

**Calreticulin in kidney function and disease: chronic low level of
calreticulin impairs Ca²⁺ homeostasis leading to mitochondrial
dysfunction and chronic renal injury**

In partial fulfillment of the requirements for the degree of

“Doctor rerum naturalium (**Dr. rer. nat.**)”

Division of Mathematics and Natural Sciences

Georg-August University Goettingen

Submitted by

Asima Bibi

From Gujrat, Pakistan

Goettingen, 2012

Supervisor: Prof. Dr. Hassan Dihazi

Department of Nephrology and Rheumatology,
University Medical Center,
Georg-August University, Goettingen, Germany.

Reviewer 1: Prof. Dr. Sigrid Hoyer-Fender

Johann-Friedrich-Blumenbach-Institute of Zoology and Anthropology,
Georg-August University, Goettingen, Germany.

Reviewer 2: Prof. Dr. Jürgen Brockmöller

Department of Clinical Pharmacology,
University Medical Center,
Georg-August University, Goettingen, Germany.

Date of oral examination: 11/10/2012

DECLARATION

I hereby declare that the Ph.D. thesis entitled “**Calreticulin in kidney function and disease: chronic low level of calreticulin impairs Ca²⁺ homeostasis leading to mitochondrial dysfunction and chronic renal injury**” has been written independently, with no other sources than quoted, and no portion of the work referred to in the thesis has been submitted in support of an application for another degree.

Asima Bibi

To the loving memory of my Taia Aba (Uncle)

Dr. Muhammad Fazal

TABLE OF CONTENTS

| | |
|---|-------------|
| List of Abbreviations | viii |
| List of Tables..... | xii |
| List of Figures..... | xiii |
| 1. General Introduction..... | 1 |
| 1.1 Chronic kidney diseases | 2 |
| 1.1.1 Etiopathology of CKD..... | 3 |
| 1.1.2 Risk factors of CKD..... | 4 |
| 1.2 Endoplasmic reticulum | 5 |
| 1.2.1 ER protein folding and ER resident proteins | 5 |
| 1.2.2 ER stress..... | 6 |
| 1.2.3 Intracellular Ca ²⁺ homeostasis..... | 8 |
| 1.3 Calreticulin..... | 10 |
| 1.3.1 Structure of calreticulin | 11 |
| 1.3.2 Functions of calreticulin | 13 |
| 1.4 Objectives | 17 |
| 2. Calreticulin is crucial for Ca²⁺ homeostasis mediated adaptation and survival of thick ascending limb of Henle's loop cells under osmotic stress | 18 |
| 2.1 Abstract | 19 |
| 2.2 Introduction..... | 20 |
| 2.3 Materials and Methods | 23 |
| 2.3.1 Cell line and culture procedure | 23 |
| 2.3.2 Osmotic stress experiments | 23 |
| 2.3.4 Protein extraction and estimation | 24 |
| 2.3.5 In-gel digestion and mass spectrometry analysis of protein spots | 25 |
| 2.3.6 Western blot analysis | 26 |
| 2.3.8 MTT cell viability assay | 26 |
| 2.3.9 Ca ²⁺ measurements | 27 |
| 2.3.10 Quantitative real-time PCR..... | 28 |
| 2.3.11 Construction of CALR expression and CALR siRNA vectors and cellular transfection..... | 28 |

| | |
|--|-----------|
| 2.3.12 Indirect immunofluorescence staining..... | 29 |
| 2.3.13 Antibodies..... | 29 |
| 2.4 Results | 30 |
| 2.4.1 ER Ca ²⁺ binding proteins and osmotic stress | 30 |
| 2.4.2 CALR and Ca ²⁺ homeostasis under osmotic stress | 37 |
| 2.4.3 CALR and cell death under osmotic stress | 40 |
| 3. Reduced calreticulin level results in oxidative stress mediated mitochondrial damage and kidney injury | 49 |
| 3.1 Abstract | 50 |
| 3.2 Introduction..... | 51 |
| 3.3 Materials and Methods | 54 |
| 3.3.1 Animals..... | 54 |
| 3.3.2 Morphometric analysis of kidneys | 54 |
| 3.3.3 Histological analysis of kidneys | 54 |
| 3.3.4 Immunohistological analysis of kidneys..... | 55 |
| 3.3.5 Electron microscopy | 55 |
| 3.3.6 Protein extraction, precipitation and estimation..... | 56 |
| 3.3.7 2-D gel electrophoresis (2-DE)..... | 56 |
| 3.3.8 In-gel digestion and mass spectrometry analysis..... | 57 |
| 3.3.9 Bioinformatic Analyses | 58 |
| 3.3.10 Western blot analysis | 58 |
| 3.3.11 Isolation of mitochondria | 58 |
| 3.3.12 Cytochrome c oxidase activity assay | 59 |
| 3.3.13 Data analysis..... | 59 |
| 3.3.14 Antibodies..... | 59 |
| 3.4 Results | 59 |
| 3.4.1 Low Calr level results in progressive kidney damage in Calr ^{+/-} mice | 59 |
| 3.4.3 Ultrastructural analysis shows glomerular and tubular cell damage in Calr ^{+/-} mice | 64 |
| 3.4.4 Enhanced expression of ECM proteins in advanced kidney injury in Calr ^{+/-} mice..... | 66 |
| 3.4.5 ER stress pathway is not operative in Calr ^{+/-} mice kidney damage | 67 |
| 3.4.6 Comparative proteomic analysis show strong metabolic dysregulation in Calr ^{+/-} mice kidneys..... | 70 |
| 3.4.7 Alteration of energy metabolism in Calr ^{+/-} mice kidneys | 75 |
| 3.4.8 Chronic low levels of Calr induces kidney injury through oxidative stress induction | 78 |

| | |
|---|------------|
| 3.4.9 Activation of iNos dimerization in Calr ^{+/-} mice | 80 |
| 3.4.10 Mitochondrial damage in Calr ^{+/-} mice | 81 |
| 3.5 Discussion | 88 |
| 4. Summary | 95 |
| Bibliography | 100 |
| Appendix | 114 |
| Acknowledgements | 120 |
| Curriculum Vitae | 122 |

LIST OF ABBREVIATIONS

Δ: Mutant

2D DIGE: 2 dimensional differential in gel electrophoresis

ACN: Acetonitrile

ACTB: β-actin

ALS: Amyotrophic lateral sclerosis

ANOVA: Analysis of variance

ATP: Adenosine triphosphate

GBM: Glomerular basement membrane

BSA: Bovine serum albumin

Ca²⁺: Calcium ions

Calr: Calreticulin mouse

CALR: Calreticulin rabbit, human

cDNA: Complementary DNA

CHAPS: 3-[(3-cholamidopropyl)dimethylammonio]-1-propanesulfonate

CKD: Chronic kidney diseases

Cnx: Calnexin

Cox: Cytochrome c oxidase

CT: Threshold cycle

DMEM: Dulbecco's modified Eagle's medium

DMF: Dimethylformamide

DMSO: Dimethyl sulfoxide

DNA: Deoxyribonucleic acid

dNTPs: Deoxyribonucleotides

DTT: Dithiothreitol

ECM: Extra-cellular matrix

EF-2: Elongation factor 2

eif2 α : Eukaryotic translation initiation factor-2 α subunit

EMT: Epithelial to mesenchymal transition

ER: Endoplasmic reticulum

ERAD: ER-associated degradation

Erp72: Endoplasmic reticulum protein 72

ESI-QTOF-MS: Electrospray ionization time of flight mass spectrometry

ESRD: End stage renal disease

Ezr: Ezrin

FCS: Fetal calf serum

FITC: Fluorescein isothiocyanate

Fn1: Fibronectin

FSP1: Fibroblast specific protein 1

G: Gravitational (unit of centrifugation)

GFR: Glomerular filtration rate

Grp78: Glucose regulated protein 78

H&E: Hematoxylin and eosin

H₂O₂: Hydrogen peroxide

HCl: Hydrochloric acid

HE: Heparin

HRP: Horse radish peroxidase

IC: Interstitial cells

IEF: Iso-electric focusing

IgA: Immunoglobulin-A

IMCD: Inner medullary collecting duct

iNos: Induced nitric oxide synthase

InsP3: Inositol 1,4,5-trisphosphate receptor

IPG: Immobilised pH gradient

kDa: Kilo dalton

KEGG: Kyoto Encyclopedia of Genes and Genomes

Lam: Laminin

LC: Liquid chromatography

LDH: Lactate dehydrogenase

mGA: Mean glomerular area

mMA. Mean mesengial area

MS: Mass spectrometry

NaCl: Sodium chloride

NADH: Nicotinamide adenine dinucleotide

NCX: Na⁺ Ca²⁺ exchanger

NMR: Nuclear magnetic resonance

NO: Nitric oxide

OD: Optical density

OxPhos: Oxidative phosphorylation

P: Probability

PAGE: Polyacrylamide gel electrophoresis

PAS: Periodic acid shift

PBS: Phosphate buffer saline

PCR: Polymerase chain reaction

PDI: Protein disulphide-isomerase

PMCA: Plasma membrane calcium pump

PMSF: Phenylmethanesulfonylfluoride or phenylmethylsulfonyl fluoride

Prdx1: Peroxiredoxin 1

RNA: Ribonucleic acid

ROS: Reactive oxygen species

RT: Reverse transcriptase

SD: Standard deviation

SDS: Sodium dodecyl sulfate

SERCA: Sarco/endoplasmic reticulum Ca²⁺ ATPase

siRNA: Small interfering RNA

Sod: Superoxide dismutase

STD: Standard

TALH: Thick ascending limb of Henle's loop

TBS-T: Tris boric acid-tween

TCA: Tricarboxylic acid cycle

TFA: Trifluoroacetic acid

TG: Thapsigargin

TGFβ1: Transforming growth factor beta 1

TJ: Tight junctions

TM: Tunicamycin

UPR: Unfolded protein response

WT: Wild type

Zn²⁺: Zinc ions

LIST OF TABLES

| | |
|---|----|
| Table 2.1: Differentially regulated proteins in TALH-NaCl cells compared to TALH-STD cells..... | 44 |
| Table 3.1: Proteins differentially regulated in the kidneys of WT and Calr ^{+/-} mice..... | 86 |

LIST OF FIGURES

| | |
|--|----|
| Figure 1.1: The ER stress response pathway. | 7 |
| Figure 1.2: Schematic representation of intracellular calcium homeostasis. | 10 |
| Figure 1.3: A model of linear and 3D structure of Calreticulin..... | 13 |
| Figure 1.4: Calreticulin-Calnexin cycle representing the proper folding of glycoproteins in ER..... | 15 |
| | |
| Figure 2.1: 2D gel electrophoresis expression of differentially regulated proteins under osmotic stress conditions. | 34 |
| Figure 2.2: Time dependent expression changes of ER Ca ²⁺ binding proteins under varied osmotic stress conditions..... | 36 |
| Figure 2.3: Impact of hyperosmotic stress on expression of ER Ca ²⁺ binding proteins under TM (5µg/ml) induced ER stress..... | 37 |
| Figure 2.4: Time dependent increase of free Ca ²⁺ in TALH cells exposed to hyper-osmotic stress. | 38 |
| Figure 2.5: Impact of HE and hyperosmotic stress on expression of proteins and cell viability in TALH cells. | 39 |
| Figure 2.6: Effect of overexpression of CALR on cell viability of TALH cells under hyperosmotic stress. | 41 |
| Figure 2.7: Knockdown of CALR enhances the resistance of TALH cells to hyperosmotic NaCl stress. 43 | |
| | |
| Figure 3.1: Morphometric analysis of embryonic and adult kidneys of Calr KO mice. | 61 |
| Figure 3.2: Progressive structural alterations in Calr ^{+/-} mice. | 63 |
| Figure 3.3: Electron microscopy analysis of Calr ^{+/-} and WT kidneys. | 65 |
| Figure 3.4: Immune expression of glomerular and tubulointerstitial injury markers..... | 67 |
| Figure 3.5: Effects of low Calr level on expression of ER stress marker and EF-hand Ca ²⁺ binding proteins. | 70 |
| Figure 3.6: 2D gel map expression of differentially regulated proteins in Calr ^{+/-} mice kidneys compared to WT..... | 72 |
| Figure 3.7: Gene Ontology (GO) classification of differentially regulated proteins by DAVID Bioinformatics. | 74 |
| Figure 3.8: Energy metabolism pathways. | 78 |
| Figure 3.9: Induction of oxidative stress in Calr ^{+/-} mice kidneys. | 79 |
| Figure 3.10: Activation of iNos in Calr ^{+/-} mice kidneys. | 81 |
| Figure 3.11: Electron micrographs demonstrating mitochondrial damage in Calr ^{+/-} mice. | 84 |
| | |
| Figure 4.1: Schematic representation of potential pathway of low calreticulin level in the progression of renal injury. | 99 |

1. GENERAL INTRODUCTION

1.1 Chronic kidney diseases

Kidney, a major homeostatic organ or highly specialized “Natural filters” of the body, mainly functions to remove waste products, excess of water and salts from the blood and excretes them outside the body in the form of urine. The kidneys filter about 180 liters of blood every day and produce about two liters of urine. The kidneys also produce certain hormones such as erythropoietin, which stimulates the bone marrow to make red blood cells, renin which regulates blood pressure, calcitriol the active form of vitamin D, which helps maintain Ca^{2+} for bones and for normal chemical balance in the body. Loss of renal function is a life threatening event due to accumulation of wastes in the blood and consequent body damage. Chronic loss of kidney function or chronic kidney disease (CKD) is becoming a major public health problem worldwide affecting 7.2% of the global adult population with the number dramatically increasing from 23.4% to 35.8% in the elderly persons aged over 64 years (Zhang & Rothenbacher, 2008). However, results from an epidemiological survey of chronic kidney disease in population of older adults in Germany also showed prevalence of CKD in 17.4% subjects aged 50-74 which increased with age and peaked 23.9% in age of 70–74 years (Zhang et al, 2009). CKD is associated with outcomes such as progression to end-stage renal disease (ESRD), development of cardiovascular disease, hospitalization, and death in community-based populations (Go et al, 2004; Orantes et al, ; Schiffrin et al, 2007; Tonelli et al, 2006; Weir). Progressive nature of CKD to end stage renal failure, a condition requiring dialysis or renal transplantation for long-term survival is putting an extensive load on global health care costs (Hossain et al, 2009; Lysaght, 2002; Meguid El Nahas & Bello, 2005; Zhang & Rothenbacher, 2008).

1.1.1 Etiopathology of CKD

The nephron, the structural and functional unit of the kidney is progressively damaged in many chronic kidney diseases starting with either glomerular or tubular injury. Despite the start, most renal diseases eventually converge into common histopathological impairments such as glomerulosclerosis and tubulointerstitial fibrosis leading to progressive functional deterioration of the renal system (Fogo, 2006; Lopez-Novoa et al, 2010; Meguid El Nahas & Bello, 2005).

Glomerulosclerosis

Glomerulosclerosis is thought to have a central pathogenetic role in the progression from chronic glomerulopathies to end-stage renal disease (Klahr et al, 1988). It frequently complicates most renal diseases and is characterized by progressive remodeling of the glomerular structure such as thickening of the glomerular basement membrane, expansion of mesangium, podocyte damage and disruption of glomerular filtration machinery. Microinflammation of endothelial cells is the early sign of glomerular injury leading to activation and release of a wide range of cytokines and growth factors from mesangial cells (Cybulsky et al, 2010). Under the influence of growth factors, especially transforming growth factor beta 1 (TGF β 1), mesangial cells regress to an embryonic mesenchymal phenotype capable of excessive production and accumulation of extracellular matrix (ECM) such as fibronectin ultimately causing glomerular mesangial expansion and fibrosis (El-Nahas, 2003; Hohenadel & Van der Woude, 2004). These structural impairments are associated with proteinuria, disturbed glomerular filtration rate (GFR), tubule damage and fibrosis (Levey & Coresh, 2011; Lopez-Novoa et al, 2010). Stress states, such as sustained hypertension, nitric oxide and oxidative stress are commonly known to implicate in glomerulosclerosis (Modlinger et al, 2004; Oberg et al, 2004; Okada et al, 2012).

Tubulointerstitial fibrosis

Despite the primary cause, many renal diseases also lead to tubulointerstitial fibrosis. Inflammation, proliferation, apoptosis, and fibrosis are hallmarks of tubulointerstitial fibrosis (Zeisberg et al, 2000). Direct attack of disease or indirectly due to proteinuria from glomerular damage initiates the inflammation of tubular cells and interstitial fibroblasts and myofibroblasts associated with an increased synthesis and release of matrix proteins (Lopez-Novoa et al, 2010). Progressive deposition of harmful connective tissue in interstitial spaces of the kidney together with epithelial to mesenchymal transition (EMT) of tubular epithelial cells, are directing to apoptosis based tubular atrophy and the formation of atubular glomeruli. (Carew et al, ; Efstratiadis et al, 2009; Meguid El Nahas & Bello, 2005; Radisky et al, 2007; Zeisberg et al, 2000). Continuing injury, inflammation, and fibroblast activation, ECM deposition and proliferation lead to irreversible fibrosis.

1.1.2 Risk factors of CKD

Hypertension (Barri, 2008; Tedla et al, 2011), and diabetes (Bash et al, 2008; Pyram et al, 2011) are the two mainly discussed causes of kidney disease worldwide. Cytokines (Schulman, 2012), kidney infections (Barsoum, 2006), urinary obstruction or blockage with kidney stones (Rule et al, 2009), oxidative stress and hypoxia (Mimura & Nangaku, 2010), and salt-induced renal injury (Mimran & du Cailar, 2008; Susic & Frohlich, 2012; Tuomilehto et al, 2001) are also known as some of the potential risk factors of CKD. Progressive kidney injury also develops in many hereditary disorders such as atherosclerosis (Boykin et al, 2011; Kottgen et al, 2010; Vehaskari, 2011). Regardless of the underlying cause, CKD is characterized by appearance of glomerulosclerosis, and tubulointerstitial fibrosis with subsequent progression toward end stage renal disease (ESRD) (Meguid El Nahas & Bello, 2005).

In the last few decades, the progression of the disease process is well documented. Much interest has focused on investigating potential mechanisms to prevent or reverse the damage. However, the intracellular mechanisms responsible for renal disease initiation leading to complete damage are mostly not well understood. There is an immense need to explore the approaches to minimize the risks of renal diseases. Over the past few decades, intensive investigations of the molecular and cellular mechanisms revealed the association of ER function alteration in normal kidney structure and function, with the early-onset and pathogenesis of renal diseases (Cunard & Sharma, 2011; Cybulsky et al, 2010; Hebert & Molinari, 2007; Inagi, 2009; Inagi et al, 2008; Liu et al, 2008).

1.2 Endoplasmic reticulum

The ER is a perinuclear, cytoplasmic compartment comprising membranous network of branching tubules and flattened sacs. It is mainly recognized as a protein-folding factory involved in synthesis, proper folding, trafficking, and modification of proteins, degradation of proteins, as well as for synthesis of steroids, cholesterol, and other lipids. Ca^{2+} storage and Ca^{2+} signaling regulation is another basic important role of ER in cell (Baumann & Walz, 2001; Bedard et al, 2005; Inagi, 2009; Nauseef et al, 1995). Importantly, the ER contains numerous molecular chaperones and catalysts to aid in the ER functions.

1.2.1 ER protein folding and ER resident proteins

Newly synthesized proteins translocate to ER, where they are covalently modified and attain their correctly folded three dimensional conformation through ER resident chaperones including BiP /Grp 78, calreticulin (CALR), calnexin (Cnx), Grp94 and the thiol oxidoreductases PDI and ERp57, all involved in generating conformationally competent and functional proteins (Bedard et al, 2005; Brodsky & Skach, ; Ellgaard & Helenius, 2003;

Kleizen & Braakman, 2004). Each of these proteins follows their distinctive chaperon system for specific types of proteins.

1.2.2 ER stress

Environmental insults like ischemia, glucose deprivation, oxidative stress, osmotic stress or genetic mutation can cause expression regulation of ER chaperone proteins. This expression changes the result in aberrant ER function due to inefficient protein folding (Buchberger et al, 2010; Chevet et al, 2001; Wu & Kaufman, 2006; Yoshida, 2007; Zhao & Ackerman, 2006). Improper protein folding results in accumulation of misfolded proteins leading to ER stress and induction of ER stress response pathways (Figure 1.1). Misfolded proteins are corrected by either activation of unfolded protein response (UPR) (Hetz, 2012; Ron & Walter, 2007; Wu & Kaufman, 2006), a coordinated stress response that upregulates the capacity of the ER to process abnormal proteins or ER quality control CALR -Cnx cycle (Discussed later). UPR is an adaptive mechanism that targets the transcription regulation of proteins which can restore the proper folding of proteins through induction of chaperone such as Grp78 (Lee, 1992; Lee, 2007; Zhang et al, 2010).

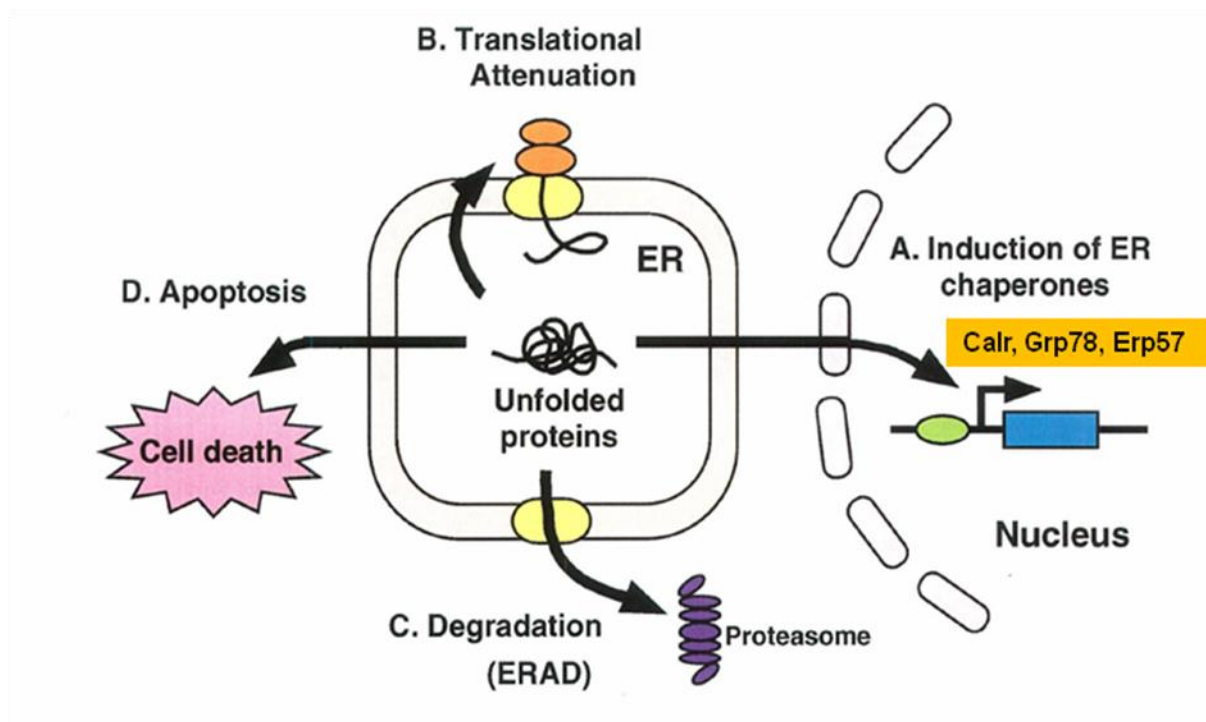


Figure 1.1: The ER stress response pathway.

ER stress leads to accumulation of unfolded proteins in ER resulting in induction of four responses. A: Induction of ER chaperones such as Calr, Grp78 and Erp57 to correctly fold the misfolded proteins and avoid protein aggregates (Hong et al, 2004). B: Translation attenuation which reduces ER load by turning down the general translation (Lee do et al, 2010) C: ERAD is the ER quality-control system which detects and exposes to cytosolic proteasomal degradation of the misfolded proteins through ubiquitylation . D: apoptosis of cells in which severe and prolonged ER stress extensively impairs the ER functions and threatens the integrity of the organism (Timmins et al, 2009). ER: endoplasmic reticulum, ERAD: ER-associated degradation. Adapted from Araki et al. (Araki et al, 2003).

Accumulating data suggest a pathophysiological role of ER stress in renal diseases. Patient biopsies and animal models of kidney diseases demonstrate the implication of ER stress in the development and progression of both glomerular and tubular injuries (Chiang et al,2011; Inagi, 2009; Inagi et al, 2008). ER stress is also associated with many risk factors of CKD such as hypertension, diabetes, hypoxia/ischemia and genetic disorders giving a possible mechanistic link between disease mediators and final diseased state (Lindenmeyer et al, 2008;

Okada et al, 2012; Yoshida, 2007). In vitro studies further show an expression regulation of ER chaperones along with UPR activation in renal cells treated with cytokines, oxidative stress, or osmotic stress mediators (Bibi et al, 2011; Dihazi et al, 2005; Dihazi et al, 2011; Eltoweissy et al, 2011; Lindenmeyer et al, 2008; Yoshida, 2007). Using proteomics, Dihazi and coworkers demonstrated a clear correlation between upregulation of ER stress-related proteins and the fibrosis phenotype highlighting an important role of ER proteins in fibrosis progression (Dihazi et al, 2011).

1.2.3 Intracellular Ca²⁺ homeostasis

Ca²⁺ is an universal signal transduction element. Free intracellular Ca²⁺ is the physiologically active form of Ca²⁺ (Means & Rasmussen, 1988). It plays an important role in the regulation of diverse cellular processes from contraction, secretion, gene transcription, cell growth and movement to cell differentiation and death (Berridge, 1993). Maintenance of a constant luminal level of Ca²⁺ is also essential for the post-translational processing, folding and export of proteins (Verkhatsky, 2007). Therefore, the maintenance of free Ca²⁺ to certain critical limits called intracellular Ca²⁺ homeostasis is of prime importance in the cell to keep it functioning normally. Intracellular Ca²⁺ homeostasis refers to a cytosolic concentration as low as ~100 nM compared to 10,000 folds more in extracellular environment. Figure 1.2 represents the simple pathways and organelles involved in the intracellular Ca²⁺ homeostasis.

ER, being a major intracellular Ca²⁺ store plays an important role in the regulation of intracellular Ca²⁺ homeostasis (Berridge, 1993). Ca²⁺ signalling between ER and cytoplasm is tightly regulated by ER membrane Ca²⁺ entry and exit channels. Ca²⁺ enters the ER through SERCA, a Ca²⁺ pump that transfers Ca²⁺ from the cytosol to the lumen of the SR/ER at the expense of ATP hydrolysis (Kubala, 2006), whereas InsP3 (inositol 1,4,5-trisphosphate

receptor) and ryanodine receptors are used for Ca^{2+} release from the ER (Arendshorst & Thai, 2009; Vanderheyden et al, 2009). Moreover, ER luminal Ca^{2+} is also in homeostasis with total ER Ca^{2+} concentration (up to 1 mM) and the free ER Ca^{2+} concentration (200 μM). ER resident proteins, in particular the molecular chaperones and folding enzymes; Cnx, CALR, BiP, Grp94, and PDI have both high- and low-affinity Ca^{2+} -binding sites and are responsible for mediating intracellular Ca^{2+} dynamics (Michalak et al, 2002). Because of the sheer abundance and number of Ca^{2+} -binding sites, CALR is considered the most important protein for Ca^{2+} storage and buffering. It binds to over 50% of ER luminal Ca^{2+} (Nakamura et al, 2001) and engages in intracellular Ca^{2+} homeostasis due to two Ca^{2+} binding domains with different affinities and capacities. The protein is involved in a variety of cellular processes and functions from cell to organ level (discussed later in part 1.3).

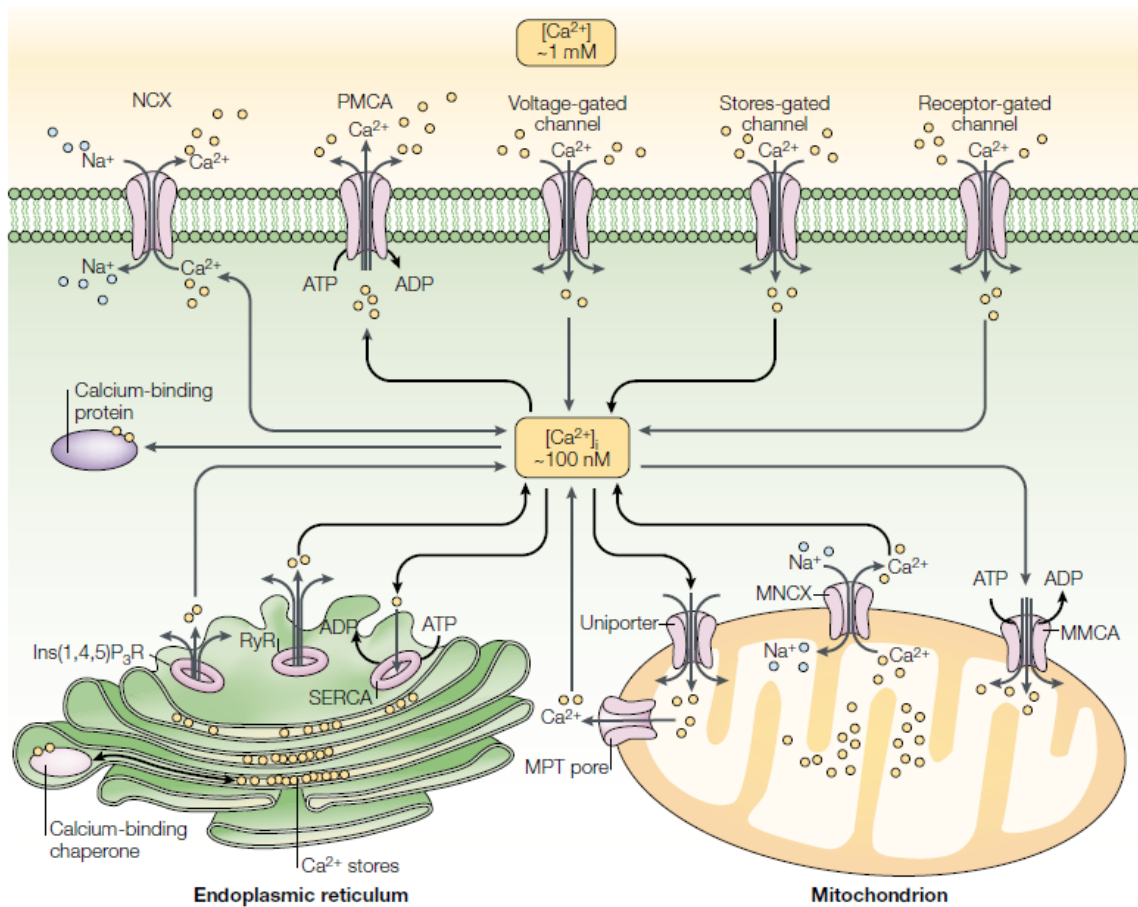


Figure 1.2: Schematic representation of intracellular calcium homeostasis.

A schematic representation of intracellular calcium homeostasis mechanism showing tightly regulated Ca^{2+} concentrations across the cell and cellular components like organelles and channels that may take part in this regulation. $[Ca^{2+}]_i$: calcium concentration, iNCX: $Na^+ Ca^{2+}$ exchanger, MNCX: mitochondrial $Na^+ Ca^{2+}$ exchanger, PMCA: plasma membrane calcium pump, MPT: mitochondrial permeability pore, RyR: ryanodine, Ins(1,4,5)P₃R: inositol-1,4,5-trisphosphate receptors, SERCA: sarco-endoplasmic reticulum Ca^{2+} ATPase. Adapted from Popi Syntichaki and Nektarios Tavernarakis (Syntichaki & Tavernarakis, 2003).

1.3 Calreticulin

CALR also known as high-affinity Ca^{2+} binding protein, Calreguiin, Erp60, CRP55, CAB-63 and CaBP3 and calsequestrin-like protein (Michalak et al, 1992) is an endoplasmic reticulum resident protein. The protein was first identified in the 70s as a Ca^{2+} binding protein in

skeletal muscle sarcoplasmic reticulum (Ostwald & MacLennan, 1974). Fifteen years later, with advances in molecular biology, two groups, Koch and Michalak, isolated simultaneously the cDNA encoding this Ca^{2+} -binding protein (Kottgen et al, 2010; Michalak et al, 1992). The authors named this protein calreticulin (Kottgen et al, 2010). Since then, CALR emerged as a ubiquitously expressed protein in a wide range of species and in almost all cell types studied. CALR is highly conserved protein with over 90% amino acid identity existing between human, rabbit, rat and mouse forms of the protein (Michalak et al, 1992).

1.3.1 Structure of calreticulin

CALR, is a 46 kDa (400 amino acid residues) ER Ca^{2+} binding chaperon. Biochemical and structural studies have demonstrated three distinct structural domains of CALR: the amino-terminal N-domain, the middle P-domain, and the carboxyl-terminal C-domain. The protein also contains a cleavable amino acid signal sequence at the beginning of N-terminal directing the protein to ER and an ER retention/retrieval signal at the C-terminal (Fliegel et al, 1989; Kottgen et al, 2010; Mesaeli et al, 1999). (Figure 1.3A)

N-domain: The N-domain (residues 1–170) is an extremely conserved and highly folded globular domain composed of eight antiparallel β -strands (Opas et al, 1996) as shown in Figure 1.3B. The N-domain of CALR also has a lectin binding site and a polypeptide binding site (Kapoor et al, 2003; Leach et al, 2002). It also binds with protein disulphide-isomerase (PDI) and ERp57 mediated by Zn^{2+} (Baksh et al, 1995; Leach et al, 2002; Michalak et al, 1999; Pollock et al, 2004). N-domain has a binding site for rubella virus RNA, a putative phosphorylation site and a segment which binds to steroid hormone receptors and the cytoplasmic domains of integrin α subunits and is recently known to have a single high-affinity Ca^{2+} binding site (Chouquet et al, 2011; Kozlov et al, 2010; Pocanschi et al, 2011).

P-domain: The middle P-domain (residues 170–285) of CALR is a proline rich domain. The P domain is also known as “extended arm” based on its three-dimensional structure obtained by NMR technique (Figure 1.3B). Moreover, this hairpin loop is also known to interact with Erp57 (Ellgaard et al, 2002; Martin et al, 2006). The P-domain also binds Ca^{2+} with high affinity ($K_d = 1 \mu\text{M}$) and low capacity (approximately 1 mol of Ca^{2+} per mol of protein) (Baksh et al, 1995; Tjoelker et al, 1994). The P domain, having a lectin binding site, together with the N-domain is involved in the chaperoning of nascent polypeptides (Pocanschi et al, 2011; Vassilakos et al, 1998). (Figure 1.3)

C-domain: The C-domain (residues 285– 400) of CALR is highly acidic Ca^{2+} binding and storage domain (Figure 1.3B). Depending on negatively charged residues of the C-domain, protein binds Ca^{2+} with low affinity ($K_d = 2 \text{mM}$) and high capacity (approximately 25 mol of Ca^{2+} per mol of protein) (Baksh et al, 1995; Mesaeli et al, 1999) and works as a Ca^{2+} -buffer in ER. The C-domain of CALR is also known to regulate the protein-protein interactions of CALR with PDI, Erp57 and other chaperones (Michalak et al, 1999).

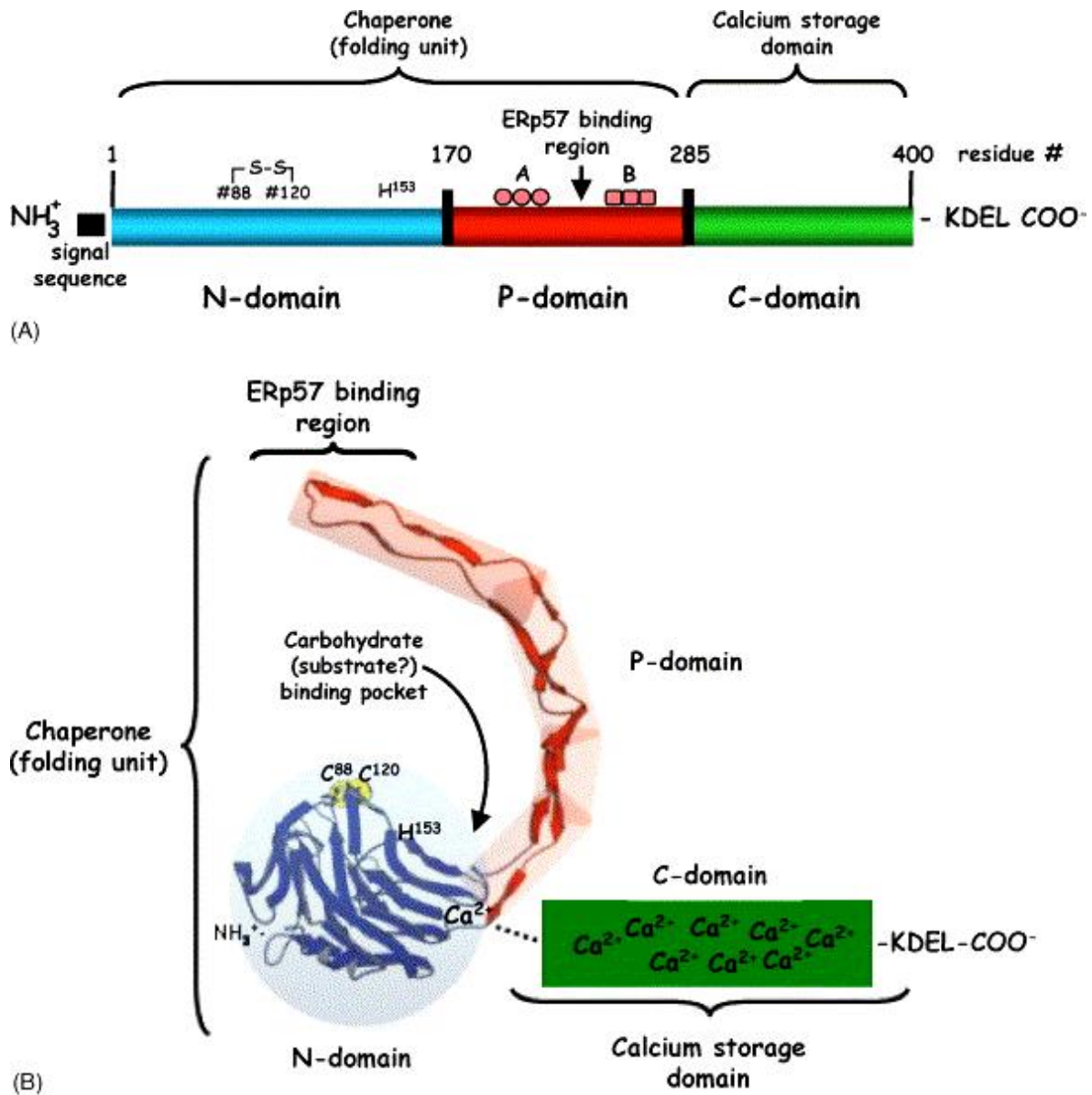


Figure 1.3: A model of linear and 3D structure of Calreticulin.

(A) Linear representation of CALR domains. (B) 3D model of the CALR domains. Adapted from Gelebart et al. (Gelebart et al, 2005).

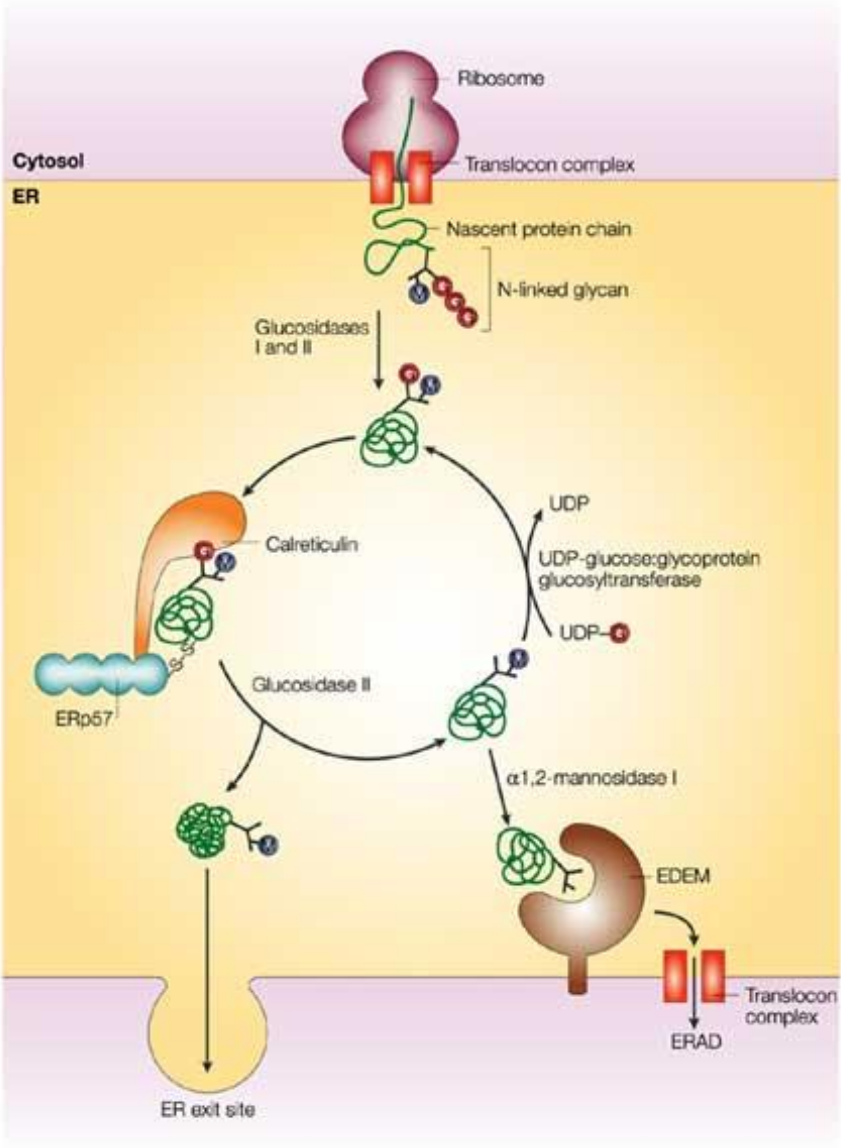
1.3.2 Functions of calreticulin

CALR is a multi-functional Ca²⁺ binding chaperon of ER. It plays two main functions in ER as a chaperon and as a Ca²⁺ binding and storage protein. CALR is also found in several other sub-cellular locations: the cell surface, cytoplasm, and ECM (Gold et al, 2010). The presence

of CALR, a protein with ER retention signal KDEL, in other cell compartments was a mystery. However, Afshar and coworkers (Afshar et al, 2005) demonstrated the retrotranslocation process of CALR, which is safe from proteasomal degradation. Many extracellular function of CALR have been reported including roles in immunogenic cell death in cancer, cellular adhesion, cell migration, phagocytosis, inflammation, cell signaling, and enhancing wound healing (Gold et al, 2010). Cytosolic CALR is also involved in certain processes such as adhesion, gene expression, translation and nuclear export (Hsu et al, 2005).

Calreticulin, an ER quality control protein

CALR functions as a molecular chaperone in the folding of many proteins and especially glycoproteins. The property of CALR to help other proteins to fold correctly and become functional, assigns the protein as a quality control unit in ER. The majority of growing polypeptides asparagine side chains bind to glycans and are translocated to ER in N-glycosylated form and are correctly folded into functional transportable forms as shown in Figure 1.4. Briefly, Glucosidase I and Glucosidase II are two independent enzyme systems, which bring these unfolded nascent proteins to monoglucosylated form by trimming two terminal glucose residues. Chaperon systems of ER, which recognize and fold specifically N-linked monoglucosylated proteins comprises of CALR, Cnx and Erp57. CALR and Cnx are homologous lectin molecular chaperones in ER. Their central P-domain binds to the hydrophilic N-linked monoglucosylated glycans of unfolded and misfolded proteins in ER leading to their proper, functional and transportable folded conformations (Hebert & Molinari, 2007; Kapoor et al, 2003; Meunier et al, 2002; Trombetta & Helenius, 1998). On the other hand, misfolded proteins are degraded through ERAD system. In contrast, folding is significantly impaired in CALR or Cnx-deficient cells having accelerated folding with an accumulation of misfolded proteins (Hebert & Molinari, 2007).



Nature Reviews | Molecular Cell Biology

Figure 1.4: Calreticulin-Calnexin cycle representing the proper folding of glycoproteins in ER.

Adapted from Ellgard and Helenius (Ellgard & Helenius, 2003). EDEM: ER degradation-enhancing 1,2-mannosidase-like protein, ERAD: ER-associated degradation

Calreticulin and Ca²⁺ homeostasis regulation

ER, being a major store of intracellular Ca²⁺, exerts a key role in the complex and precise mechanism of Ca²⁺ signalling and homeostasis. The ER lumen Ca²⁺ storage capacity is enhanced by Ca²⁺-binding proteins. CALR is one of the most important Ca²⁺ binding proteins of ER. CALR plays a critical role in the regulation of intracellular Ca²⁺ homeostasis directly through Ca²⁺ storage capacity of ER. Earlier studies with overexpression of CALR in various cell lines show increased ER Ca²⁺ storage capacity with almost no impact on protein folding (Bastianutto et al, 1995; Bibi et al, 2011; Mery et al, 1996; Opas et al, 1996). On the other hand, downregulation and deficiency of CALR decreases the ER Ca²⁺ storage (Bibi et al, 2011; Coe & Michalak, 2009; Michalak et al, 1999). It also controls the Ca²⁺ homeostasis through store operated Ca²⁺ influx. CALR interacts with Ca²⁺ entry and exit channels called SERCA and IP3R and modulates Ca²⁺ influx by controlling the extent of inositol 1,4,5-trisphosphate-induced Ca²⁺ store depletion (Mery et al, 1996; Michalak et al, 2002; Xu et al, 2000). Michalak et al. showed that CALR knockout is lethal due to impaired cardiac development (Michalak et al, 1999). They further demonstrated that this impairment of heart development is due to Ca²⁺ homeostasis regulation and not because of chaperon function of protein.

Short-term increase in Ca²⁺ is an essential signal for vitally important cell processes whereas, long-term increase in Ca²⁺ leads to irreversible impairment of cellular functions and/or structure, up to cell death. There is convincing evidence that sustained increase in intracellular Ca²⁺ alters cell functions and is associated with various diseases such as diabetes mellitus, hypertension, Alzheimer`s disease, neurodegenerative disorders, cardiac ischemia, and atherosclerosis and renal diseases (Chan et al, 2009; Lajdova et al, 2009; Rivera et al, 1996; Vamvakas & Anders, 1990; Zile & Gaasch, 2011). The role of intracellular Ca²⁺ homeostasis

disturbances has also been discussed in some renal diseases but very little is known about its the role in normal kidney function and mechanisms undergoing in renal impairments.

1.4 Objectives

The general aim of our group is to understand the molecular mechanisms, which are involved in renal function or lead a normal functioning kidney towards disease state. In this regard we have undertaken proteomic screening of several renal cell line models exposed to different physiological conditions, such as osmotic stress, oxidative stress, and cytokines. Moreover, proteome of renal cells derived from fibrotic human kidney were also compared to healthy renal cells. All these studies highlighted the involvement of a group of ER resident proteins mainly CALR, Grp78, Erp72 and Erp57 in kidney injury. The present work is focused on one of these proteins, CALR and its physiological importance in renal structure and function, specifically through the following aims:

- i) To investigate the role of CALR in renal cells functions and adaptation specifically, the potential mechanism of CALR downregulation under conditions of osmotic stress. This is addressed in Chapters 2.
- ii) To examine the *in vivo* role of chronic low level of CALR in kidney structure and function. Especially, to analyze the intracellular signaling pathways that regulates the development of chronic kidney injury in mice with chronic low level of CALR. This aim is addressed in Chapters 3.

2. CALRETICULIN IS CRUCIAL FOR Ca^{2+} HOMEOSTASIS MEDIATED ADAPTATION AND SURVIVAL OF THICK ASCENDING LIMB OF HENLE'S LOOP CELLS UNDER OSMOTIC STRESS

Asima Bibi, Nitin K. Agarwal, Gry H. Dihazi, Marwa Eltoweissy, Phuc Van Nguyen,
Gerhard A. Mueller, Hassan Dihazi

The International Journal of Biochemistry and Cell Biology, 43 (2011): 1187-97.

2.1 Abstract

The thick ascending limb of Henle's loop (TALH) is normally exposed to variable and often very high osmotic stress and involves different mechanisms to counteract this stress. ER resident calcium ions (Ca²⁺) binding proteins especially calreticulin (CALR) play an important role in different stress balance mechanisms. To investigate the role of CALR in renal epithelial cells adaptation and survival under osmotic stress, two-dimensional fluorescence difference gel electrophoresis combined with mass spectrometry and functional proteomics were performed. CALR expression was significantly altered in TALH cells exposed to osmotic stress, whereas renal inner medullary collecting duct cells and interstitial cells exposed to hyperosmotic stress showed no significant changes in CALR expression. Moreover, a time dependent downregulation of CALR was accompanied with continuous change in the level of free intracellular Ca²⁺. Inhibition of the Ca²⁺ release, through IP3R antagonist, prevented CALR expression alteration under hyperosmotic stress, whereas the cell viability was significantly impaired. Overexpression of wild type CALR in TALH cells resulted in significant decrease in cell viability under hyperosmotic stress. In contrast, the hyperosmotic stress did not have any effect on cells overexpressing the CALR mutant, lacking the Ca²⁺-binding domain. Silencing CALR with siRNA significantly improved the cell survival under osmotic stress conditions. Taken together, our data clearly highlight the crucial role of CALR and its Ca²⁺-binding role in TALH adaptation and survival under osmotic stress.

2.2 Introduction

The osmoregulation of the body is one of the most controlled physiological mechanisms, regulated by a balance of hydration and solute concentrations (Bourque, 2008). The kidney is one of the main organs of the body which maintain osmolality. As a consequence of this, the kidney cells are exposed to very hyper-osmotic environment compared to the rest of the body (Marsh & Azen, 1975). The thick ascending limb of Henle's loop (TALH) segment is the part of the kidney nephron, which plays a vital role in urinary concentration mechanism by generating concentrated urine in antidiuresis and dilutes urine in water diuresis. Hyperosmolality affects numerous cellular functions and causes cell cycle delay and apoptosis in renal cells (Burg et al, 2007; Michea et al, 2000). To study the adaptive changes under variable osmotic stress conditions in this segment of the kidney, the TALH-cell line from rabbit kidney provides a unique tool. The ability at the cellular level to alter gene expression and metabolic activity in response to changes in the osmotic environment provides an additional regulatory mechanism. TALH cells adapt to an increased levels of NaCl by morphological shrinkage (Grunewald et al, 2001). These morphological adaptations are accompanied by dramatic change in the proteome of the cells. Especially the downregulation of the ER Ca²⁺ binding chaperones like calreticulin (CALR), Erp72, and GRP78 is debatable, since such a reaction of a protein with chaperone function is quite unlikely under stress conditions in TALH cells (Dihazi et al., 2005). The aim of the current study is to understand the role of CALR in terms of Ca²⁺ homeostasis regulation in the adaptation mechanism of TALH cells under osmotic stress. CALR is a 46 kDa protein, which is ubiquitously expressed in nearly all cells of higher organisms (Mesaeli et al, 1999). It is subdivided into three structural and functional regions: a highly conserved N-domain, a proline-rich P-domain and a

very acidic C-domain, which binds Ca^{2+} with high capacity and low affinity. Different cellular functions have been characterized for CALR, intracellular as well as extracellular. Mainly due to its ability to bind monoglucosylated high mannose oligosaccharides, CALR plays an important role as a lectin-like chaperon by binding to incompletely folded proteins that contain one terminal glucose on N-linked oligosaccharides, retaining the protein inside the ER until proper folding (Peterson et al, 1995). Directing proper conformation of misfolded proteins and glycoproteins under stress conditions, CALR, is generally induced as stress response protein to protect the cells against various toxic insults (Ihara et al, 2005; Little & Lee, 1995; Liu et al, 1997; Marber et al, 1995; Morris et al, 1997; Sugawara et al, 1993) and is involved in various cellular functions and signaling, including apoptosis, stress responses, organogenesis, and transcriptional activity (Michalak et al, 2002). Ca^{2+} is an important signaling molecule and stored mainly in the lumen of the ER. Fluctuations of the ER luminal Ca^{2+} concentration result in disturbance of intracellular Ca^{2+} homeostasis. Intracellular Ca^{2+} homeostasis has received considerable attention

as a cell death signal and as an activator of gene expression (Nicotera et al, 1992; Nicotera & Orrenius, 1998). CALR due to its Ca^{2+} binding C-domain and accumulation of large amounts of Ca^{2+} without an excessive increase in the free ER intraluminal Ca^{2+} concentration was proved to regulate the intracellular Ca^{2+} homeostasis and ER Ca^{2+} storage capacity (Fliegel et al, 1989; Gelebart et al, 2005; Nakamura et al, 2001; Treves et al, 1990; Vassilakos et al, 1998). Additionally, CALR appears to play an essential role in the development of heart and brain since CALR-deficient mice develop embryonic lethality due to decreased ventricular wall thickness, whereas cells derived from CALR knockout embryos have impaired Ca^{2+} homeostasis (Gelebart et al, 2005). Intracellular Ca^{2+} concentration (Ca^{2+}) also plays an important role in the signal transduction processes within the TALH cells and regulates the

Calreticulin is crucial for Ca^{2+} homeostasis mediated adaptation and survival of thick ascending limb of Henle's loop cells under osmotic stress

transepithelial transport of sodium across the renal epithelial tubular cells (Friedman et al, 1981; Taylor & Windhager, 1979).

2.3 Materials and Methods

2.3.1 Cell line and culture procedure

The epithelial cell line used in these experiments was derived from a rabbit kidney's outer medulla. Cultured cells were immortalized by SV 40 early region DNA (Bartek et al, 1991). They showed a high degree of differentiation and specialization and provided a suitable model to study TALH cell function in vitro. The TALH cell line was maintained as a monolayer culture in DMEM (Gibco) including 5.5 mmol/l d-glucose supplemented with 10% fetal calf serum (Roche), 1% MEM nonessential amino acids, 1% l-glutamine and 1% Penicillin/Streptomycin (Gibco). Cells were routinely cultured in 75 cm² tissue culture flasks (Falcon) at 37 °C in a humidified 5% CO₂/95% air atmosphere.

2.3.2 Osmotic stress experiments

After reaching 70% confluence, TALH cells cultivated in 300 mosmol/kg medium (TALH-STD) were stressed with 600 mosmol/kg NaCl medium. TALH-cell lines exhibiting a high resistance to osmolality (600 mosmol/kg) (TALH-NaCl) were established. The osmolality was adjusted with 3 M NaCl solution and was controlled routinely. Later on, the TALH-NaCl cells, which were growing for a long time in hyperosmolality NaCl medium (600 mosmol/kg) were transferred back to hypoosmotic medium (300 mosmol/kg) in a time dependent manner for 12, 24, 48 and 72 h. All osmotic stress experiments were repeated at least three times.

Isolation of IMCD and IC cells

Inner medullary collecting duct (IMCD) and interstitial cells (IC) were isolated from rat kidney by following the protocol of Grupp et al. (Grupp et al, 1998).

2.3.4 Protein extraction and estimation

75% confluent cultures were scraped and washed three times with PBS with the corresponding osmolality (300 or 600 mosmol/kg). The cells were harvested by centrifugation at 200×g for 10 min, the pellet was treated with 0.3-0.5 mL lysis buffer (9.5 M urea, 2% CHAPS (w/v), 2% ampholytes (w/v), 1% DTT, 10 mM PMSF). Ampholytes, DTT, pepstatin (to a final concentration of 1.4 μM), and complete from Roche Diagnostic (according to the manufacturer's protocol) were added before use. To remove the cell debris, sample centrifugation was carried out at 13,000×g and 4°C for 45 min. Supernatant was recentrifuged at 13,000×g and 4 °C for an additional 45 min to get maximal purity. The resulting samples were used immediately or stored at -80°C until use. Protein concentration was estimated according to Bradford (1976), using bovine serum albumin as a standard.

2.5. Two-dimensional fluorescence difference gel electrophoresis (2D DIGE) Protein extraction was performed as described above. The resulting pellet was solubilized in labeling buffer (30 mM Tris-HCl pH 8.5, 9.5 M urea, 2% CHAPS, 10mM PMSF), centrifuged (5 min, 13,000 × g) and the protein concentration of the supernatant was determined as described above. For the fluorescence labeling, each dye was freshly dissolved in anhydrous N,N-dimethylformamide (DMF) (Sigma-Aldrich, St. Louis, USA) to a stock solution containing 1000 pmol/μl. One volume of CyDye solution was added to 1.5 volumes of high grade DMF, to make a 400 pmol CyDye solution. For minimal labeling 400 pmol of the amine-reactive cyanine dyes Cy3 and Cy5 was added respectively to 50 μg proteins from each TALH-STD and TALH-NaCl, following the manufacturer's protocol (GE Healthcare). The labeling reaction was carried out at 4°C in the dark for 30 min and the reaction was terminated by addition of 10 nmol lysine at 4°C in the dark for 10 min. Equal volumes of 2× sample buffer (30mM Tris-HCl pH 8.5, 9.5 M urea, 2% CHAPS, 10 mM PMSF, 130 mM DTT and 2%

ampholytes 3-10) were added to each of the labeled protein samples. To avoid the dye-specific protein labeling, every pair of protein samples from two independent cell extract preparations was processed in duplicate while swapping the dyes. Thereby, four replicate gels were obtained which allowed monitoring regulation factors down to two-fold changes. 50µg of an internal standard consisting of a mixture of all cell samples under investigation were labeled with 400 pmol Cy2 and included on all gels to facilitate gel matching, thereby eliminating experimental variation. The three differentially labeled fractions were pooled. Rehydration buffer (8 M urea, 1% CHAPS, 13 mM DTT and 1% ampholytes 3-10) was added to make a total volume of 185 µl prior to IEF. The 2-DE was performed with 11cm 3–10 IPG strips. The CyDye-labeled gels were scanned at 50µm resolution on a Fuji FLA5100 scanner (Fuji Photo, Kanagawa, Japan) with laser excitation light at 473nm and long pass emission filter 510LP (Cy2), 532nm and long pass emission filter 575LP (Cy3), and 635nm and long pass emission filter 665LP (Cy5). Fluorescent images were acquired in 16-bit TIFF files format. Spot matching across gels and normalization based on the internal standard was performed with Delta2D software (Decodon, Greifswald, Germany). To analyze the significance of protein regulation, a Student's t-test was performed, and statistical significance was assumed for p values <0.01. For protein visualization, 2-DE was poststained with colloidal Coomassie blue (Roti-Blue) overnight. Differentially regulated proteins were excised and processed for identification by MS.

2.3.5 In-gel digestion and mass spectrometry analysis of protein spots

Differentially expressed spots were manually excised from the gels and in-gel digestion, mass spectrometry analysis and protein identification with database search was performed as described by Dihazi et al. (Dihazi et al, 2005).

2.3.6 Western blot analysis

In order to confirm the protein expression differences during 2-D DIGE analysis, Western blot analysis was performed for the proteins of interest according to a standard protocol of Towbin et al. (Towbin et al, 1979).

2.3.7 Tunicamycin (TM), heparin (HE) and thapsigargin (TG) treatment.

TALH-cells were cultured in 96-well microtiter plates at a concentration of 5×10^3 cells per well (for cell viability assay) and to 70% confluence in 75 cm² tissue culture flasks (for Western blot analysis). A stock solution of TM, an ER stress inducer was prepared by dissolving in DMSO. Heparin, an IP3R antagonist and blocker was used to block the IP3R. A low molecular weight, water soluble heparin which can enter the cell was purchased from Sigma. It was dissolved in culture media. Cells were treated with a concentration of 5 μ M TM and 25 μ M HE alone and coupled with NaCl stress separately, for 24 hours compared to control groups with normal and NaCl stress media. Cells grown in normal media also received equivalent volumes of DMSO as a control. After 24 hours of treatments cells cultured in 96 well plates were further processed for MTT cell viability assay and samples were collected for Western blot analysis.

A stock solution of Thapsigargin (Sigma), a SERCA inhibitor was prepared by dissolving in DMSO and a concentration of 0.3 μ M was used to treat the TALH-cells cultured in 6-well plate in a time dependent manner for 0-50 min. mRNA samples were collected for RT-PCR.

2.3.8 MTT cell viability assay

Cell viability was tested using cell Proliferation Kit I (MTT), a colorimetric assay for the non-radioactive quantification of cell proliferation and viability (Roche Applied Bioscience, Mannheim, Germany). Cells were plated in 200 μ l of medium at a concentration of 5×10^3

cells per well in 96-well microtiter plates (tissue culture grade, Falcon) and MTT cell viability was performed according to manufacturer's protocol. GraphPad Prism 4 software (GraphPad Software Inc., San Diego, CA) was used for statistical analysis. Comparisons of two groups were conducted using paired two-tailed t-test. A one-way ANOVA test was performed for comparisons among multiple groups, and statistical significance was set at $p < 0.05$. All assays were performed using at least three separate experiments in triplicate, and data were expressed as mean \pm SD in comparison to untreated cells (controls).

2.3.9 Ca²⁺ measurements

Imaging of intracellular free Ca²⁺

Cells grown on cover slides were incubated with 2.5 mM probenecid (an inhibitor of organic ion transport by blocking multidrug resistance-associated proteins) for 30 min at 37 °C in standard medium. Loading of cells with fura-2/AM (Invitrogen) was performed according to Vamvakas et al. (Vamvakas & Anders, 1990) in 3 ml standard medium for cover slides in four well plates respectively, both containing fura-2/AM in a final concentration of 8 μ M, 2.5 mM probenecid and 1:1000 Pluronic® F-127. After loading the cells for 1 h at room temperature, the samples were washed two times with standard medium containing 2.5 mM probenecid to prevent leakage of fluorescent dye. Subsequently, cells were allowed to incubate for 30 min at room temperature to deesterify fura-2/AM dye. The cover slides were removed from the well plates and imaging was carried out at 37 °C on the stage of an inverted microscope (Zeiss, Oberkochen) equipped for epifluorescence with objectives ranging from magnifications of 10 \times to 100 \times with oil-immersion.

Measurement of intracellular free Ca²⁺ with FlexStation

Measurement of free Ca²⁺ was also made with a fluorescence microplate reader (FlexStation, Molecular devices). Cells were plated in 200 µl of medium at a concentration of 5×10³ cells per well in 96-well microtiter plates (tissue culture grade, Falcon). Fura-2/AM was loaded as described above. Fura-2/AM fluorescence was measured by illuminating the cells with an alternating 340/380 nm light every 5 s. Fluorescence intensity was measured at 510 nm. Automated pipette was settled for the addition of 45 ml of thapsigargin to remove extracellular Ca²⁺. Changes in intracellular Ca²⁺ concentration are presented as the change in the ratio of fluorescence intensity for excitation at 340 and 380 nm.

2.3.10 Quantitative real-time PCR

Short-term stress dependent CALR mRNA expression levels were determined by quantitative real-time PCR. Briefly, total RNA was isolated from TALH-STD and TALH-NaCl cells exposed for different times to NaCl stress with the column-based RNeasy Mini Kit (Qiagen, Hilden) according to the manufacturer's protocol. RNA was transcribed using the SuperScriptTM II RNase H-Reverse Transcriptase Kit. PCR was performed with a PCR kit (Invitrogen) according to the manufacturer's directions. Primer sequences were as follows:

Rabbit-CALR forward, 5'-GAA ATC GAC AAC CCC GAG TA-3'; reverse, 5'-CCT CGT CCT GCT TGT CTT TC-3' (MWG Biotech, Ebersberg D). Quantitative real-time PCR was carried out on an Mx3000P PCR system (Stratagene, Amsterdam). Reaction conditions were adopted according to Hsu et al. (Hsu et al. 2005).

2.3.11 Construction of CALR expression and CALR siRNA vectors and cellular transfection

The construction procedure of wild type (WT-CALR), mutant without the Ca²⁺ binding C-domain (Δ CALR) and CALR siRNA vectors has been provided in detail in supplementary

data. All constructs were verified by sequencing. The transfection was performed using transfection reagent Lipofectamine 2000TM (Invitrogen) according to manufacturer's standard protocol. In brief, 2 µg of plasmids and 8 µl of Lipofectamine 2000TM were added to 100 µl OptiMEM (Gibco). The mixture was gently mixed, incubated at room temperature for 20 min, and then added drop-wise to TALH cells cultured to approximately 80% confluence in 100-mm plates. The analysis of the transfection was carried out after three days of incubation. After 24 h, transfection media was changed with selection media for stable transfection. Cells were maintained in the selection medium for 14 days to achieve stable transfection and assessed for CALR expression by Western blot and immunofluorescence staining.

2.3.12 Indirect immunofluorescence staining

For the indirect immunofluorescence staining 10×10³ cells from each TALH-STD and TALH-NaCl were cultivated overnight in 16-well chamber slides. The medium was removed and the cells were washed twice with PBS-buffer. Fixation of the cells was carried out for 30 min at -20 °C with methanol/acetone (1:1, v/v). The fixed cells were blocked with 1:5 normal goat serum (DAKO)/PBSbuffer for 1 h and incubated with primary antibodies overnight.

Alexa Fluor labeled goat anti-rabbit antibody was used as secondary antibodies. The incubation was performed for 60 min at room temperature in the dark. Thereafter the samples were counterstained with DAPI in mounting medium. Afterwards samples were analyzed with immunofluorescence microscopy (Carl Zeiss Axiovert S100TV).

2.3.13 Antibodies

Rabbit anti-Erp72 polyclonal antibody was from Stressgen, mouse anti-β-actin monoclonal antibody and rabbit anti- GRP78/BiP polyclonal antibody were from Sigma, mouse anti-CALR monoclonal antibody was from BD Bioscience. Anti-CALR was purified from rat liver

according the procedure of Nguyen Van and Soling (Nguyen Van, 1989). Alexa Fluor dye conjugated to secondary anti-rabbit antibody and Alexa dye conjugated to secondary anti-mouse antibody were from Molecular Probes. Anti-flag antibody was from Sigma.

2.4 Results

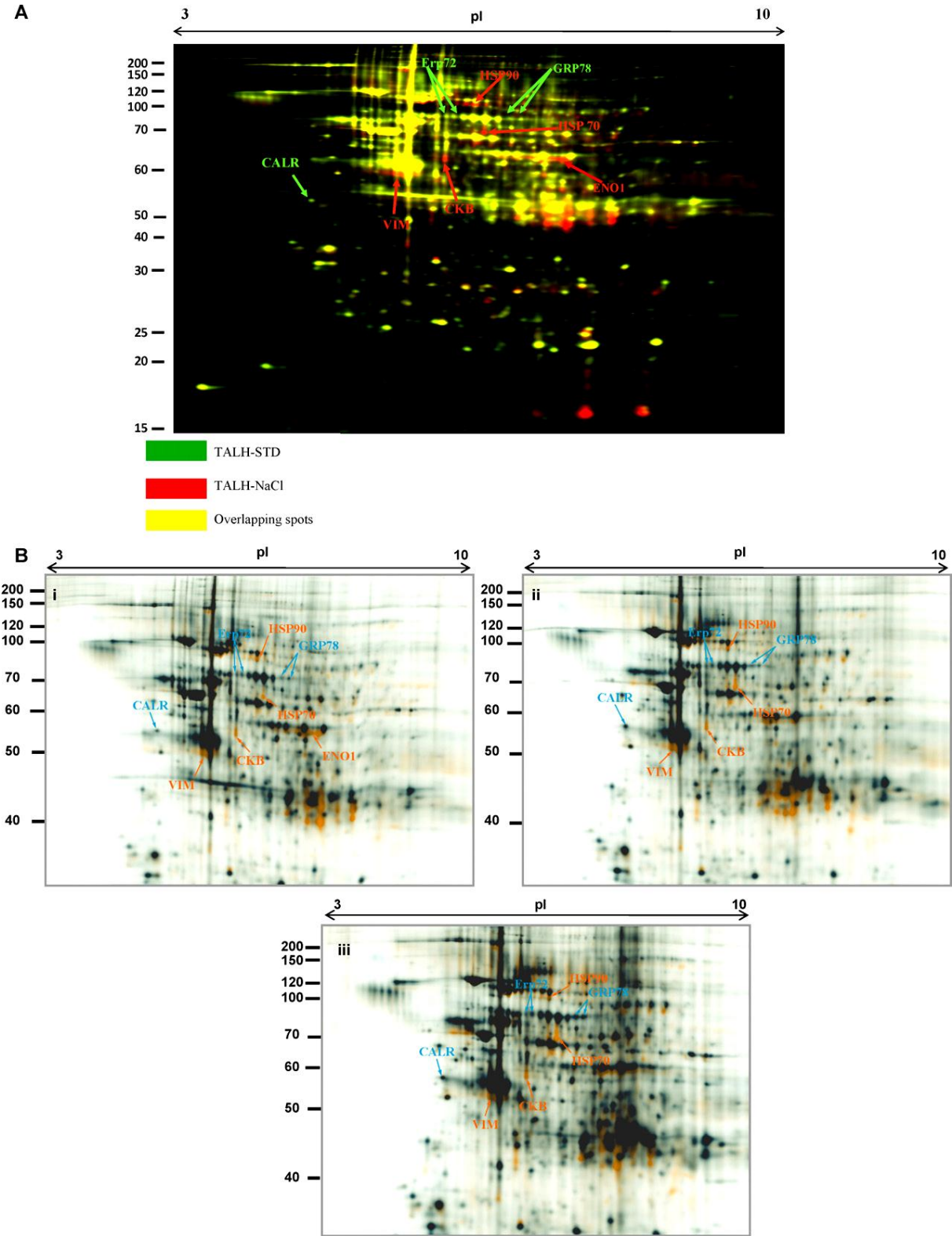
2.4.1 ER Ca²⁺ binding proteins and osmotic stress

In order to understand the molecular mechanism of TALH cells adaptation and survival under osmotic stress, cell extracts were prepared from TALH-STD and TALH-NaCl cells. The protein extracts were subjected to DIGE analysis. The 2D DIGE images were analyzed with the Delta2D software (Decodon); interesting protein spots were excised and analyzed by mass spectrometry. The proteins were identified using MASCOT Database. 2D DIGE coupled with mass spectrometry analysis showed that many proteins were differently expressed in the stressed TALH-NaCl cells compared to TALH-STD cells. Among these differentially expressed proteins, a group of ER resident proteins, GRP78, Erp72 and especially CALR, were downregulated in TALH-NaCl cells as reaction on hyperosmotic stress. In contrast, other ER stress proteins like the heat shock proteins, HSP 70 and HSP 90 were found to be upregulated (Figure 2.1A) (Table 2.1).

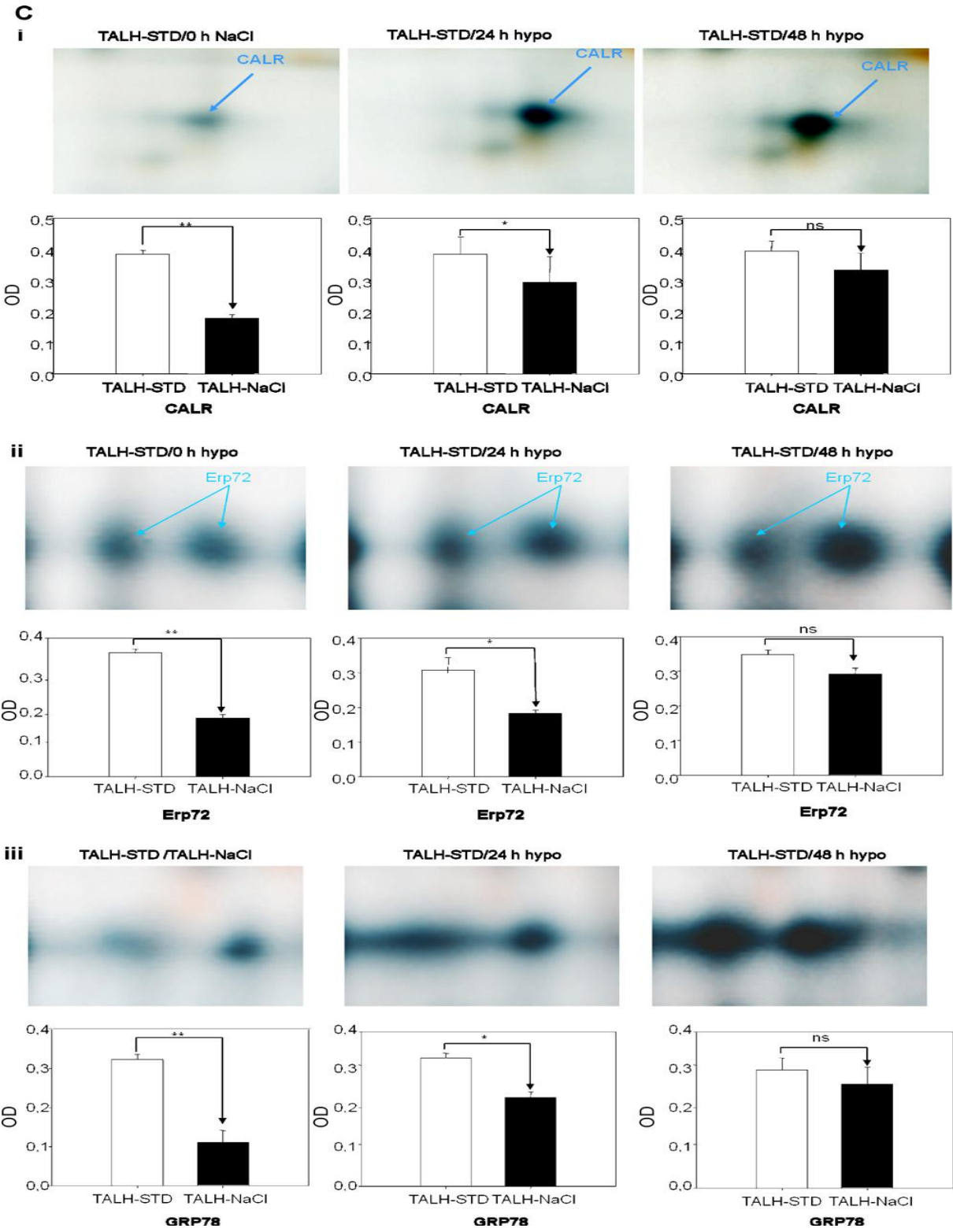
In order to further investigate the effects of osmolality changes on the expression of these proteins in TALH cells, TALH-NaCl cells were exposed to hypoosmotic stress by culturing the cells back in isoosmotic medium (300 mosmol/kg). To assess the time dependent effect of osmolality changes on protein expression the cell were harvested after 24 and 48 h upon incubation in hypoosmotic medium. The protein extract were subjected to 2D DIGE analysis. TALH-STD was used as a control (Figure 2.1B). Quantitative analysis of the protein spots

revealed that the expression of CALR, GRP78 and Erp72 increased progressively after the transfer of the TALH-NaCl cells to isoosmotic medium and achieves the level of the proteins in TALH-STD after 48 h of incubation (Figure 2.1C).

Calreticulin is crucial for Ca²⁺ homeostasis mediated adaptation and survival of thick ascending limb of Henle's loop cells under osmotic stress



Calreticulin is crucial for Ca²⁺ homeostasis mediated adaptation and survival of thick ascending limb of Henle's loop cells under osmotic stress



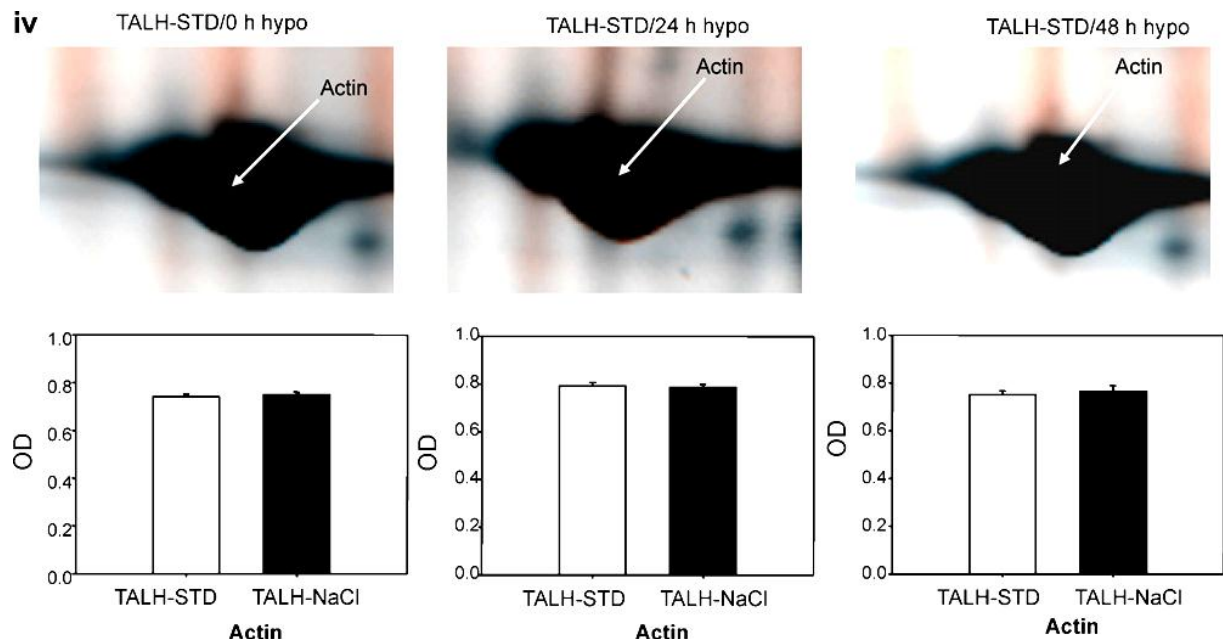


Figure 2.1: 2D gel electrophoresis expression of differentially regulated proteins under osmotic stress conditions.

(A) Downregulation of ER Ca²⁺ binding proteins under hyperosmotic stress conditions: dual color 2-D DIGE images of proteins extracted from TALH-STD control and TALH-NaCl cells. Cy3-labeled proteins are shown in green color (TALH-STD) and Cy5-labeled proteins are in red color (TALH-NaCl), whereas protein spots in yellow color are present in both samples. (B) 2D DIGE proteome analysis of the TALH-STD and TALH-NaCl cultured in hypoosmotic medium in a time dependent manner for 0 h (i), 24 h (ii) and 48 h (iii). Cy3 labeled proteins are false colored in blue (TALH-STD) and Cy5 labeled proteins are false colored in orange (TALH-NaCl). (C) Enlargement of the gel regions of interest showing protein spots found to be differentially expressed: (i) CALR, (ii) Erp72, (iii) GRP78 and (iv) ACTB (β -actin). The protein expression quantification for selected proteins is given in form of bar diagrams. Expression of the same protein was quantified under different hypo-osmotic conditions shown in the form of black bar while control is shown in the form of white bar. Results are given as the means \pm SD from three independent DIGE experiments.

To validate the data obtained from 2D DIGE and protein identification, we confirmed the regulation profiles of the three differentially expressed key proteins by Western blot, namely CALR, GRP78 and Erp72. The Western blot analysis showed a downregulation of these proteins when TALH-STD cells were transferred to hyperosmotic NaCl medium in a time

dependent manner from 12 to 72 h (Figure 2.2A). In contrast, the TALH-NaCl cells showed an upregulation of these proteins when they were cultured back to hypoosmotic standard medium in a time dependent manner from 12 to 72 h (Figure 2.2B). To compare the results obtained with TALH cells under hyperosmotic stress, similar experiments were performed with IMCD and IC primary cells, which were isolated from rat kidney. After three passages of cell culture, the cells were subjected to NaCl stress for 72 h and samples were collected for Western blot analysis. In contrast to TALH cells, IMCD and IC cells showed that CALR expression was not affected with osmotic stress in both cell types. Whereas Erp72 was found to be upregulated in IMCD cells, IC cells showed no regulation of Erp72 under hyperosmotic stress (Figure 2.2C).

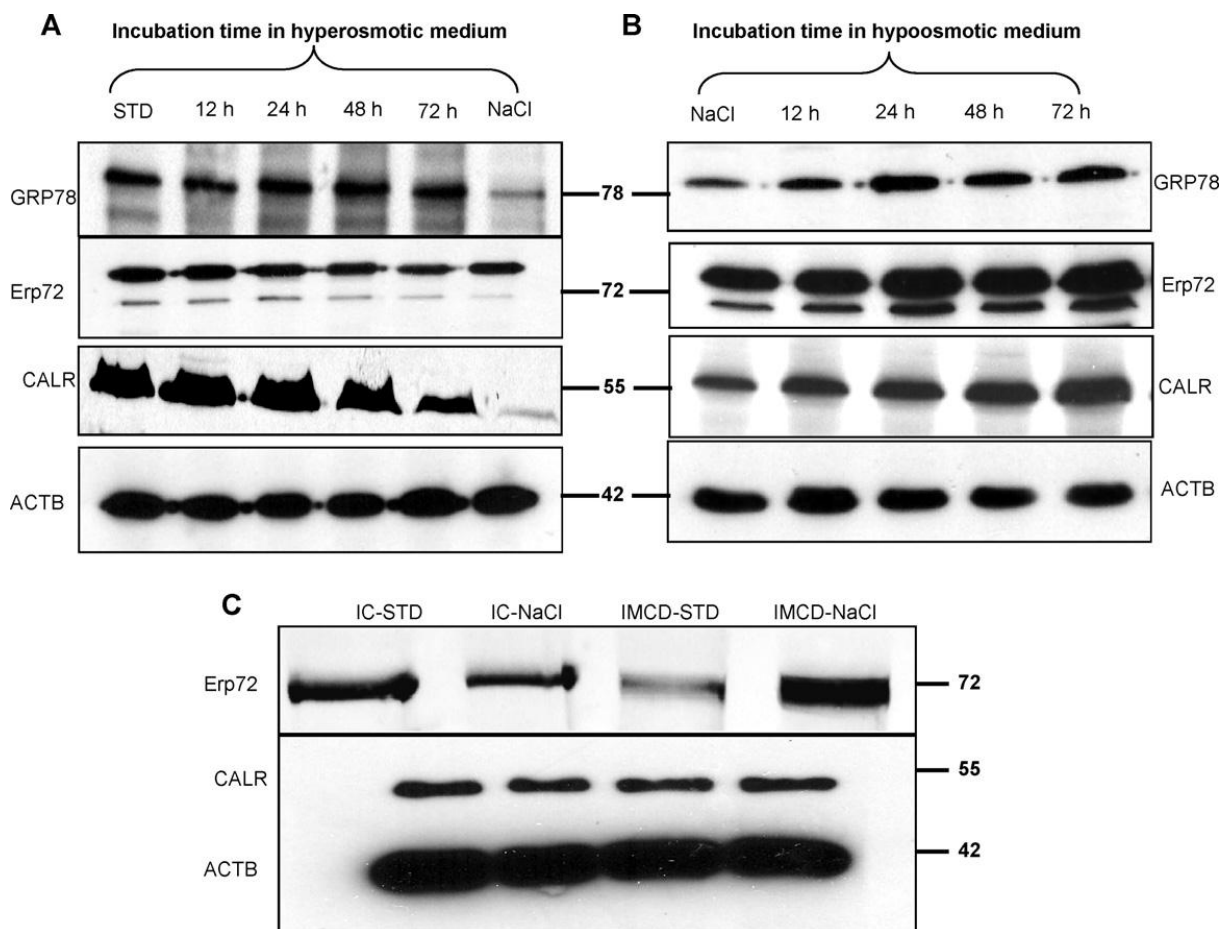


Figure 2.2: Time dependent expression changes of ER Ca²⁺ binding proteins under varied osmotic stress conditions.

Western blot analysis of ER Ca²⁺ binding proteins (CALR, Erp72 and GRP78) found to be differentially expressed in time dependent manner under osmotic stress. Protein expression was investigated with respective antibodies for CALR, Erp72 and GRP78, while ACTB was kept as control: (A) TALH-STD cells cultivated in hyper-osmotic stress of NaCl for 24, 48 and 72 h. (B) TALH-NaCl cells cultivated back to hypo-osmotic medium for 24, 48 and 72 h. (C) IC and IMCD kidney cells under control and exposed to NaCl stress for 72 h.

To further characterize the role of the downregulation of these proteins for the TALH cell survival under hyperosmotic stress, we investigated the impact of upregulation of these proteins on cells subjected to osmotic stress. As expected TALH cell treated with TM resulted in ER-stress reflected in upregulation of CALR, GRP78 and Erp72. Cells exposed to a combination of tunicamycin and hyperosmotic stress showed a downregulation of the three

investigated proteins (Figure 2.3A) accompanied by a significant increase in cell death revealed by the cell viability assay (Figure 2.3B).

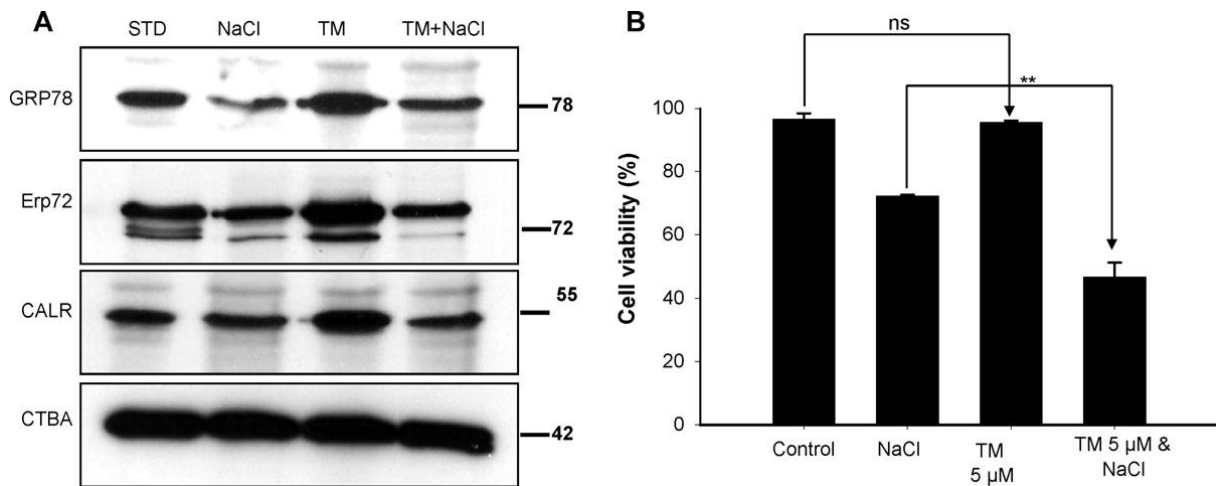


Figure 2.3: Impact of hyperosmotic stress on expression of ER Ca²⁺ binding proteins under TM (5µg/ml) induced ER stress

(A) Western blot analysis of the expression changes of CALR, GRP78 and Erp72 in TALH-STD cells treated with TM and exposed to NaCl stress for 72 h. ACTB was kept as control. (B) MTT cell viability assay, 5000 cells/well were cultured in 96 well cell culture plates, incubated with NaCl stress or 5µM TM or both for 72 h. The cell viability was measured and plotted in the form of bar diagrams with the cell treatment on x-axis and cell viability on y-axis. TM: tunicamycin ns, non significant and ** shows significance.

2.4.2 CALR and Ca²⁺ homeostasis under osmotic stress

To investigate the impact of stress on Ca²⁺ store in ER, TALH cells growing in isoosmotic medium were transferred in hyperosmotic environment and the ER- Ca²⁺ release was monitored using fura-2/AM fluorescence dye, fluorescence microscopy and AnalySIS software. 10 min after stress application, a significant increase in ER- Ca²⁺ release could be detected (Figure 2.4A). A time dependent increase of Ca²⁺ release could be observed: the Ca²⁺ release was 1.6-fold higher after 20 min and 1.8 after 30 min of incubation in hyperosmotic medium when compared to the cell in isoosmotic one (Figure 2.4B). Parallel to Ca²⁺ imaging, RT-PCR was carried out for CALR. The increase in CALR threshold cycles (CT) confirmed

an alteration in CALR-expression under osmotic stress. Parallel to the increase in Ca^{2+} release, a time dependent downregulation of CALR could be measured (Figure 2.4C). RT-PCR analysis of CALR expression from TALH cells treated with thapsigargin and exposed to hyperosmotic stress revealed an upregulation of CALR in the first 50 min as showed by a diminution in CT, while this decrease was stabilized afterwards. The decrease in CT value reflects the upregulation of CALR after thapsigargin treatment in contrast to downregulation of CALR when exposed to NaCl stress (Figure 2.4D). As reaction on Ca^{2+} loss upon thapsigargin treatment, the cells increase the expression of CALR to prevent excessive attenuation in Ca^{2+} and to rescue the homeostasis.

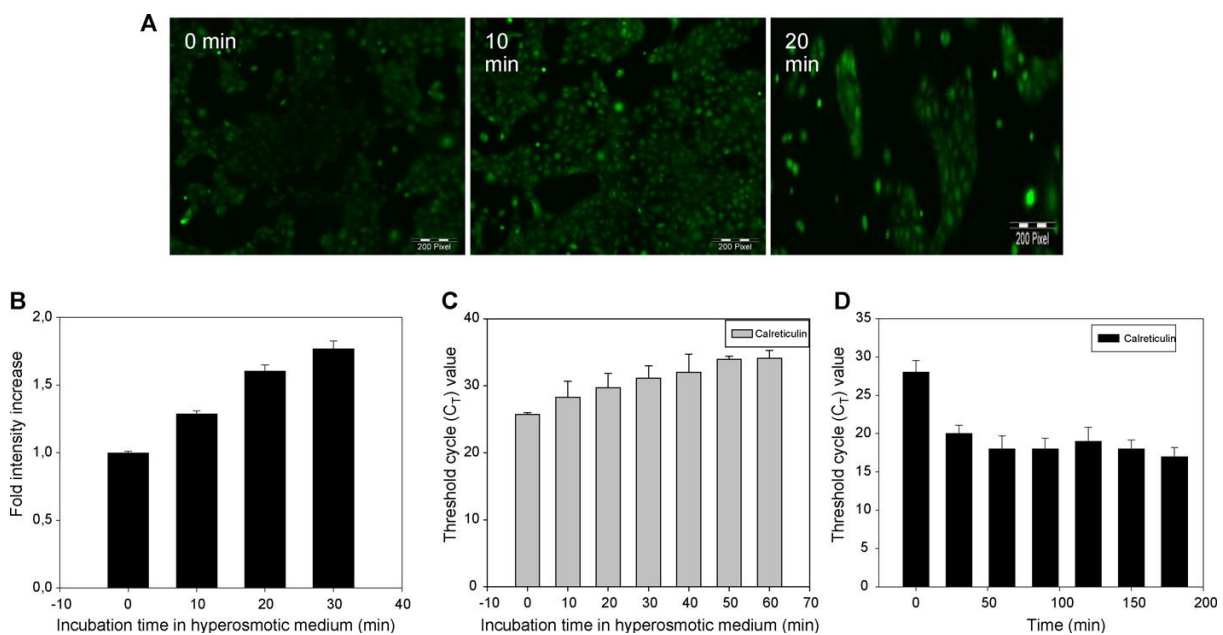


Figure 2.4: Time dependent increase of free Ca^{2+} in TALH cells exposed to hyperosmotic stress.

(A) Control cells in isoosmotic medium (STD), and cells exposed to NaCl stress for 10 and 20 min. (B) Quantitative analysis of fluorescence intensity in fura-2/AM-stained TALH cells after osmotic stress treatment. Results are given as the means \pm SD from three independent experiments. (C) Quantitative real-time PCR for the mRNA of CALR in TALH cells from 0 to 70min in NaCl stress. (D) Real-time PCR analysis of CALR

expression in TALH cells treated with 0.3 μ M TG. The bar diagram showed the CALR mRNA in the form of CT value on y-axis while time is plotted on x-axis. TG: thapsigargin.

To investigate the impact of Ca²⁺ release inhibition on ER Ca²⁺ binding protein expression and cell viability under osmotic stress, TALH cell treated with 25 μ M heparin, to block the IP3R mediated Ca²⁺ release, were exposed to hyperosmotic stress with NaCl. Cells treated with heparin alone showed no pronounced effect on the expression of CALR. In contrast, we could demonstrate a significant downregulation of GRP78 and Erp72 in TALH cells under NaCl stress with and without heparin treatment (Figure 2.5A). In comparison CALR was only downregulated in TALH cells under NaCl stress without heparin. Cells treated with heparin or heparin combined with NaCl stress showed no significant effect on CALR expression (Figure 2.5A). To determine the effect of alteration of Ca²⁺ traffic combined with osmotic stress on cell viability and proliferation, MTT test was carried out with TALH cells exposed to different conditions of heparin treatment with and without NaCl stress. The cell viability assay revealed a significant increase in cell death of heparin treated cells upon exposition to NaCl stress compared to NaCl or heparin treatment separately (Figure 2.5B).

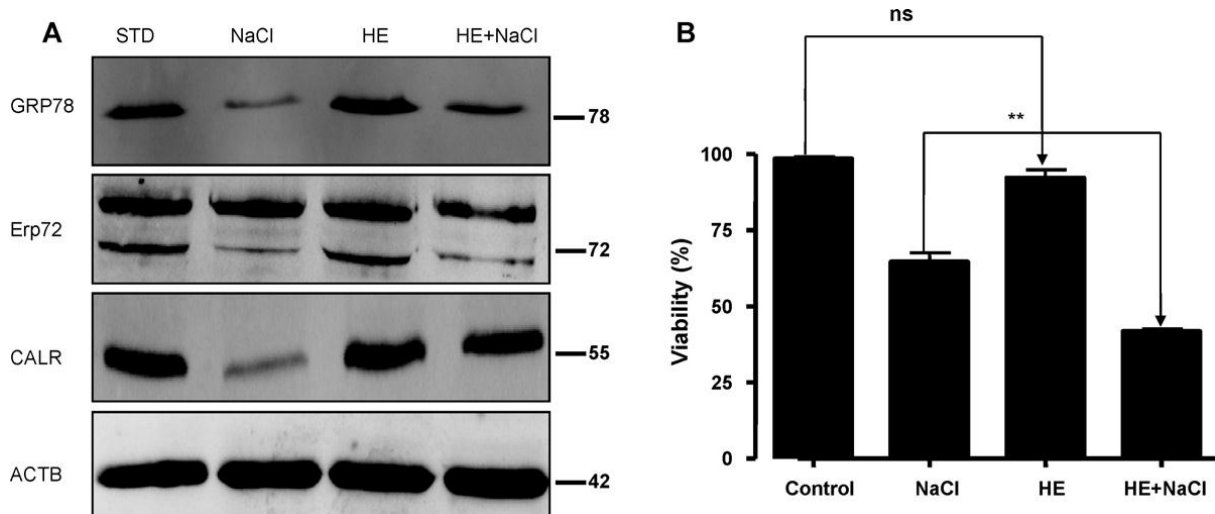


Figure 2.5: Impact of HE and hyperosmotic stress on expression of proteins and cell viability in TALH cells.

(A) Western blot analysis of the TALH-STD cells treated with HE and exposed to NaCl stress for 72 h compared to untreated control cells for the expression of CALR, Erp72, and GRP78 while ACTB was kept as control. (B) MTT cell viability assay, 5000 cells/well cultured in 96 well cell culture plates, incubated with NaCl stress or 25µM heparin or both. The cell viability (%) was measured from values obtained from the assay and plotted in form of bar diagrams with the cell treatment on x-axis and cell viability on y-axis. HE: heparin.

2.4.3 CALR and cell death under osmotic stress

CALR is an ER- Ca²⁺ binding protein, to investigate the impact of CALR due to its Ca²⁺ binding capacity on cell adaptation and survival in hyperosmotic stress, vectors expressing WT-CALR and ΔCALR (mutant without the Ca²⁺ binding site) were constructed and transfected into TALH cells separately. Intracellular localization of CALR and ΔCALR was examined by indirect immunofluorescence staining. As shown in Figure 2.6A, CALR showed a perinuclear reticular pattern in all cases, including the control and gene-transfected cells, although the signal intensity was increased in the transfectants compared to the control cells. Moreover, the Figure 2.6A also shows the transfection efficiency analyzed with anti-flag antibody against the flagged CALR transfected cells. To assess whether the increase in CALR expression interfered with ER Ca²⁺ storing capacity and Ca²⁺ homeostasis, we measured the free intracellular Ca²⁺ in cells transfected with WT-CALR and ΔCALR compared with control TALH cells. FlexStation and imaging analyses showed almost same basal levels of free intracellular Ca²⁺ in both WT-CALR and ΔCALR transfected cells. However thapsigargin induced a significant increase in free intracellular Ca²⁺ in cells overexpressing WT-CALR compared to ΔCALR and control, whereas the difference between ΔCALR and control was not significant (Figure 2.6B, Supplemental Figure 2.1). These results revealed the higher Ca²⁺ storing capacity of WT-CALR compared to ΔCALR and that the Ca²⁺ buffering capacity of the cells is directly correlated to CALR level in ER. The cell viability assay was

performed with WT-CALR and Δ CALR transfected cells exposed to hyperosmotic NaCl stress compared to non-transfected control cells. We observed a significant decrease in cell viability (%) in cells overexpressing WT-CALR under NaCl stress conditions compared to control non-stressed conditions. Moreover these cells also showed significant increase in cell death compared to cells over-expressing Δ CALR with no Ca²⁺ binding region (almost 70%) and non-transfected cells exposed to NaCl stress (almost 70%) (Figure 6C).

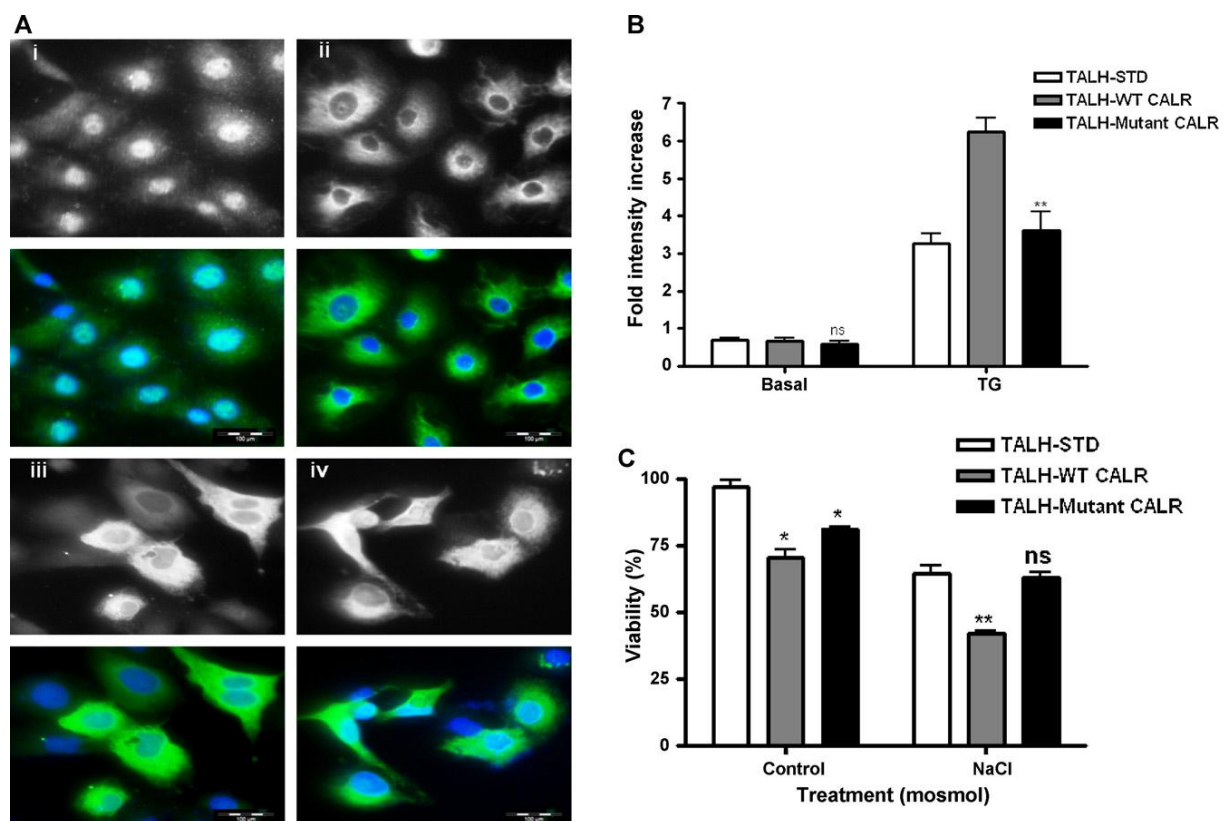


Figure 2.6: Effect of overexpression of CALR on cell viability of TALH cells under hyperosmotic stress.

(A) Immunolocalization of transfected and endogenous CALR in TALH cells. (i) Endogenous CALR. (ii) Transfected CALR with anti-flag antibody. (iii) Transfected WT-CALR. (iv) Transfected mutant CALR (Δ CALR). (B) Quantitative analysis of free Ca²⁺ using FlexStation in cells overexpressing WT-CALR and Δ CALR. Transfected cells were loaded with fura-2/AM dye. Free Ca²⁺ was measured in terms of fluorescence intensity of fura-2/AM at basal and TG induced levels. Results are given as the means \pm SD from three independent experiments. (C) MTT cell viability assay, TALH cells transfected with WT-CALR and Δ CALR

were cultured to approximately 70% confluence in 96-well culture plates. After 24 h, cells were incubated to hyperosmotic NaCl medium for 72 h and proceeded for MTT cell viability assay. The cells expressing Δ CALR showed significant less cell death compared to cells overexpressing WT-CALR under hyperosmotic stress conditions. Results are given as the means \pm SD from three independent experiments. TG: thapsigargin.

To further evaluate the role of CALR expression in TALH cells under hyperosmotic stress, we knocked down the expression of CALR in TALH cells with siRNA vector. Western blot analysis and immunofluorescence staining showed an efficient reduction in endogenous CALR protein levels compared to control (Figure 2.7A and B). Interestingly, the knockdown of CALR led to significant reduction in cell death under hyperosmotic stress condition compared to control cells under the same conditions (Figure 2.7C).

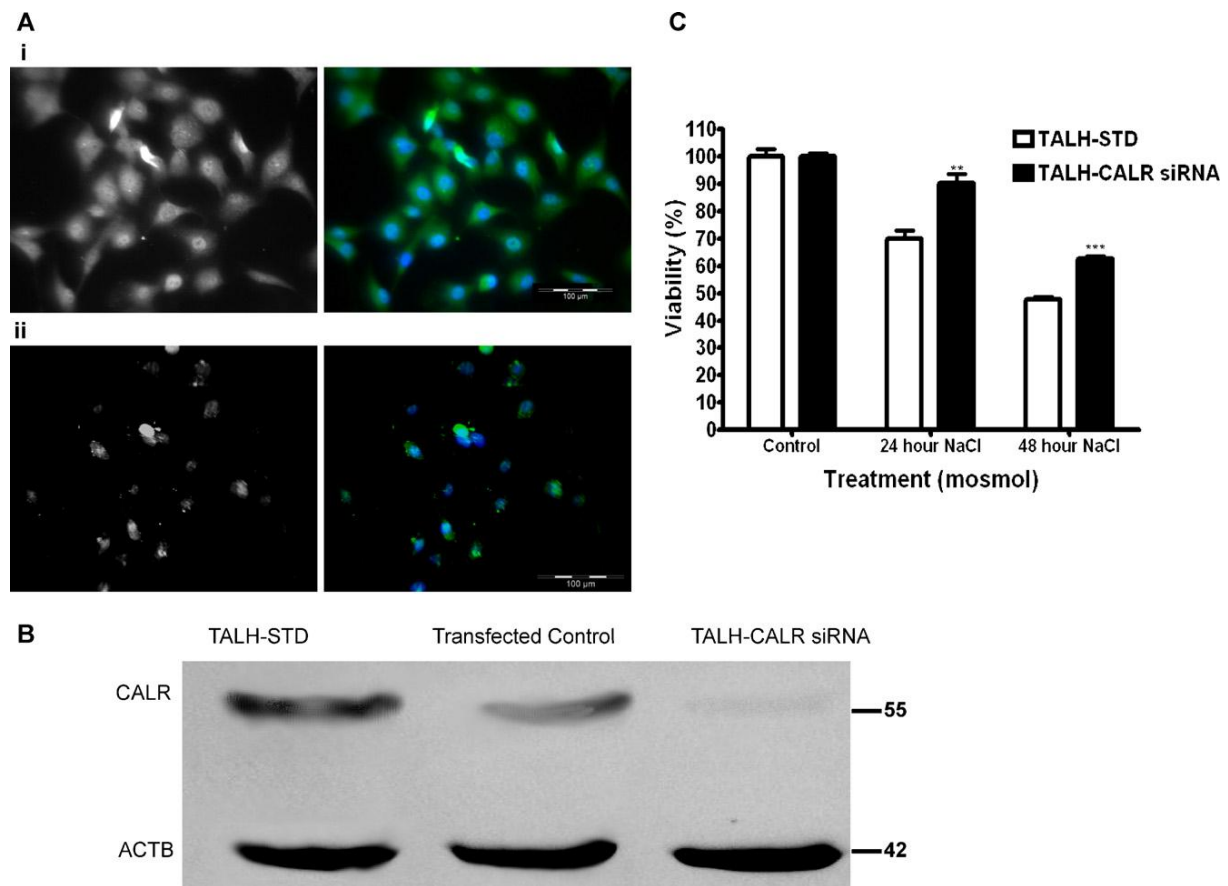


Figure 2.7: Knockdown of CALR enhances the resistance of TALH cells to hyperosmotic NaCl stress.

(A) Immunofluorescence staining of CALR in non-transfected cells (i) and cells transfected with siRNA vector for the knockdown of CALR (ii) showing the knockdown of CALR. (B) Western blot analysis of TALH-STD, cells transfected only with vector (transfected control) and cells transfected with siRNA vector targeting CALR (TALH-CALR siRNA) against CALR antibody showing almost 100% knockdown of CALR in siRNA transfected cells compared to controls. (C) MTT cell viability assay, cell viability assay was performed to assess the effect of knockdown of CALR with siRNA on the viability of TALH cells under hyperosmotic NaCl stress. The cells with CALR knockdown showed significant decrease in cell death after 24 and 48 h NaCl stress compared to TALH cells under NaCl stress as a control. Results are given as the means \pm SD from three independent experiments.

Calreticulin is crucial for Ca²⁺ homeostasis mediated adaptation and survival of thick ascending limb of Henle's loop cells under osmotic stress

Table 2.1: Differentially regulated proteins in TALH-NaCl cells compared to TALH-STD cells.

| Spot | Name of protein | Gene Name | Uniprot Accession | MS/MS Score | Nominal Mass (KDa) | Up/down regulation |
|-------------|----------------------------------|------------------|--------------------------|--------------------|---------------------------|---------------------------|
| | Calreticulin | CALR | P15253 | 215 | 48.274 | ↓ |
| 2 | 78 kDa glucose-regulated protein | GRP78 | P20029 | 325 | 72.422 | ↓ |
| 3 | Protein disulfide isomerase A4 | Erp72 | P08003 | 98 | 71.973 | ↓ |
| 4 | Heat shock protein 70 | Hsp70-1 | Q9MYS2 | 110 | 57.484 | ↑ |
| 5 | Heat shock protein HSP 90-alpha | HSP90AA1 | P30946 | 72 | 46.811 | ↑ |
| 6 | Vimentin | Vim | Q6S5G2 | 144 | 68.946 | ↑ |
| 7 | Alpha-enolase | Eno1 | P17182 | 165 | 47.140 | ↑ |
| 8 | Creatine kinase B-type | Ckb | Q04447 | 85 | 42.713 | ↑ |

2.5 Discussion

In recent years, CALR was described to play a role in many biological systems, including functions outside the ER, indicating that the protein is a multi-process molecule. Regulation of Ca²⁺ homeostasis and ER Ca²⁺ buffering by CALR might be the key for the explanation of its multi-process property. CALR due to its chaperon function is generally induced as a stress response protein to correct misfolded proteins. In proteomic analysis of cellular response to osmotic stress in TALH cells, Dihazi et al. described the downregulation of CALR under hyperosmotic stress as part of the osmotic stress resistant in kidney cells (Dihazi et al, 2005). In contrast to TALH cells, IMCD cells and IC of kidney showed no regulation under hyperosmotic stress conditions. Furthermore renal fibroblast cell lines subjected to hyperosmotic stress showed a significant upregulation of ER-stress proteins, e.g. CALR, GRP78 and Erp72 (Dihazi et al, 2011). This revealed a TALH cells specific role of CALR downregulation. In the present study, we investigated the role of downregulation of CALR in TALH cells adaptation to osmotic stress. Reversible regulation of CALR in TALH-NaCl under hypoosmotic stress conditions showed that the downregulation of the protein is a part of the cell resistance to osmotic stress. Furthermore, TM treatment of TALH cells strengthens our theory of the non-chaperon function of CALR under osmotic stress conditions. TM is an antibiotic that inhibits N-linked glycosylation of proteins leading to accumulation of misfolded proteins in the endoplasmic reticulum. Incorrect folding of proteins in the ER causes ER stress and upregulation of ER stress proteins, e.g. CALR and GRP78 (Elbein, 1987). Upregulation of CALR under TM treatment did not have any significant impact on cell viability, whereas TM treatment combined with hyperosmotic stress which resulted in significant reduction in the cell viability. CALR is one of the major Ca²⁺ buffering chaperones

in the endoplasmic reticulum. It plays a critical role in Ca²⁺ signaling in the endoplasmic reticulum lumen and has significant impacts on many Ca²⁺ dependent pathways (Coe & Michalak, 2009). CALR is involved in regulation of intracellular Ca²⁺ homeostasis and ER Ca²⁺ capacity. Regulation of Ca²⁺ homeostasis and ER Ca²⁺ buffering by CALR might be the key to explain its multiprocess properties (Coe & Michalak, 2009; Fliegel et al, 1989; Nakamura et al, 2001; Treves et al, 1990). Time dependent increase in the intensity of free intracellular Ca²⁺ coupled with continuous decrease of mRNA levels of CALR under NaCl stress revealed that CALR expression is interconnected with Ca²⁺ homeostasis. Our results suggested that the unusual downregulation of a protein with chaperon function under stress condition is necessary to free Ca²⁺ from ER store and to increase cytosolic Ca²⁺ levels to inhibit the excessive NaCl transport across the plasma membrane. Despite the increased free Ca²⁺ ions, it does not elicit cell death directly like excessive Na⁺, which may damage cells by direct osmotic effects (Nicotera & Orrenius, 1998) . Further, a recent study on murine renal epithelial cells showed that Ca²⁺ inhibits the Na⁺ transport (Sugawara et al, 1993) and changes in cytosolic Ca²⁺ levels play a critical role in the regulation of transepithelial sodium transport. This suggest the involvement of a process of coupled Na⁺/Ca²⁺ exchange across the plasmamembrane by the sodium gradient (Friedman et al, 1981; Taylor & Windhager, 1979). Therefore, it is possible that cytosolic Ca²⁺ buffering system consisting of mitochondria, endoplasmic reticulum, and Ca²⁺ binding proteins may also play a role in this control system. Inositol 1,4,5-trisphosphate receptor (IP3R) is an intracellular Ca²⁺ release channel on the endoplasmic reticulum of all types of cells and controls via Ca²⁺ mobilization which ultimately attributed to a perturbation in intracellular Ca²⁺, the Ca²⁺ homeostasis (Elbein, 1987; Kottgen et al, 2010; Thastrup et al, 1990). Heparin is an IP3R antagonist and potentially blocks the IP3 mediated release of Ca²⁺ from endoplasmic reticulum (Walensky & Snyder,

1995). Our study revealed that blocking the Ca²⁺ release by IP3R antagonist had no impact on the expression of CALR. In contrast, emptying the ER Ca²⁺ stores by inhibition of SERCA pumps with thapsigargin resulted in upregulation of CALR. This highlights direct correlation between Ca²⁺ signaling and CALR expression alteration. On the other hand, Camacho and Lechleiter reported that CALR expression influence the IP3R mediated Ca²⁺ signaling by inhibiting the repetitive intracellular Ca²⁺ waves in ER (Camacho & Lechleiter, 1995). The fact that heparin significantly increased the cell death under NaCl stress conditions, supported the theory, that downregulation of CALR accompanied with Ca²⁺ signaling regulation is essential for the cell survival under hyperosmotic stress. The further evidence for the involvement of CALR due to its Ca²⁺ storage capacity under osmotic stress was provided by overexpression of WT-CALR and Δ CALR, without the Ca²⁺ binding C-domain in TALH cells. It is evident that overexpression of CALR increases ER Ca²⁺ storage capacity and Ca²⁺ buffering power of the ER lumen with increased intracellular free Ca²⁺ on induction (Xu et al., 2000; Bastianutto et al., 1995; Mery et al., 1996). The C-domain of CALR is a highly acidic region that binds 20–50 mol of Ca²⁺ per mole of protein and has been shown to be the major site of Ca²⁺ storage within the endoplasmic reticulum. The work done on the expression of the high capacity Ca²⁺-binding domain of CALR suggested that ectopic expression of the CALR C-domain increases Ca²⁺ stores (Wyatt et al, 2002). Cells overexpressing WT-CALR binds Ca²⁺ and prevents the Ca²⁺ release from ER to cytosol when exposed to NaCl. In contrast, cells overexpressing Δ CALR cannot bind efficiently Ca²⁺ resulting in increased release of Ca²⁺ from ER under NaCl stress conditions. This allowed a faster adaptation to hyperosmotic stress conditions. Similar effects were described on *Xenopus* oocytes by Xu et al. that deletion mutant with an increase in intracellular free Ca²⁺, requires the CALR high capacity Ca²⁺-binding domain to reduce the elevations of Ca²⁺ ions due to Ca²⁺ influx (Xu et

al, 2000). Moreover, knockdown of CALR with siRNA showed no significant impact of hyperosmotic stress on cell viability compared to control. Increased osmotic stress resistance in cells expressing Δ CALR or in siRNA CALR knockdown cells confirmed the role of CALR in cell survival under NaCl stress. Taken together, the results directly support the notion that CALR plays a crucial role in the adaptation and survival of TALH cells under hyperosmotic NaCl stress conditions due to its Ca²⁺ binding and storage capacity. The presented data are good basis for *in vivo* studies to highlight the role of CALR and Ca²⁺ signaling in the onset and progression of kidney diseases.

3. REDUCED CALRETICULIN LEVEL RESULTS IN OXIDATIVE STRESS MEDIATED MITOCHONDRIAL DAMAGE AND KIDNEY INJURY

Asima Bibi, Hassan Dihazi

3.1 Abstract

Calreticulin (Calr) is an important endoplasmic reticulum resident calcium binding protein. Recently, our work showed that calreticulin expression alteration is involved in the functioning of renal cells coupled with disturbances in Ca^{2+} homeostasis. The aim of the present study was to investigate if there is any critical role of Calr level in the renal function and in onset and progression of kidney diseases. The chronic physiological low level of Calr was achieved by using heterozygote Calr mice ($\text{Calr}^{+/-}$). Histological analysis illustrated that low expression of Calr caused progressive renal injury in $\text{Calr}^{+/-}$ mice as evidenced by an age-dependent development of the glomerulosclerosis and tubulointerstitial damage. Upregulation of the cytosolic calcium buffering proteins with almost no significant change in ER stress proteins was observed in the kidneys of 40 wk old $\text{Calr}^{+/-}$ mice, ruling out ER stress and suggesting disturbance of intracellular calcium homeostasis as a causal factor for the renal injury. Further proteomic analysis revealed expression alterations in proteins associated with oxidative stress, energy production and mitochondrial damage. Here, especially the significant downregulation of Sod1 coupled with irregular, aggregated immunohistochemical expression could only be observed in the kidneys of heterozygote mice. High magnification electron microscopy analysis displayed the enlarged, swollen and vacuolated mitochondria confirming the mitochondrial damage in $\text{Calr}^{+/-}$ mice kidneys. Decrease in activity of cytochrome c oxidase in isolated intact mitochondria further confirmed the impairments of mitochondria and energy metabolism in $\text{Calr}^{+/-}$ kidneys.

Consequently, our findings suggest that chronic low level of Calr results in downregulation of Sod1 accompanied with increase in oxidative stress and mitochondrial damage. This plays an aggravating role in the progression of renal injury throughout chronic kidney disease.

3.2 Introduction

Chronic kidney disease (CKD) is becoming a major public health problem worldwide affecting 7.2% of the global adult population (Zhang & Rothenbacher, 2008). Despite the start, most renal diseases eventually converge into common histopathological impairments such as glomerulosclerosis and tubulointerstitial fibrosis leading to progressive functional deterioration of renal system (Meguid El Nahas & Bello, 2005). In the last few decades, progression of the disease process is well documented. Much interest has focused on investigating potential mechanisms to prevent or reverse the damage. However, the intracellular mechanisms responsible for renal disease initiation leading to complete damage are mostly not well understood. Accumulating evidence from focus on the molecular and cellular mechanisms of CKD, including our previous studies, revealed a pathophysiologic involvement of ER, especially ER Ca^{2+} binding proteins in renal disease progression (Bibi et al, 2011; Dihazi et al, 2011; Eltoweissy et al, 2011; Lindenmeyer et al, 2008; Yoshida, 2007). Therefore, ER Ca^{2+} binding proteins have become an area of interest to understand the possible links in renal disease initiation and progression. In the present study, we will focus on one of the major Ca^{2+} binding proteins, calreticulin (Calr), and its potential role in the progression of kidney injury.

Calr is an ubiquitously expressed ER resident Ca^{2+} binding chaperon. Biochemical and structural studies have demonstrated three distinct structural and functional domains of Calr; the amino-terminal lectin binding N-domain for chaperone function of the protein, the middle proline rich P-domain assisting in both Ca^{2+} storage and chaperone activity, and the carboxyl-terminal, highly acidic Ca^{2+} binding and storing C-domain followed by an ER retention/retrieval signal on C-terminal (Fliegel et al, 1989; Kottgen et al, 2010; Mesaeli et al, 1999). Within ER, Calr plays two important functions; as a chaperon in ER quality control

and binding to high concentration of ER luminal Ca^{2+} in ER Ca^{2+} storage and buffering. Consistent with Ca^{2+} storing property, expression (up or down) studies of Calr show direct correlation of Calr expression with ER Ca^{2+} storage capacity (Bastianutto et al, 1995; Bibi et al, 2011; Martin et al, 2006; Michalak et al, 1999; Opas et al, 1996) . In addition to storage of Ca^{2+} , Calr is also known to modulate Ca^{2+} signalling and homeostasis through store operated Ca^{2+} influx from plasma membrane. It interacts with Ca^{2+} entry and exit channels SERCA and IP3R and modulates Ca^{2+} influx by controlling the extent of inositol 1,4,5-trisphosphate-induced Ca^{2+} store depletion (Mery et al, 1996; Michalak et al, 2002; Xu et al, 2000).

A major breakthrough in Calr research was made in 1999, when Mesaeli et al. showed that Calr deficiency in mice is lethal and homozygote animals mostly die between E12/E15 due to impaired heart development (Michalak et al, 1999). Further studies showed development of cardiomyopathy, exencephaly, and omphalocele in Calr deficient mice. Calr is also stated to perform an anti-oxidative role in protecting human type II alveolar epithelial cells against hypoxic injury (Xu et al, 2000). Many extracellular functions of Calr have been reported including roles in immunogenic cell death in cancer, cellular adhesion, cell migration, phagocytosis, inflammation, cell signaling, and enhancing wound healing (Gold et al, 2010). Additionally, we have recently demonstrated that Calr level is playing important role in the functioning and survival of renal cells through Ca^{2+} homeostasis (Bibi et al, 2011).

Since the generation of Calr KO mice in 1999, most of the work has been done at different embryonic stages, whereas viable Calr heterozygotes has not been enough investigated. In the present study, we have focused on the viable Calr heterozygote mice. The aim of the study was to analyze the impact of chronic low level of Calr on kidney structure and function. Results obtained showed a significant effect of low Calr level on the development of kidney injury. Proteomic screening further highlighted the impact of Calr low level, through Sod1

repression mediated oxidative stress induction and mitochondrial damage in the progression of kidney injury.

3.3 Materials and Methods

3.3.1 Animals

Calreticulin heterozygote ($\text{Calr}^{+/-}$) and wild type (WT) littermate mice in identical C57BL/6J genetic backgrounds were obtained from Prof. Marek Michalak, University of Alberta, Edmonton, Alberta, Canada. Mice were bred under specific-pathogen-free housing conditions and genotyped as previously described in Michalak et al. (Michalak et al, 1999). A total of 25 $\text{Calr}^{+/-}$ and 25 WT mice were sacrificed. For embryonic studies, ages of embryos subject to analysis were given as embryonic day (E). The presence of a copulation plug was defined at E0.5. Embryos were removed from euthanized mothers, analyzed and genotyped at E17.5. To assess morphological and further biochemical analyses of adult kidney, three time points of average age 15, 30 and 40 weeks (wk) were decided. All experimental procedures were performed according to the German animal care and ethics legislation and were approved by the local government authorities.

3.3.2 Morphometric analysis of kidneys

Immediately after cervical dislocation, the freshly excised kidneys from embryos (WT, $\text{Calr}^{+/-}$ and $\text{Calr}^{-/-}$) and adult mice (WT, $\text{Calr}^{+/-}$) were quickly removed, cleaned of surrounding fat, washed in sterile saline solution, and weighed. Kidneys were dissected along sagittal section for macroscopic and microscopic analyses of the renal injury in $\text{Calr}^{+/-}$ mice. The macroscopic differences in $\text{Calr}^{+/-}$ kidneys compared to WT controls were recorded using a Nikon D5000 Camera. Data were recorded from all the 50 mice used in the present study.

3.3.3 Histological analysis of kidneys

Freshly excised embryonic and adult kidneys were immediately fixed overnight in a freshly prepared 5% paraformaldehyde solution. Fixed kidneys were processed for paraffin

embedding and sectioning using standard procedures. 3 µm thick tissue sections were stained with PAS reagent and hematoxylin-eosin, separately for light microscopic examination and histological evaluation. Histological analysis was performed with ImageJ software as described by Rangan and Tesch (Rangan & Tesch, 2007). Briefly, the mean glomerular areas (mGA) of at least 30 glomeruli tuft /animal group were measured. PAS-positive material in each of these glomeruli was quantified and expressed as the mean mesangial area (mMA).

3.3.4 Immunohistological analysis of kidneys

Immunostaining of deparaffinized and rehydrated sections was performed to detect the expression of several proteins. Following antigen retrieval pretreatment in 0.01 M citric acid using Braun Electrical steamer for 25 min, endogenous peroxidase was inactivated with 3% H₂O₂ in PBS for 10 min at room temperature in the dark. Sections were blocked with 10% goat serum in PBS for 1 h and incubated with primary antibodies overnight at 4°C. Primary antibodies were detected with HRP labeled secondary antibody for 1 h at room temperature (GE Healthcare). For negative controls tissue sections were incubated only with the secondary antibody. The detection reaction was developed with 3,3-diaminobenzidine (Sigma) for 10 min at room temperature in the dark. Nuclei were counterstained with hematoxylin before examination. All tissue sections were dehydrated in graded alcohols and xylene and embedded in mounting solution Entellan (Merck).

Some primary antibodies were also detected with fluorescence Alexa 555–conjugated goat anti-rabbit or Alexa 488–conjugated goat anti-mouse secondary antibody (Invitrogen) as recommended. Slides were rinsed and mounted with Vectashield 4,6-diamidino-2-phenylindole (DAPI) (Vector Laboratories) for visualization of nuclei.

3.3.5 Electron microscopy

For ultrastructural electron microscopy, 4mm³ kidney samples were taken from three mice per group, fixed in Karnovsky solution. After dehydration in graded series of ethanol, tissue samples were cleared in propylene oxide, and embedded in epoxy resin as described previously (Girgert et al). Ultrathin sections (70 nm) were prepared (Reichert-Jung Ultracut E; Leica, Wetzlar, Germany) and examined under an electron microscope (LEO 906E; Zeiss, Oberkochen, Germany).

3.3.6 Protein extraction, precipitation and estimation

Kidneys were homogenized in buffer containing Tris-HCl 50 mmol/L (pH 7.4), 1% Triton X-100, 100 mmol/L NaCl and protease inhibitors. After incubation for 30 min at 4°C, kidney tissue homogenates were centrifuged two times at 14,000 rpm for 30 min, and the supernatant was collected. To reduce the salt contamination and to enrich the proteins, protein precipitation was performed. Whole tissue homogenate was precipitated by methanol-chloroform as previously described by (Dihazi et al, 2005). The precipitation eliminates lipids, nucleotides, and salts, which improves the resolution of 2D gel analysis (Gorg et al, 1997). Protein concentration was measured according to Bradford assay (Bradford, 1976), using bovine serum albumin as a standard.

3.3.7 2-D gel electrophoresis (2-DE)

2-D gel electrophoresis (2-DE) analysis of Calr^{+/-} kidneys compared to WT kidneys was performed according to Dihazi et al., 2011. Briefly, a total protein concentration of 150 µg in rehydration buffer (8 M urea, 1% CHAPS, 1% DTT, 0.2% ampholytes, and a trace of bromphenol blue) was loaded on 11-cm IPG strips pH 5-8 from Bio-Rad (Hercules, CA) using passive rehydration at 20 °C. Isoelectric focusing was performed using the Protean IEF cell (Bio-Rad) for 50,000 Vh. After equilibration, IPG strips were loaded on 12% BisTris

Criterion precast gels (Protean Xi, Bio-Rad) and run at 200 V for second dimension separation of proteins.

For image analysis, 2D gels were fixed in a solution containing 50% methanol and 12% acetic acid for 2 h and stained with Flamingo fluorescent gel stain (Bio-Rad, Hercules, CA, USA) for minimum 5 h. After staining, gels were scanned at 50 μ m resolution on a Fuji FLA5100 scanner. The digitalized images were analyzed; spot matching across gels and normalization were performed using Delta2D 3.4 (Decodon, Braunschweig, Germany). In order to ensure that the same spot area was quantified in all gels, a master gel was created by fusing all gel images with the maximum intensity option selected in Delta2D. To analyze the significance of protein regulation, a Student's t-test was performed, and statistical significance was assumed for P values less than 0.01.

3.3.8 In-gel digestion and mass spectrometry analysis

Significantly regulated spots were excised from the gels and tryptic in-gel digestion and peptide extraction were performed as previously described by Dihazi et al. (Dihazi et al, 2011). Briefly, gel spots were rinsed twice in 25 mM ammonium bicarbonate (amBic) and once in water, shrunk with 100% acetonitrile (ACN) for 15 min, and dried in a Savant SpeedVac for 20–30 min. All excised spots were incubated with 12.5 ng/ μ l sequencing grade trypsin (Roche Molecular Biochemicals, Basel, CH) in 25 mM amBic overnight at 37 °C. Peptide extraction was carried out twice using first 50% CAN/1% trifluoroacetic acid (TFA) and then 100% ACN. All extracts were pooled, and the volume was reduced using SpeedVac. Tryptic peptides were subjected to mass spectrometric sequencing using a Q-TOF Ultima Global mass spectrometer (Micromass, Manchester, UK) equipped with a nanoflow ESI Z-spray.

Protein identification was carried out with Mascot search engine against MSDB and Swissprot databases through using a peptide mass tolerance and fragment tolerance of 0.5 Da.

3.3.9 Bioinformatic Analyses

To examine potential protein function categories and pathways of significantly regulated proteins, we performed bioinformatic analysis using a public protein software named DAVID Functional Annotation Bioinformatics Microarray Analysis (<http://david.abcc.ncifcrf.gov/>).

3.3.10 Western blot analysis

Western blot analyses were performed according to Towbin et al. (Towbin et al, 1979). Equal amount of proteins (50-75 μ g) were separated by polyacrylamide gel electrophoresis (SDS-PAGE) and transferred on nitrocellulose membranes (Amersham Pharmacia Biotech, Buckinghamshire, UK). The membranes were blocked in 5% non-fat dry milk in Tris buffer and incubated with the indicated primary antibody at 4°C overnight. To visualize the protein bands, fluorescence labeled secondary antibody was used. To confirm equal protein loading, the blots were reprobed with β -actin (Actb).

3.3.11 Isolation of mitochondria

Kidney mitochondria were isolated from average 40 weeks old WT and Calr^{+/-} mice following the mitochondria isolation kit for tissues and cultured cells protocol (amsbio, UK). 150 mg of mice kidneys were minced and homogenized with a Douncer homogenizer in 2 ml mitochondrial isolation buffer provided with kit. The suspension was centrifuged at 600 xg for 10 min and the resulting supernatant at 10,000 g for 15 min at 4°C. After centrifugation, the mitochondrial pellet was collected from the lower interface and washed in mitochondrial isolation buffer by repeating the above centrifugation steps. Isolated mitochondrial pellet were

either resuspended in mitochondria storage buffer for intact mitochondria for functional assay or lysed with mitochondria lysis buffer for Western blot analysis of mitochondrial proteins.

3.3.12 Cytochrome c oxidase activity assay

Cytochrome c oxidase (Cox) activity was determined in intact isolated mitochondria from kidney tissues using the Cox Kit according to the manufacturer's instructions (Mitochondrial activity assay kit, amsbio, UK). The colorimetric assay is based on the observation that a decrease in absorbance at 550 nm of ferrocytochrome c is caused by its oxidation to ferricytochrome c by Cox.

3.3.13 Data analysis

All blots were quantified using the ImageJ software. Graphpad prism was used for graphical presentation and analysis by Student's t-distribution. Results are expressed as the average of three or more independent experiments. Results are presented as the mean \pm SD of at least three independent experiments. Differences were considered statistically significant when $p < 0.05$.

3.3.14 Antibodies

Monoclonal rabbit anti-Fn1, anti-Lamc1, anti-Grp78, anti-Park7, and mouse anti- Actb antibodies were from Sigma. Polyclonal rabbit anti- Ddit3/Chop and anti-Sod1 antibodies were from Abnova. Rabbit monoclonal anti- Pvalb, anti-Cam, anti-Prdx6, anti- Nos1, anti- Phb, anti-Vdac1 antibodies were from Abcam. Rabbit anti-Hsp47 monoclonal antibody was purchased from Sigma.

3.4 Results

3.4.1 Low Calr level results in progressive kidney damage in Calr^{+/-} mice

As reported earlier Calr gene knockout is embryonic lethal and Calr^{-/-} embryos die during embryonic stages with multiple developmental defects especially heart development (Mesaeli et al., 1999). To investigate the role of Calr in kidney development, viable and fertile heterozygote Calr^{+/-} mice were mated. Viable embryos were obtained at E17.5 and kidneys were excised. Gross morphological analysis showed significant reduction in the size of the Calr^{-/-} embryos. However, phenotype of the kidneys of the Calr^{+/-} embryos did not show any significant differences compared to WT (Figure 3.1A). H&E staining of E17.5 kidney sections further revealed severe developmental defects in Calr^{-/-} especially the formation of comma- and S-shape was impaired compared to WT. Moreover, the ureter bud formation seems to be affected resulting in less developed kidneys. In contrast, the staining of the kidneys from Calr^{+/-} embryos showed normal renal embryonic structures (comma and S-shapes), but their number was reduced compared to WT (Figure 3.1B) revealing a disadvantage in kidney development of Calr^{+/-} embryos.

Our previous studies (Dihazi et al., 2005, Bibi et al 2011) revealed that chronic reduction of Calr could play a significant role in kidney function. Despite the major differences in kidney development, we investigated adult Calr^{+/-} mice to study the chronic low level of Calr in structure and function of the kidney. Morphological examination of freshly excised adult kidneys from 5 different animals from 12, 30 and 40 wk old mice showed a progressive deterioration of kidneys with development of hypertrophy (Figure 3.1C). 70% of Calr^{+/-} animals at an average age of 40 wk showed severely affected kidneys with remarkable morphological differences compared to young Calr^{+/-} and WT controls of same age. 10% Calr^{+/-} mice of total Calr^{+/-} animals displayed hemizygous kidneys with one missing kidney (Fig 3.1D) whereas 20% showed heterozygous kidneys with one hypoplastic kidney.

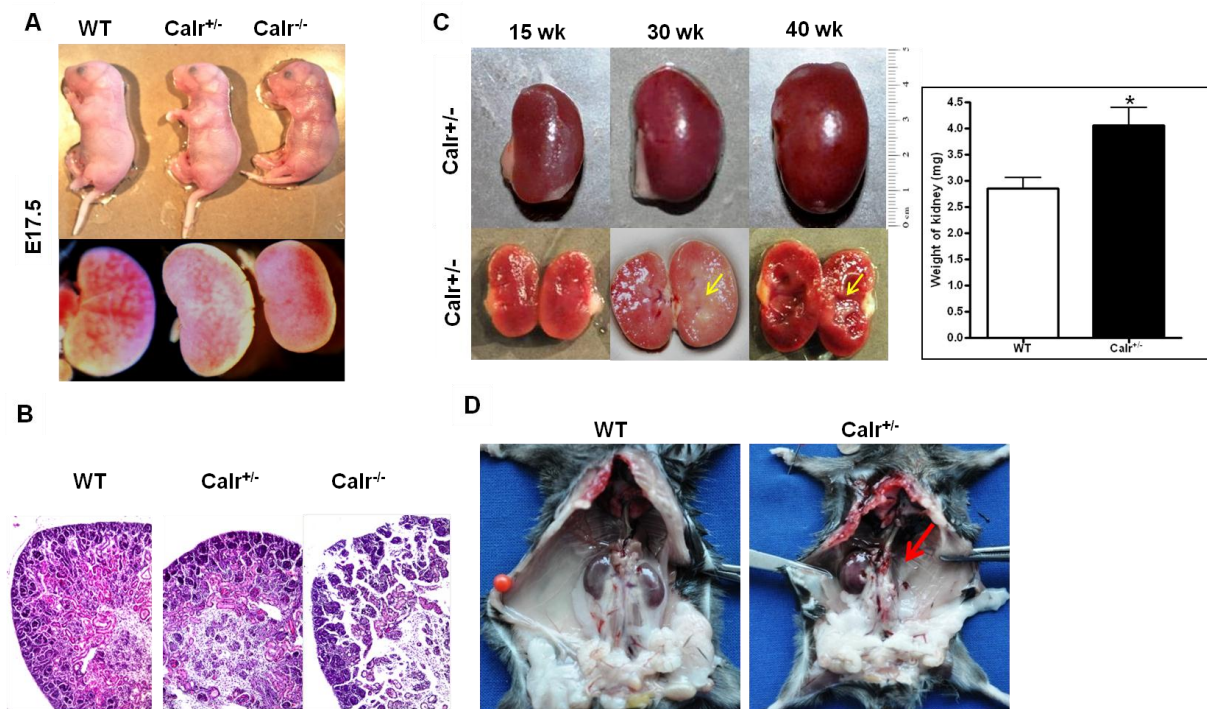


Figure 3.1: Morphometric analysis of embryonic and adult kidneys of Calr KO mice.

(A) Whole mount views of control and mutant fetuses of the indicated genotypes of WT, Calr^{+/-} and Calr^{-/-} at E17.5 in upper lane with corresponding kidneys in lower lane. The size and gross morphology of Calr^{+/-} embryos and kidneys are comparable to WT whereas, Calr^{-/-} shows significant morphological alteration with remarkable reduced size. (B) Histological staining of embryonic kidney section with H&E stain shows similar structures in Calr^{+/-} and WT kidneys compared to severely affected Calr^{-/-} kidneys. (C) Gross morphology of kidneys from 15, 30 and 40 weeks Calr^{+/-} mice (from left to right) from external sight (upper lane) showing a progressive enlargement and impairment of kidneys. Bar diagram represents the significant increase in kidney weight at 40 wk of age. Longitudinal sections of kidneys showing progressive internal impairments (lower lane) indicated with arrows (yellow) in Calr^{+/-} mice. Genotypes are indicated at the top. wk: weeks

3.4.2 Calr^{+/-} mice develop progressive glomerulosclerosis and tubulointerstitial damage

Histological examination of kidneys from 15 to 40 wk old mice revealed the development of progressive pathological changes in both glomerular tufts and interstitial tubular parts of Calr^{+/-} kidneys compared to WT (Figure 3.2A-D). Consistent with macroscopic examination, kidneys from 15 wk old Calr^{+/-} mice showed indistinguishable changes resulting in normal

prenatal and postnatal nephrogenesis in Calr^{+/-} mice. At 30 wk, glomeruli of Calr^{+/-} mice demonstrated prominent mesangial expansion with increased matrix deposition. However, in Calr^{+/-} mice of 40 wk of age, more advanced glomerular damage with characteristic sclerotic lesions evolved (Figure 3.2A). In addition to glomerulosclerosis, tubulointerstitial area was also severely affected at this age with a significant number of dilated, atrophic and necrotic tubules with expanded lumen (Figure 3.2B). Measurement of mean glomerular area and volume, as a parameter for overall glomerular architecture, showed a progressive increase in the glomerular size from 15 to 40 wk (Figure 3.2C). Similar results were also observed when measuring the mean mesangial area. Moreover, at advanced stage expansion in mesangial matrix was manifested with significant increase in the PAS-positive area (Figure 3.2D). The histological impairments were confirmed with classical H&E staining (Supplemental Figure 3.1A).

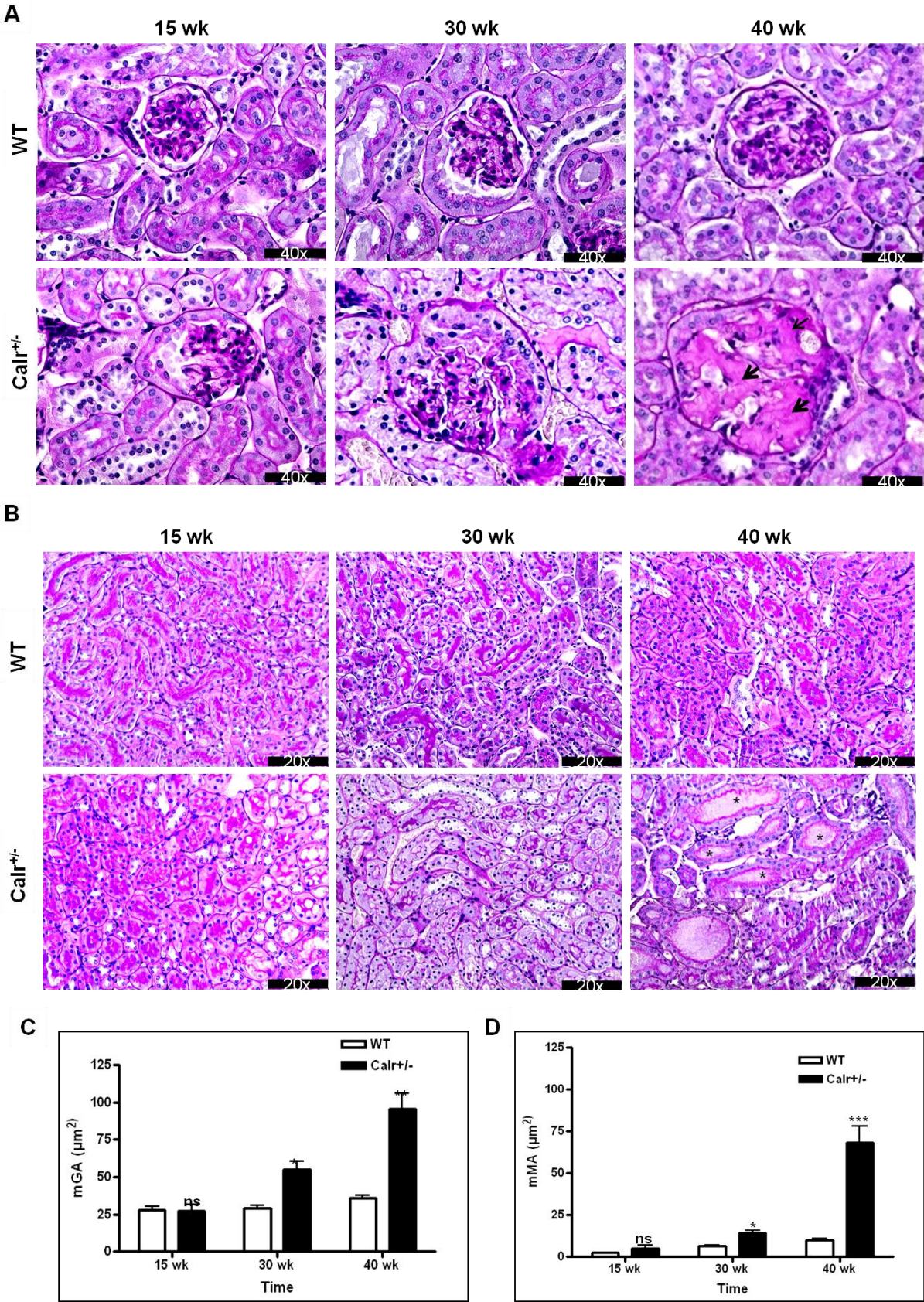


Figure 3.2: Progressive structural alterations in Calr^{+/-} mice.

Paraffin embedded kidney sections (3 μm) were stained with PAS to compare the kidney structures of $\text{Calr}^{+/-}$ at 15 wk, 30 wk and 40 wk of age. (A) Glomerular histopathology analysis. The pictures display representative glomeruli of PAS-stained sections from $\text{Calr}^{+/-}$ mice (lower lane) and WT mice (upper lane). At 15 wk of age, size and structure of glomerulus is comparable with WT mice. At 30 wk of age, size of glomerulus is significantly enlarged with little deposition of mesangial matrix compared to WT. At 40 wk of age, glomerular damage is highly significant showing expansion of mesangium with accumulation of PAS-positive material indicated with arrowhead in $\text{Calr}^{+/-}$ mice (Magnification x40). (B) Tubulointerstitial analysis. The pictures show progressive tubulointerstitial necrosis in $\text{Calr}^{+/-}$ mice (lower lane) compared to WT mice (upper lane). At 40 wk of age, tubules are damaged with necrotic debris and PAS positive brush borders indicated with asterisks (Magnification x20) and one shown in higher magnification at the corner. (C) Bar diagram show an increase in mGA in the kidneys of 30 and 40 wk old $\text{Calr}^{+/-}$ mice in comparison to that of young $\text{Calr}^{+/-}$ and WT mice of same age ($P < .05$). (D) Bar diagram show a significant increase in mMMA in 40 wk old $\text{Calr}^{+/-}$ mice compared to young $\text{Calr}^{+/-}$ mice of 15 and 30 wk old and WT of same age. The data shown are mean \pm SE ($n = 30$ glomeruli per group, $P < 0.05$). PAS: periodic acid shift, mGA: mean glomerular area, mMMA: mean mesangial area.

3.4.3 Ultrastructural analysis shows glomerular and tubular cell damage in $\text{Calr}^{+/-}$ mice

To investigate the structural changes in $\text{Calr}^{+/-}$ mice, electron microscopy analysis was performed. As expected, the electron microscopy results were consistent with the light microscopic observations. Ultrastructural analysis revealed significant alterations in 40 wk old $\text{Calr}^{+/-}$ mice compared to WT mice (Figure 3.3A-E) and young $\text{Calr}^{+/-}$ mice kidneys (Supplemental Figure 3.2). Ultrastructural changes in $\text{Calr}^{+/-}$ mice were characterized by a significant mesangial sclerosis, marked and irregular thickening of the glomerular basement membrane and enlarged vacuolated podocytes with foot process broadening and effacement. In addition to glomerular abnormalities, damage of the renal tubules was noted as focal loss of the brush border of the epithelial lining of proximal renal tubules and disturbance of tight junctions. These data indicate that a critical level of Calr is necessary to maintain glomerular and tubular architecture.

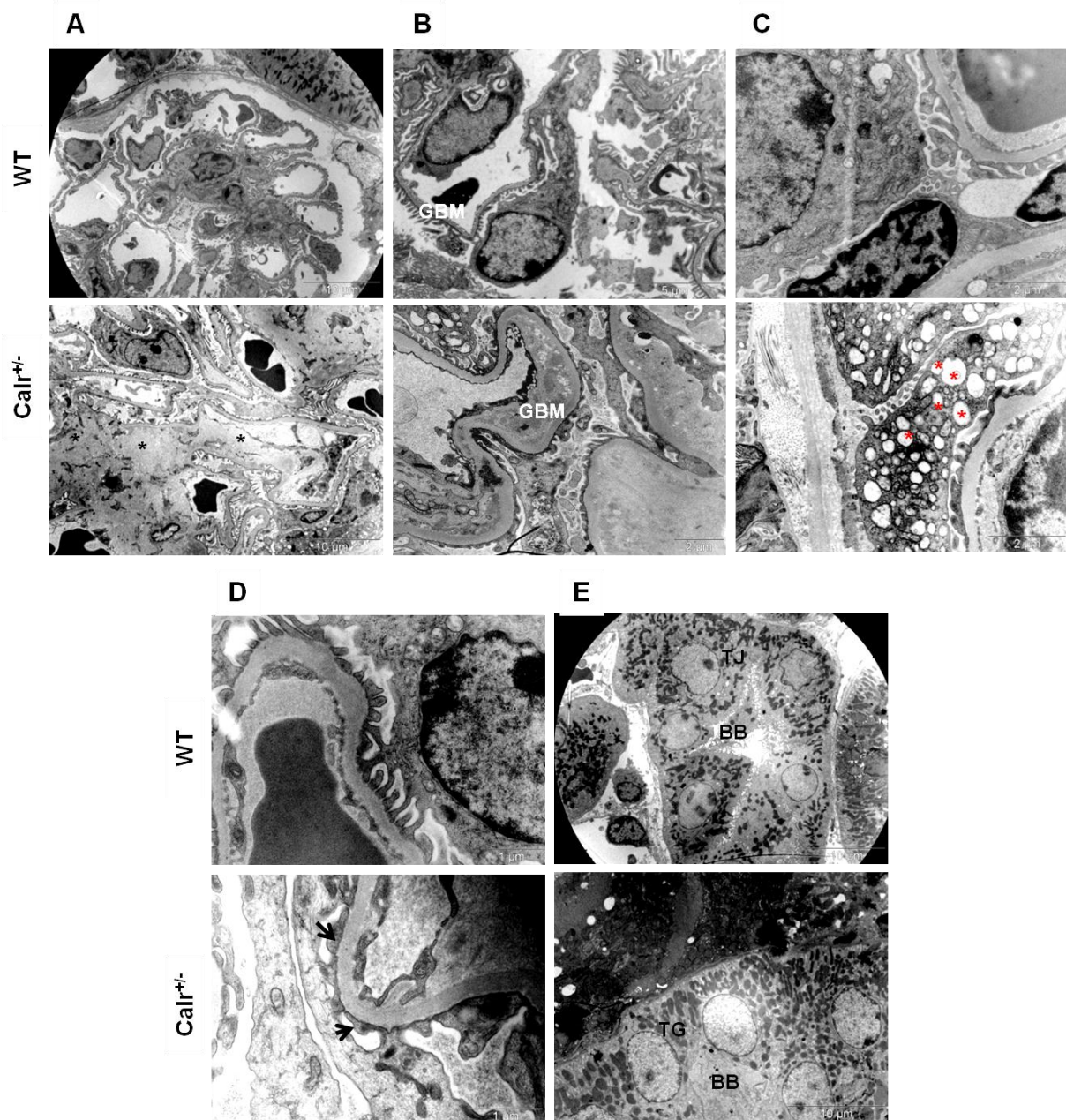


Figure 3.3: Electron microscopy analysis of Calr^{+/-} and WT kidneys.

Kidney section from 40-weeks-old WT and Calr^{+/-} mice were assessed by electron microscopy. Representative electron microscopic images show damaged structures in Calr^{+/-} (lower panel) compared with normal structures in WT (upper panel). (A) At lower magnification (10 μm), changes in glomerular matrix of Calr^{+/-} mice became visible with extensive accumulation of ECM compared to WT (*). (B) Irregular glomerular basement membrane indicated with GBM compared to normal in WT (10 μm). (C) Vacuolated podocyte indicated with red asterisks (2 μm). (D) Extensive podocyte foot process indicated with black arrows (1 μm) in Calr^{+/-} mice. (E) Representative micrographs of proximal tubular cells showing disturbance of tight junctions and brush borders in

Calr^{+/-} mice indicated with TJ and BB compared to WT (10 μm). GBM: basement membrane, BB: brush borders, TJ: tight junction

3.4.4 Enhanced expression of ECM proteins in advanced kidney injury in Calr^{+/-} mice

Following the histological findings of kidney damage, immuno-histochemical analysis of kidneys of 40 wk old Calr^{+/-} mice demonstrated the enhanced expression of ECM proteins in both glomeruli and tubulointerstitial parts. A strong deposition of Fn1 was observed in the mesangium of glomeruli and interstitial areas of Calr^{+/-} compared to WT controls (Fig 3.4A). Immunofluorescence staining of Fn1 confirming the deposition of protein in expanded mesangium of Calr^{+/-} kidney glomeruli and interstitial spaces is provided in supplementary data (Supplemental Figure 3.1B). Besides the higher expression of Fn1, Lam expression was also significantly enhanced in Calr^{+/-} mice kidneys (Figure 3.4B). However, no significant immunoreaction was observed for Ezr, a podocyte marker, in glomeruli of Calr^{+/-} kidneys compared to control confirming the severe damage of podocytes (Fig 3.4C). Western blot analysis confirmed the expression of these kidney injury markers in total protein extract of 4 different Calr^{+/-} mice kidneys, whereas WT mice kidneys were kept as control (Fig 3.4D). These data indicate that Calr level is critical for maintaining an intact kidney as well as in the progression of kidney injury.

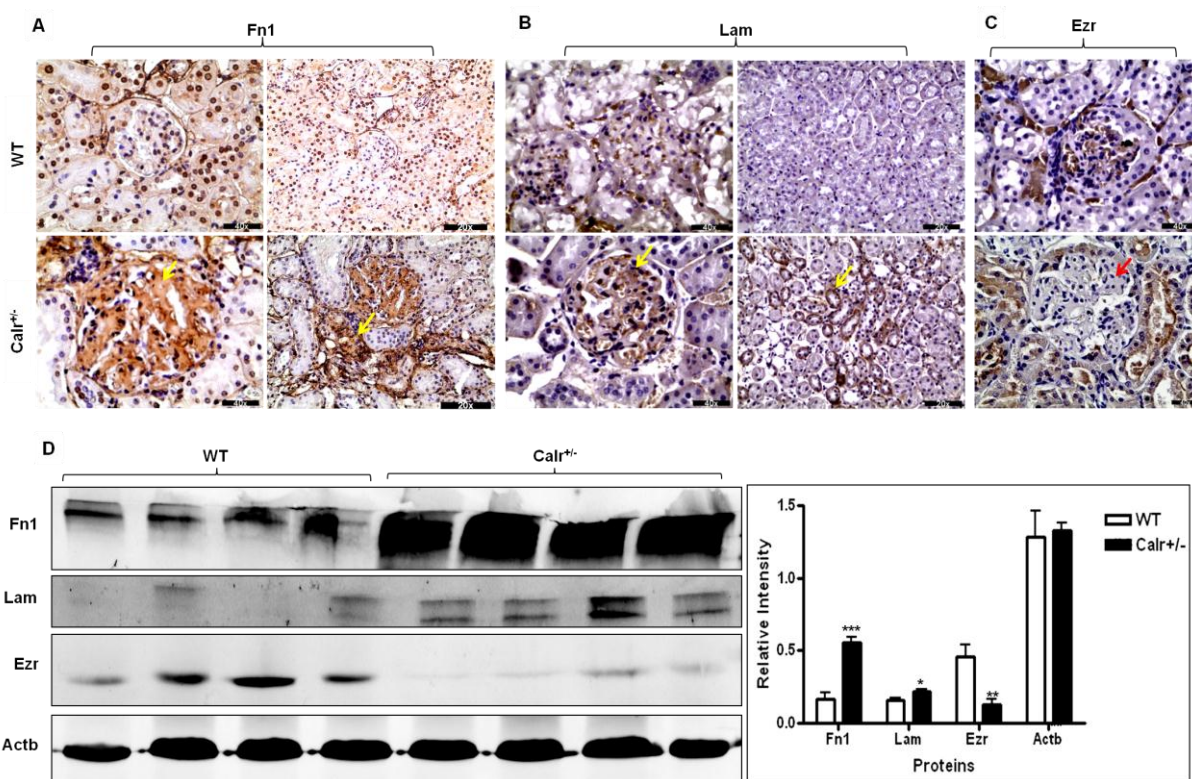


Figure 3.4: Immune expression of glomerular and tubulointerstitial injury markers.

Representative images of glomerular and tubulointerstitial areas from WT (upper panel) and Calr^{+/-} (lower panel) kidneys stained with (A) fibronectin (Fn1), (B) laminin (Lam), and (C) ezrin (Ezr). We observed a marked increase in Fn1 and Lam expression in the glomeruli (Magnification x40) and tubulointerstitial areas (Magnification x20) of Calr^{+/-} kidneys indicated with yellow arrows. Whereas expression of Ezr was less in glomeruli of Calr^{+/-} kidneys compared to WT kidneys. (D) Representative Western blot analyses of Fn1, Lam, and Ezr in whole kidney lysate of WT and Calr^{+/-} mice. (E) Bar diagram representing the quantification of the Western blot results shown in D. (n=4. *, P < 0.05). β -actin (Actb) was used as loading control.

3.4.5 ER stress pathway is not operative in Calr^{+/-} mice kidney damage

Calr is a chaperone protein implicated in protein folding and is a Ca²⁺ binding protein responsible for the Ca²⁺ storage and Ca²⁺ homeostasis regulation. To determine which functional aspect of Calr downregulation is operative in Calr^{+/-} mice kidney injury, we investigated the expression of proteins linked to downstream effects of either ER stress response or Ca²⁺ signaling regulation.

Immunohistochemical staining showed that intensity of ER chaperon Grp78 expression was not significantly altered (Figure 3.5A). Western blot and 2D gel analyses further confirmed that expression of Grp78 is unchanged demonstrating the absence of ER stress in Calr^{+/-} mice (Figure 3.5D, Figure 3.6B). In addition to ER chaperon Grp78, Hsp47 and downstream proteins of ER stress pathway, chop and eif2 α -phospho were also not altered in Calr^{+/-} mice compared to WT mice (Figure 3.5E). All these results depict that ER stress is not operative in Calr^{+/-} mice kidney damage.

Ca²⁺ homeostasis is an important cellular phenomenon. Increase in free intracellular Ca²⁺ is associated with disturbance of Ca²⁺ homeostasis. Alterations in free intracellular Ca²⁺ level result in the expression regulation of a group of EF-hand cytosolic Ca²⁺ binding proteins. Here, we examined the expression of some of the EF-hand Ca²⁺ binding proteins; S100a4, Pv and Cam with immunohistochemistry and immunoblotting in the Calr^{+/-} kidneys. The S100a4 was highly expressed in tubular epithelial cells of Calr^{+/-} kidneys compared to WT (Figure 3.5B). Specific staining of distal convoluted tubules with Pv showed tubular damage in terms of decrease in tubular lumen and damaged tubular walls (Figure 3.5C). Expression of Cam was disturbed with overall nonspecific staining compared to specific tubular staining in WT mice (Figure 3.5D). Western blot analysis further confirmed the altered expression of calcium binding proteins. Actb was kept as control (Figure 3.5E).

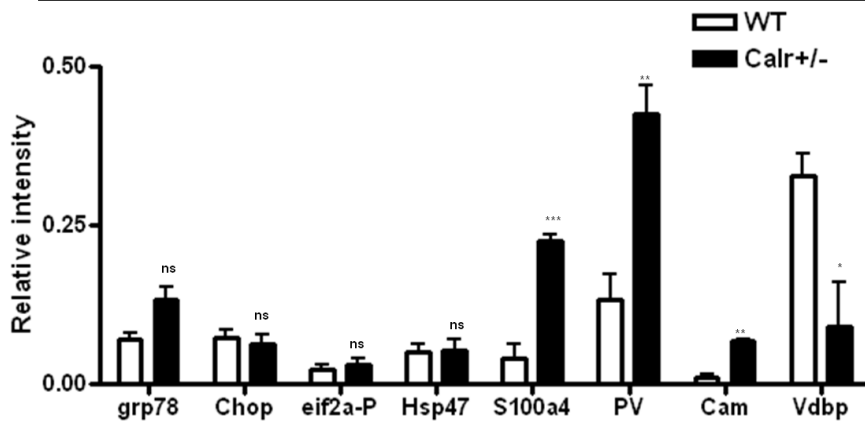
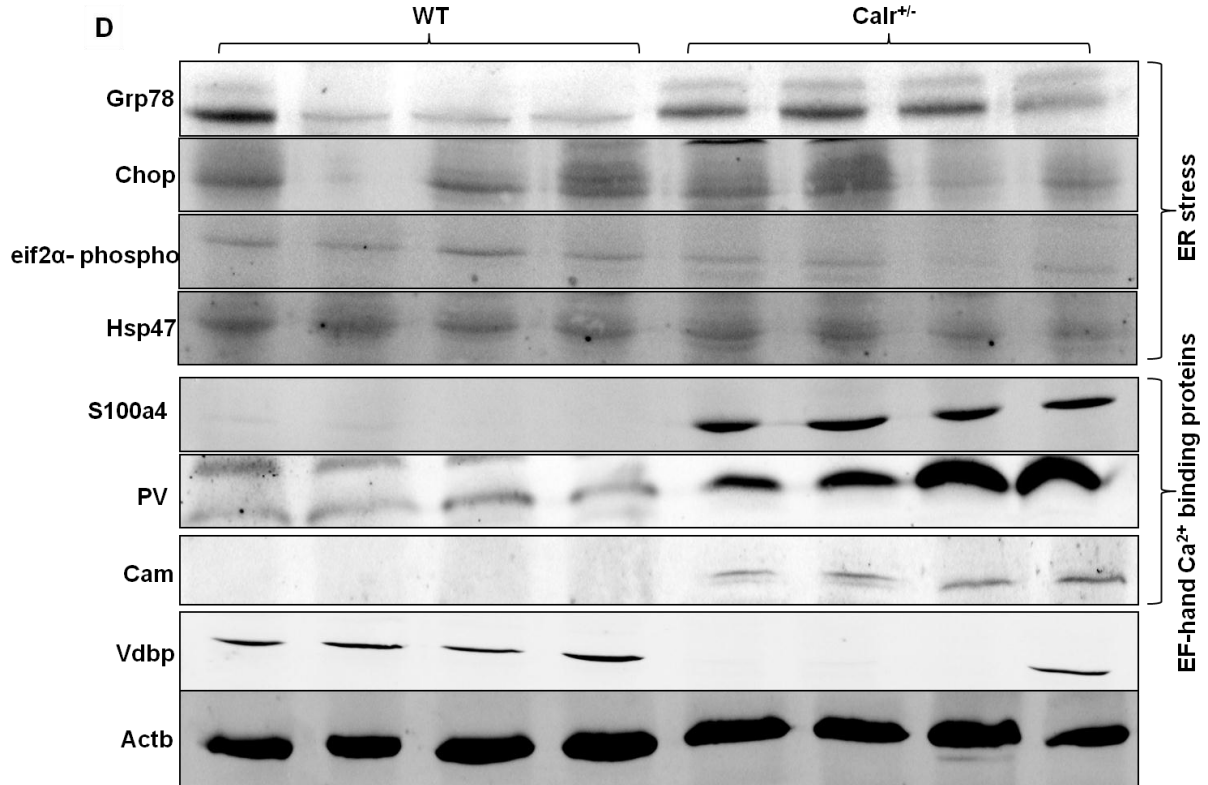
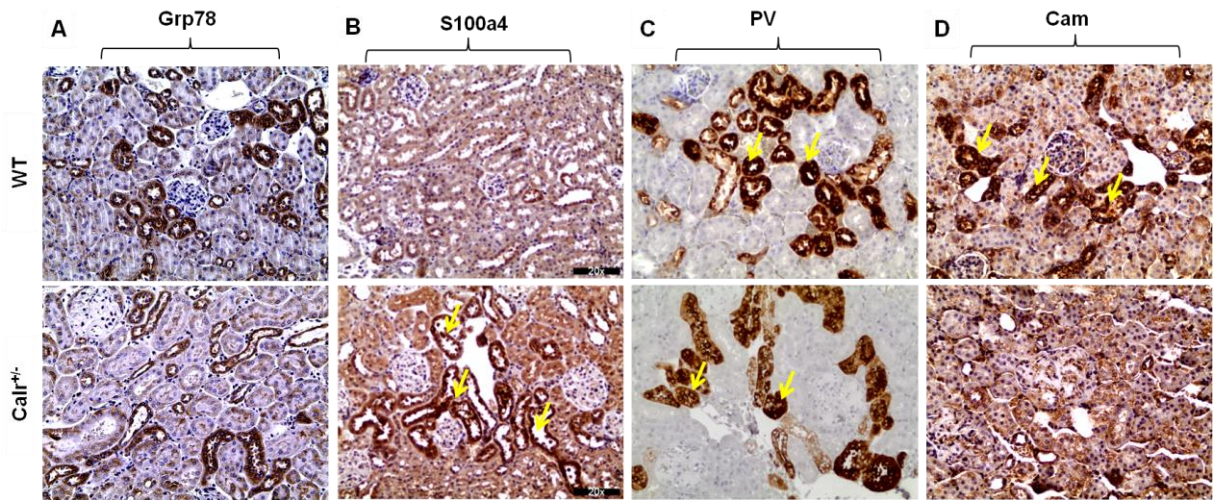


Figure 3.5: Effects of low Calr level on expression of ER stress markers and EF-hand Ca²⁺ binding proteins.

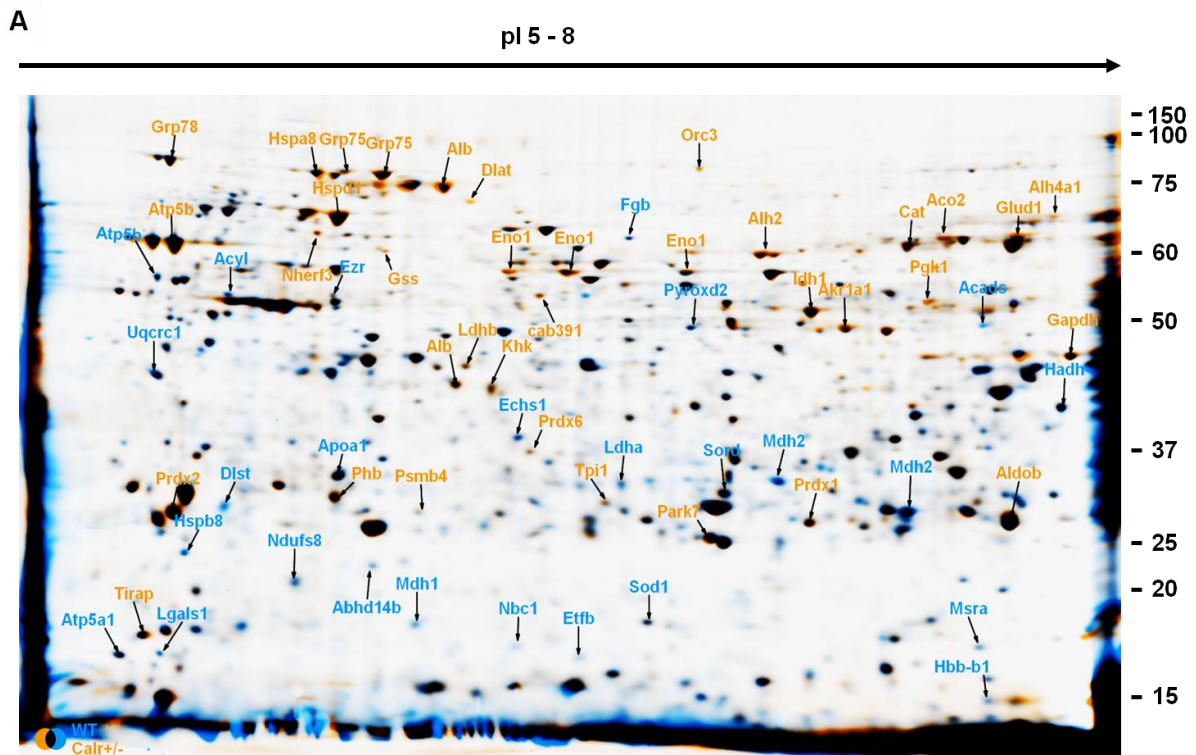
Representative images for immunohistochemical staining of Grp78, S100a4, Pv and Cam are shown in 40 wk old Calr^{+/-} (upper lane) and WT (lower lane) mice kidney sections. (A) Grp78 staining is showing no significant expression changes (B) S100a4 is overexpressed in epithelial tubular cells highlighted with arrows, (C) Pv staining shows an expression decrease in tubular lumen and damaged tubular wall indicated with arrows (D) Cam expression alters from highly specific tubular expression in WT (indicated with arrows) to overall nonspecific expression in Calr^{+/-} mice kidney section. (Magnification: x20). (E) Immunoblotting of Grp78, chop, eif2 α -phospho, Hsp47, S100a4, Pv, and Cam was performed for kidney lysate of Calr^{+/-} and WT mice. Actb was used as loading control. Bar diagram represents the quantification of the Western blot results shown in D. (n=4. *, P < 0.05).

3.4.6 Comparative proteomic analysis show strong metabolic dysregulation in Calr^{+/-} mice kidneys

To investigate the mechanism behind the kidney injury in Calr^{+/-} mice, proteomic analysis was performed. Kidneys were obtained from both WT and Calr^{+/-} mice at an average age of 40 weeks and homogenized. Proteins were extracted and purified from both WT and Calr^{+/-} mice kidney homogenates, and separated by 2-D gel electrophoresis as described in Methods part. For comparison, three independent 2-DE images of each protein extract from three independent WT and Calr^{+/-} mice were selected for statistical analysis. Significantly regulated proteins in Calr^{+/-} mice kidneys as compared to their corresponding control (Delta 2D analysis, see Materials and Methods) were excised from gels, in-gel digested with trypsin, and prepared for mass spectrometric (MS/MS) analysis. Proteins were identified by the sequence databases search using Mascot.

The low Calr level results in statistically significant changes (p<0.05) in the expression of 65 proteins, obtained from WT and Calr^{+/-} kidneys. By mass spectrometry we identified about 50 of the differentially expressed proteins in the whole lysate. Among them, 22 protein spots

were downregulated, and 28 were up regulated (Table 3.1). A proteome map from three independent experiments labeled with differentially regulated proteins is presented in Figure 3.6A. Some of the interesting proteins spots are highlighted in higher magnifications with their expression quantification (Figure 3.6B).



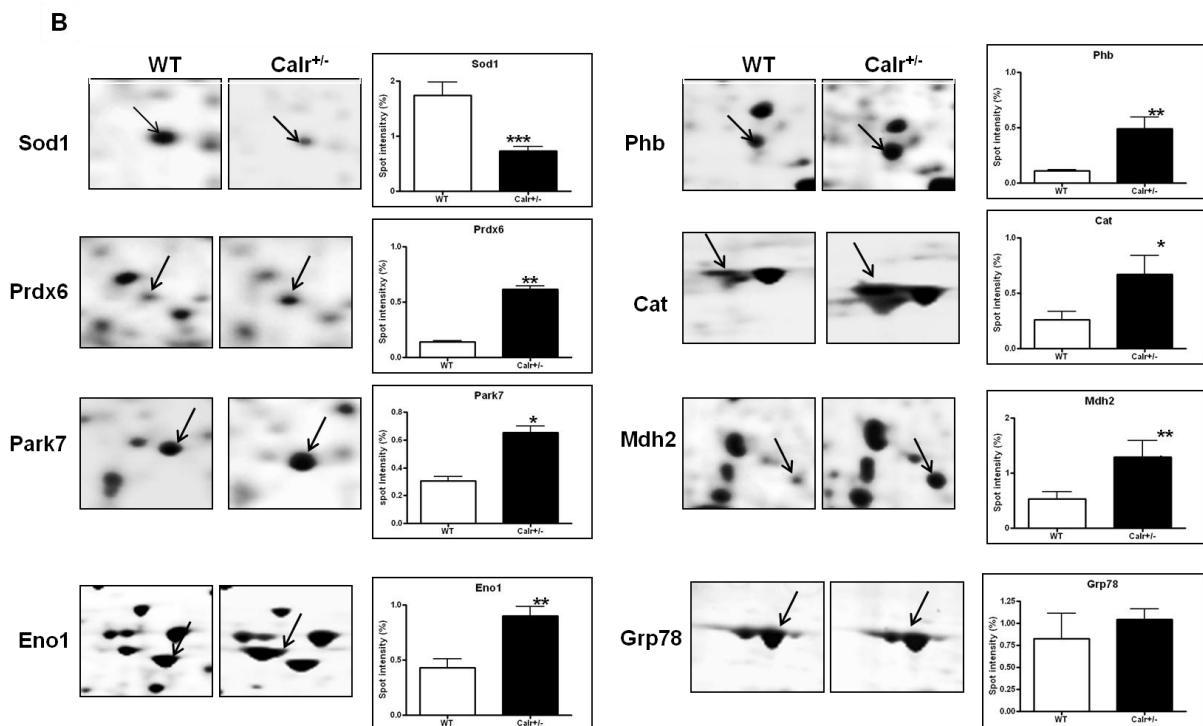
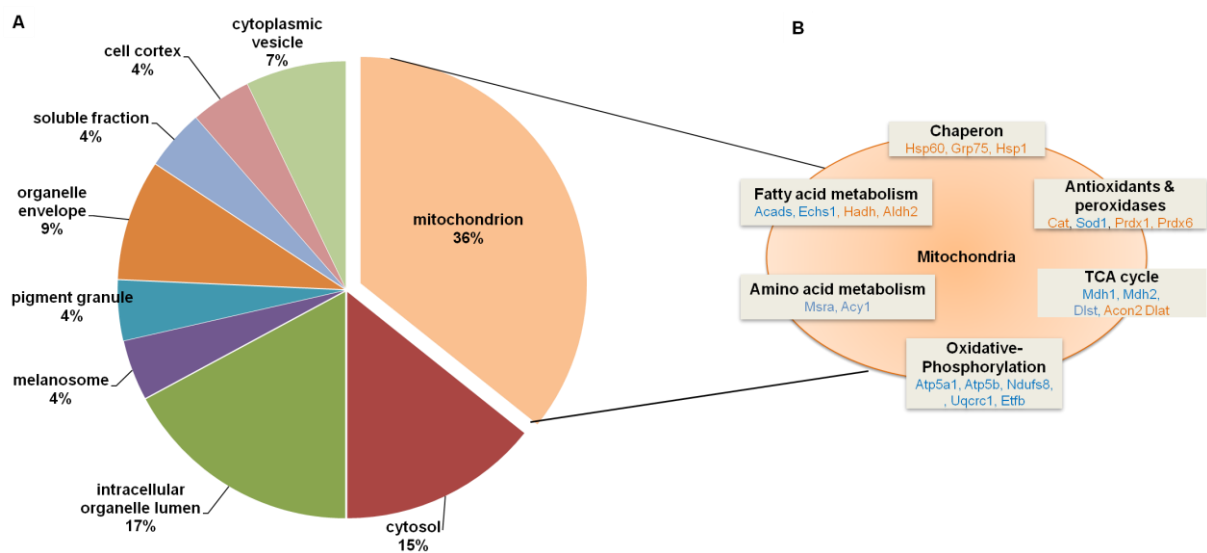


Figure 3.6: 2D gel map expression of differentially regulated proteins in $Calr^{+/-}$ mice kidneys compared to WT.

(A) Overlapping 2-DE expression map of WT and $Calr^{+/-}$ kidneys. Blue spots indicate higher expression in WT mice samples than in $Calr^{+/-}$ mice samples. Orange spots indicate the reverse. Overlapping spots are shown in black. (B) Magnified images of regions of interest showing differentially regulated proteins in the $Calr^{+/-}$ mouse kidney. The protein expression quantification for selected proteins is given in form of bar diagrams. Results are given as the means \pm SD of the percentage volume of spot from at least three independent experiments ($P < 0.05$).

Each identified protein was assigned to cellular components, functional categories and biological processes based on the Gene Ontology annotation system using the DAVID Functional Annotation Bioinformatics Microarray Analysis (<http://david.abcc.ncifcrf.gov/>). Interestingly, the largest part of the identified proteins was found to be located in the mitochondrion (Figure 3.7A). Functional analysis with DAVID Bioinformatics tool classified the differentially regulated proteins into 24 different functional protein categories according to Gene Ontology annotation, some proteins belonging to more than one category due to their

multifunctional properties (Supplemental Figure 3.3). Proteins categories belonging to mitochondria are shown (Figure 3.7B). Classification of proteins according to biological processes illustrates that many of the identified proteins were assigned into energy metabolism, response to oxidative stress and mitochondria dysfunction (Figure 3.7C). Taken together, the proteomic data provides converging evidence for perturbations in a number of key metabolic pathways and evidence for kidney injury.



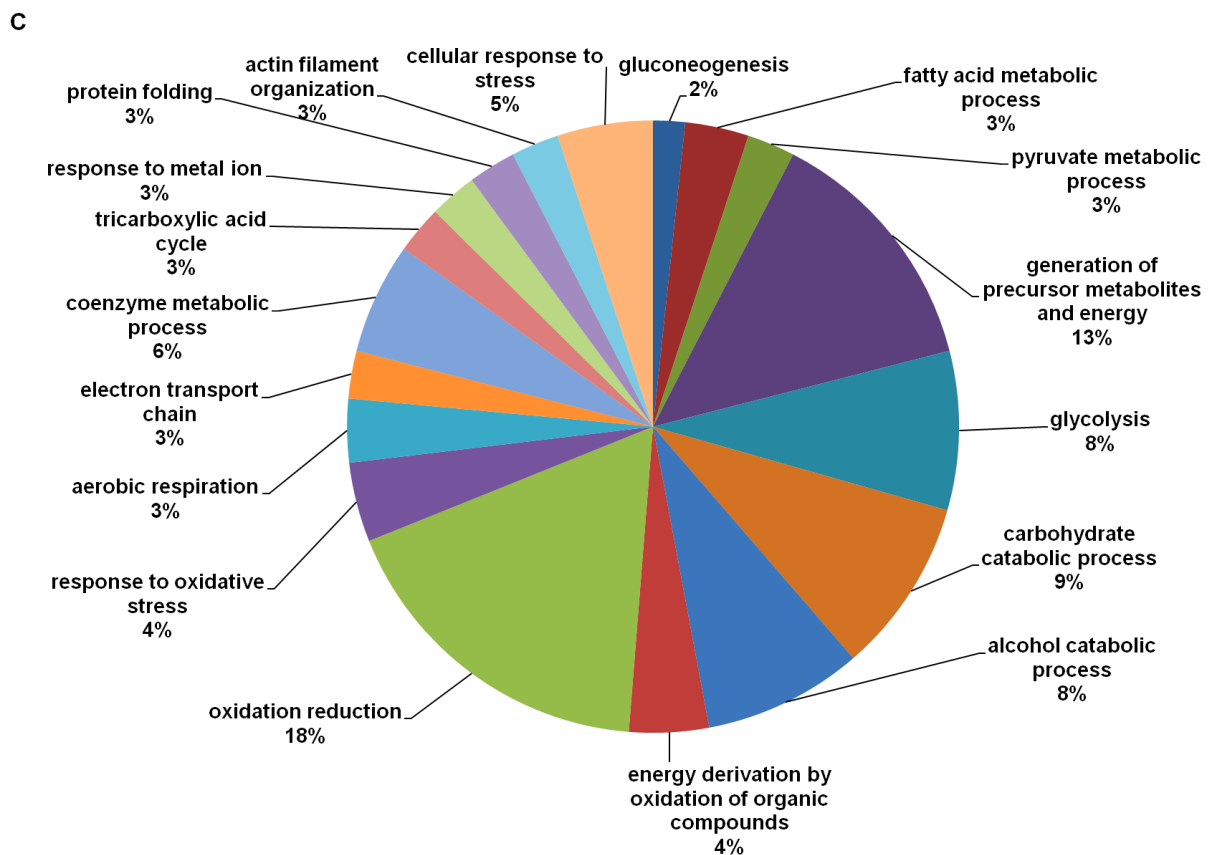


Figure 3.7: Gene Ontology (GO) classification of differentially regulated proteins by DAVID Bioinformatics.

Categorization was achieved by correlating GO identification numbers corresponding to cellular component and biological process with the regulated proteins. Values in figures presented the ratio distribution of proteins found in that respective category, (A) identified proteins categorized based upon their cellular component, (B) identified mitochondrial proteins categorized based upon their functional category. Gene names for proteins indicated in blue are downregulated, whereas, the ones in orange are upregulated in Calr^{+/-} compared to WT mice (C) identified proteins categorized based upon their biological processes.

3.4.7 Alteration of energy metabolism in Calr^{+/-} mice kidneys

Life is the interplay between structure and energy. Classification of differentially regulated proteins into functional categories and pathway analysis demonstrated that the majority of them were enzymes that catalyze reactions in intermediary energy metabolism (Figure 3.8A). For example, 5 enzymes of the cytosolic resident pathways glycolysis/gluconeogenesis were upregulated. Ldhd, an enzyme for anaerobic respiration was upregulated. However, in contrast to cytosolic energy pathways, the majority of enzymes belonging to mitochondrial energy production were downregulated. Among these, an important oxidative energy metabolism pathway is pyruvate metabolism, which is a link between glycolysis and TCA cycle. Enzymes of the pyruvate metabolism were altered with 4 downregulated enzymes and 2 upregulated. In addition to carbohydrate metabolism, 3 enzymes of fatty-acid oxidation, another major pathway for oxidative energy metabolism, were also downregulated in Calr^{+/-} mice kidneys. End products of carbohydrate and fatty acid metabolism enter the TCA cycle to produce NADH. Here, 4 enzymes of TCA cycle were significantly regulated. Among them, 3 were downregulated and 1 was upregulated. TCA cycle mainly reduces NAD⁺ to NADH, which enters the electron transport chain for ATP production on the basis of oxidative phosphorylation. Our proteomic data further demonstrated the downregulation of 3 enzymes of electron transport chain, which might result in diminished oxidative phosphorylation (Figure 3.8B). All these results showed that Calr^{+/-} mice have reduced oxidative energy metabolism enzymes, one might expect them to exhibit low energy levels leading to signs of energetic stress.

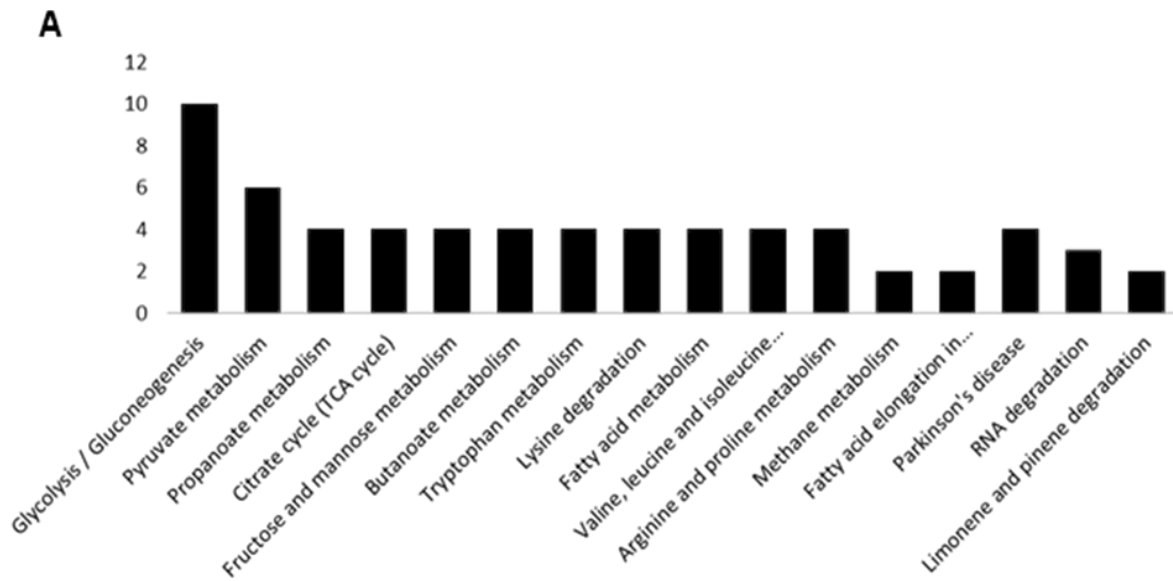


Figure 3.8 continued....

B

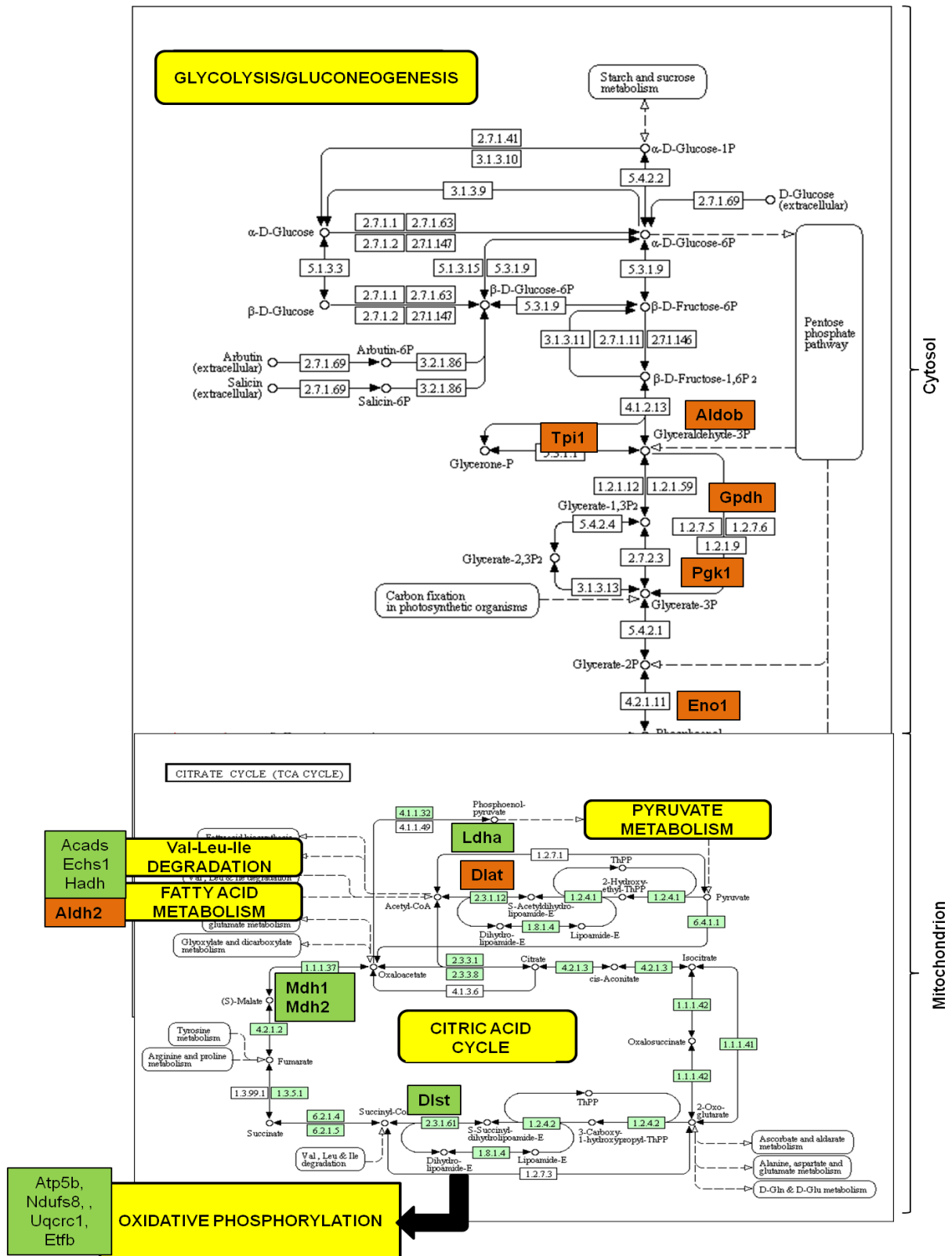


Figure 3.8: Energy metabolism pathways.

(A) Pathway analysis of regulated proteins using DAVID Bioinformatics showing majority of pathways related to energy metabolism (B) The KEGG (<http://www.genome.jp/kegg/pathway.html>) #00010 pathway diagrams shows the major carbohydrate metabolic pathways including glycolysis/gluconeogenesis, pyruvate metabolism, citric acid/TCA cycle, fatty acid metabolism, and Val-Leu-Ile degradation. Enzymes in orange color denote upregulated, while in green color denote downregulated.

3.4.8 Chronic low levels of Calr induces kidney injury through oxidative stress induction

Excessive ROS production or inefficient antioxidant system are known as major causes of oxidative stress in the target cells and tissues. Our proteomic analysis revealed that low Calr level results in impairment of the antioxidant system of kidney through significant downregulation (2.6 fold) of an important antioxidant enzyme, Sod1 in Calr^{+/-} mice. Furthermore, significant upregulation (>2 fold) of a group of proteins called peroxiredoxins; Prxd1, Prxd2 and Prdx6 validated the occurrence of oxidative stress. Peroxiredoxins (Prdxs) work as a cellular redox control via their ability to eliminate organic hydroperoxides. Their upregulation in cells and tissues under oxidative stress conditions is known as one of the cellular recovery responses after oxidative damage (Ishii & Yanagawa, 2007). Furthermore, the significant upregulation (>2 fold) of another oxidative stress response protein Park7 (Figure 3.6B), as shown by proteomic data, confirmed the high oxidative stress level in Calr^{+/-} mice.

Western blot analysis from the kidney lysate of each of the four different Calr^{+/-} and WT mice further confirmed the significant downregulation of antioxidant Sod1 and upregulation of Prdx6 and Park7 proteins in all Calr^{+/-} mouse kidney lysates on individual basis compared to the WT mice. The expression of Actb, kept as a protein loading control, was unchanged (Figure 3.9A). Immunohistochemical analysis of Sod1 further demonstrated anomalous

expression of this protein in Calr^{+/-} mice kidneys. Sod1 is expressed in irregular aggregate form in Calr^{+/-} mice compared to homogenous distribution in WT mice kidneys. Sod1 aggregates could be better observed by co-staining of Sod1 with ubiquitin (Figure 3.9B). Immunofluorescence staining of Prdx6 showed an enhanced expression in Calr^{+/-} kidneys (Figure 3.9B). These results indicate that the Calr^{+/-} mice kidneys, due to ineffective antioxidant system, were subjected to oxidative stress leading to renal injury.

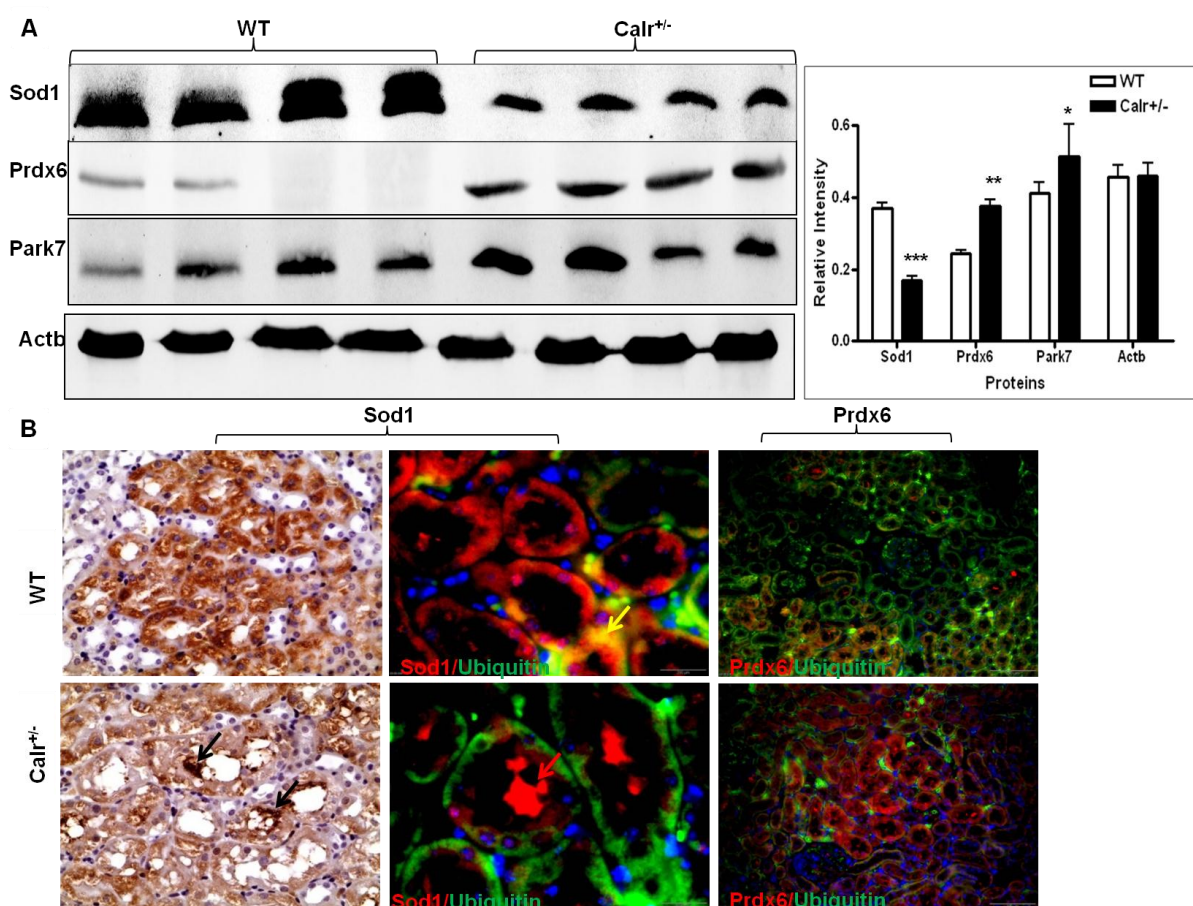


Figure 3.9: Induction of oxidative stress in Calr^{+/-} mice kidneys.

(A) Western blot analysis of oxidative stress related proteins; Sod1, Prdx6, and Park7 were performed for kidney lysate of Calr^{+/-} and WT mice. Actb was used as loading control. Bar diagram representing the quantification of the Western blot results shown in D. (n=4. *, P < 0.05). (B) Left panel: Immunohistochemistry staining show uneven Sod1 staining in Calr^{+/-} mice indicated with black arrows compared to uniform staining in WT mice. Middle panel: immunofluorescence staining of Sod1 coupled with ubiquitin further confirmed the presence of

uneven Sod1 aggregates indicated with red arrows compared to overlapped Sod1 and ubiquitin staining in WT indicated with yellow arrows. Right panel: immunofluorescence staining of Prdx6 showing an enhanced expression of the protein in Calr^{+/-} kidneys. Magnification: x40-100.

3.4.9 Activation of iNos dimerization in Calr^{+/-} mice

Nitric oxide synthase plays a critical role in ROS generation, mitochondrial function and signaling during inflammation. Overproduction of nitric oxide (NO) by inducible nitric oxide synthase (iNos) has been implicated in the pathogenesis of many disorders. It is well known that iNos is functional only in its dimer form (Kolodziejcki et al, 2003). Immunochemical staining of iNos in Calr^{+/-} showed no significant expression changes compared to WT kidneys (Figure 3.10A). In contrast, Western blot analysis showed an induction of higher molecular weight iNos dimer in Calr^{+/-} mice compared to lower molecular weight inactive monomer in WT mice (Figure 3.10B). These results provide evidence for the involvement of nitric oxide stress in Calr^{+/-} kidney.

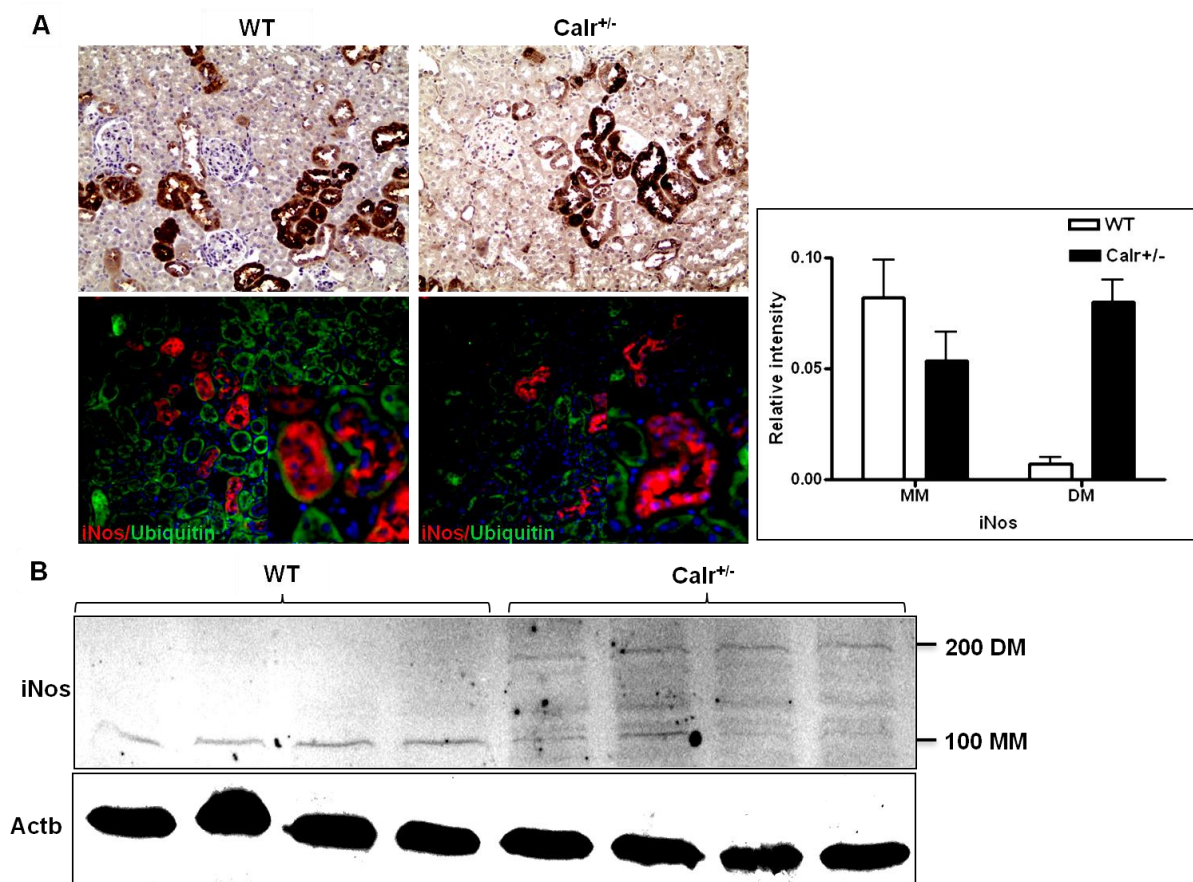


Figure 3.10: Activation of iNos in Calr^{+/-} mice kidneys.

(A) Immunohistochemical (upper lane) and immunofluorescence staining of iNos shows no significant change in expression of protein in Calr^{+/-} compared to WT with lower magnification (x20). However, zoomed tubules shown at corners represent an expression alteration of iNos in Calr^{+/-} compared to WT (Magnification: x40). (B) Western blot analysis of iNos was performed for kidney lysates of Calr^{+/-} and WT mice. Actb was used as loading control. Bar diagram representing the quantification of the MM and DM of iNos Western blot results shown in B (n=4. *, P < 0.05). MM: monomer, DM: dimer.

3.4.10 Mitochondrial damage in Calr^{+/-} mice

In order to examine the effect of oxidative stress on intracellular organelles, we used high magnification electron microscopy analysis. Interestingly, ultrastructural examination of kidney tissues showed profound alterations in mitochondrial morphology and number in both glomerular and tubular cells in Calr^{+/-} mice kidneys compared to WT ones. In comparison to

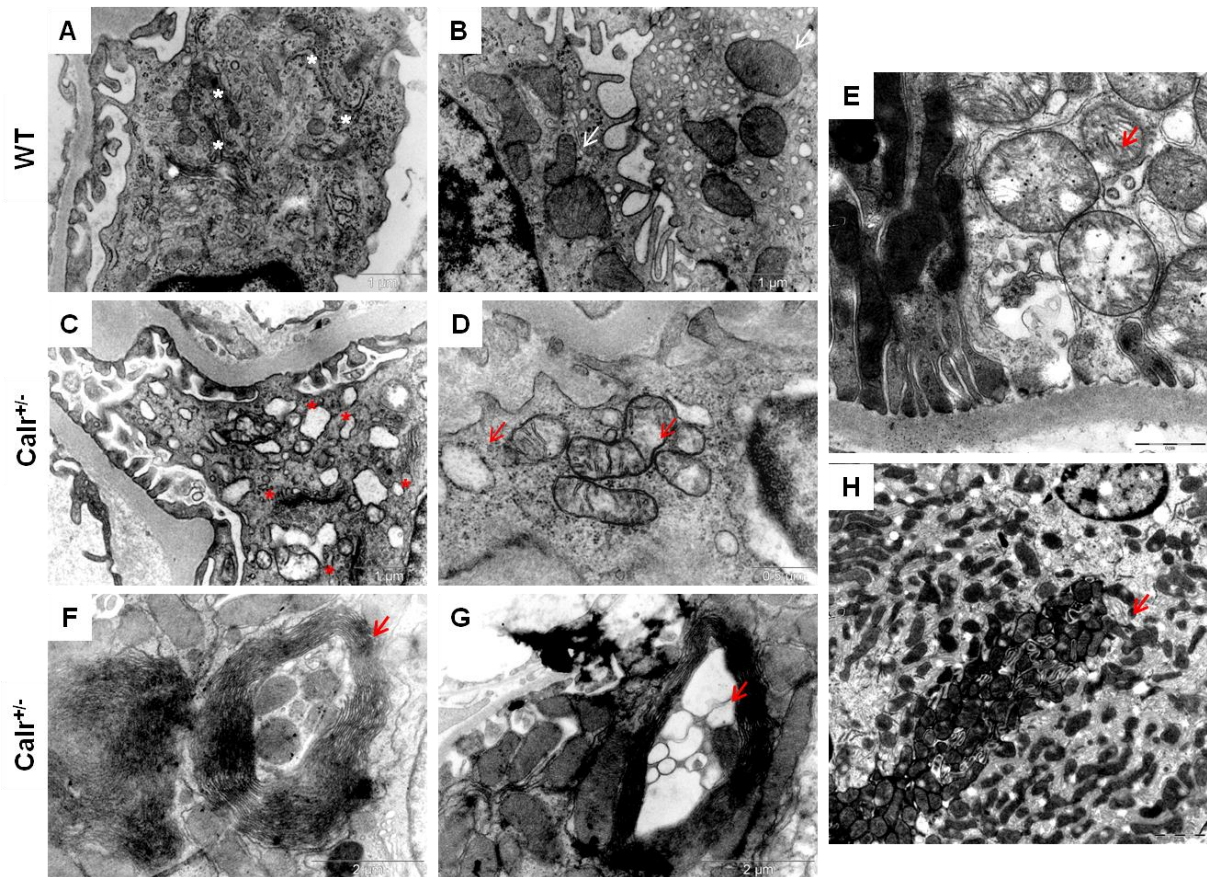
normal mitochondrial structures of WT kidney cells (Figure 3.11A-B), the Calr^{+/-} kidney mitochondria displayed vacuole like structures with prominent loss of cristae and inner mitochondrial membrane (Figure 3.11C). The latter varied widely in size and shape, from small and rounded to markedly enlarged and swollen with disorganized and fragmented cristae in podocytes (Figure 3.11D). Moreover, proximal tubular cells also showed swelling of several mitochondria with regression of their cristae and an increased number of mitochondria with loss of other cellular structures (Figure 3.11E).

Examination of electron micrographs from kidneys of Calr^{+/-} mice also revealed the presence of mitochondrial autophagy in some tubular cells. A number of mitochondria were observed enclosed in vacuoles with clear cristae (Figure 3.11F). Progressive degradation in some places with presence of myelin like structures (Figure 3.11G) provides further evidence of autophagy of mitochondria. In contrast to autophagy, certain tubular cells were densely packed with mitochondria (Figure 3.11H).

To investigate the possible expression alteration of proteins associated with mitochondria damage, mitochondria from WT and Calr^{+/-} mice kidneys were isolated and lysed as described under “Materials and Methods.” The expressions of soluble mitochondrial proteins were quantified using Western blot analysis. The data showed a significant downregulation of outer membrane channel Vdac1; whereas Phb a mitochondrial chaperon and stress induced protein was upregulated in Calr^{+/-} mice kidneys compared to control. Cat, a mitochondrial oxidative stress marker was also upregulated (Figure 3.11I). In addition, fluorescence staining of Cat showed a perturbed expression with clear translocation to nuclei (Figure 3.11J).

In addition to structural impairments coupled with protein alterations, we performed Cox activity assay with intact isolated mitochondria to evaluate the effects of the low Calr level on kidney mitochondrial ETC function (Figure 3.11K). Cox or complex IV of the mitochondrial

electron transport chain is the primary site of cellular oxygen consumption and, as such, is central to oxidative phosphorylation and the generation of ATP. The data showed that a decrease in the enzyme activity occurred in $Calr^{+/-}$ mice exhibiting the mitochondrial dysfunction leading to reduced energy metabolism.



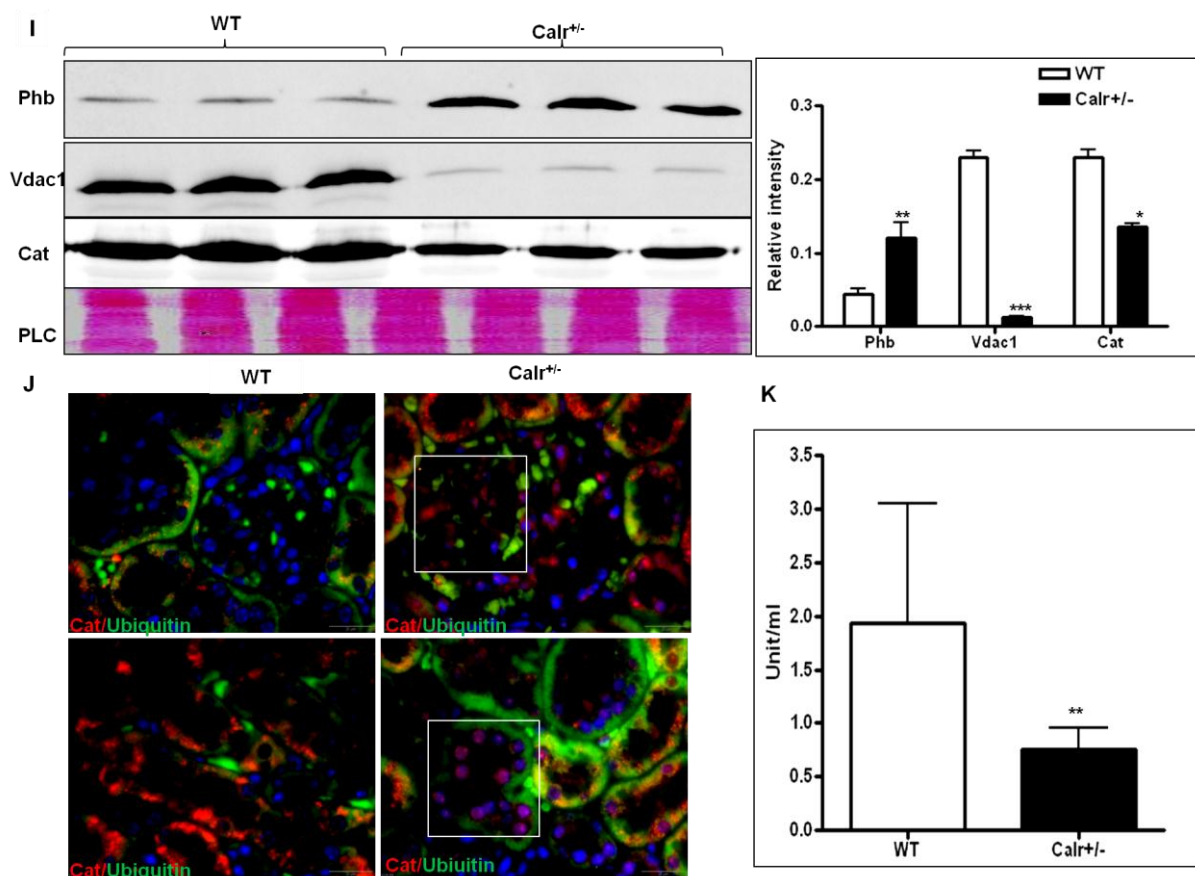


Figure 3.11: Electron micrographs demonstrating mitochondrial damage in Calr^{+/-} mice.

A-B: Representative electron micrographs for ultrastructural morphology of mitochondria from WT kidney. (A) a podocyte showing normal mitochondria pointed with white asterisks (B) Higher magnification image of normal WT mitochondria indicated with white arrows. **C-H:** Representative electron micrographs for ultrastructural morphology of mitochondria from Calr^{+/-} kidney (C) a podocyte with damaged vacuolated mitochondria highlighted with red asterisks (D) Higher magnification image of a podocyte illustrating mitochondrial swelling and damage with disordered cristae indicated with red arrows (E) Mitochondrial swelling in a proximal tubular cell indicated with arrow (F) a number of mitochondria are enclosed in a membranous network in tubular cell (G) progressive autophagous damage of mitochondria enclosed in a vacuolated structure pointed with arrow (H) Robust number of mitochondria in certain tubular cells indicated with arrow. **(I)** Western blot analysis of mitochondrial proteins; Vdac1, Phb and Cat from isolated mitochondrial lysate of WT and Calr^{+/-} kidneys. Ponso stained Cellulose membrane is used as a PLC. Quantification of protein expression is shown in bar diagram. **(J)** Immunofluorescence staining of Cat: Immunofluorescence staining of Cat coupled with ubiquitin shows enhanced expression in glomerulus (left panel indicated with box) and nuclear translocation in

proximal tubules of Calr^{+/-} kidney (right panel indicated with box) compared to WT kidney (upper row). **(K)** Quantification of cytochrome c oxidase activity. Intact mitochondria were isolated for the quantification of cytochrome c oxidase activity. Comparison of respiratory activity between Calr^{+/-} and WT kidneys revealed about 50% decrease in mitochondrial activity in Calr^{+/-} compared to WT kidneys. Results are given as the means \pm SD of the percentage volume of spot from at least three independent experiments ($P < 0.05$). PLC: protein loading control.

Table 3.1: Proteins differentially regulated in the kidneys of WT and Calr^{+/-} mice

| Spot | Name of protein | Gene Name | Uniprot Accession | MS/MS Score | Nominal Mass (KDa) | Fold change |
|------|--|-----------|-------------------|-------------|--------------------|-------------|
| 1 | Abhydrolase domain-containing protein 14B | Abhd14b | Q8VCR7 | 99 | 22,451 | 2,06 ↓ |
| 2 | Alcohol dehydrogenase [NADP+] | Akr1a1 | Q9JII6 | 262 | 36,587 | 3.49 ↑ |
| 3 | Aldehyde dehydrogenase, mitochondrial | Aldh2 | P47738 | 63 | 56,538 | 3.31 ↑ |
| 4 | Alpha-enolase | Eno1 | P17182 | 110 | 47,141 | 2.84 ↑ |
| 5 | Aminoacylase-1 | Acy1 | Q99JW2 | 113 | 45,781 | 4,50 ↓ |
| 6 | ATP synthase subunit alpha, mitochondrial | Atp5a1 | Q03265 | 236 | 59,753 | 3,49 ↓ |
| 7 | ATP synthase subunit beta, mitochondrial | Atp5b | P56480 | 505 | 56,300 | 2,04 ↓ |
| 8 | Catalase | Cat | P24270 | 54 | 59,795 | 1.92 ↑ |
| 9 | Cytochrome b-c1 complex subunit 1, mitochondrial | Uqcrc1 | Q9CZ13 | 58 | 52,852 | 1,91 ↓ |
| 10 | Delta-1-pyrroline-5-carboxylate dehydrogenase, mitochondrial. | Alh4a1 | Q8CHT0 | 83 | 61,841 | 1.69 ↑ |
| 11 | Dihydrolipoyllysine-residue acetyltransferase component of pyruvate dehydrogenase complex, mitochondrial | Dlat | Q8BMF4 | 110 | 67,942 | 5.8 ↑ |
| 12 | Dihydrolipoyllysine-residue succinyltransferase component of 2-oxoglutarate dehydrogenase complex, mitochondrial | Dlst | Q9D2G2 | 98 | 22,23 | 6,82 ↓ |
| 13 | Electrogenic sodium bicarbonate cotransporter 1 | Nbc1 | O88343 | 43 | 121,484 | 3,47 ↓ |
| 14 | Electron transfer flavoprotein subunit beta | Etfb | Q9DCW4 | 50 | 27,623 | 3,95 ↓ |
| 15 | Enoyl-CoA hydratase, mitochondrial | Echs1 | Q8BH95 | 384 | 31,474 | 3,53 ↓ |
| 16 | Ezrin | Ezr | P26040 | 95 | 69,407 | 1.91 ↓ |
| 17 | Fibrinogen beta chain | Fgb | Q8K0E8 | 132 | 54,753 | 2,42 ↓ |
| 18 | Fructose-bisphosphate aldolase B | Aldob | Q91Y97 | 271 | 39,507 | 2.18 ↑ |
| 19 | Fructose-bisphosphate aldolase B | Aldob | Q91Y97 | 71 | 39,507 | 3.25 ↑ |
| 20 | Glutamate dehydrogenase 1, mitochondrial | Glud1 | P26443 | 79 | 61,337 | 2.16 ↑ |
| 21 | Glutathione synthetase | Gss | P51855 | 67 | 52,247 | 3.03 ↑ |
| 22 | Glyceraldehyde-3-phosphate dehydrogenase | Gapdh | P16858 | 194 | 35,810 | 2.13 ↑ |
| 23 | Heat shock cognate 71 kDa protein | Hspa8 | P63017 | 158 | 68,779 | 2.16 ↑ |
| 24 | Heat shock protein beta-8 | Hspb8 | Q9JK92 | 151 | 21,533 | 2.19 ↑ |
| 25 | Hemoglobin subunit beta-1 | Hbb-b1 | P02088 | 461 | 15.840 | 4,24 ↓ |
| 26 | Hydroxyacyl-coenzyme A dehydrogenase, mitochondrial | Hadh | Q61425 | 366 | 34,464 | 2.00 ↓ |
| 27 | Ketohexokinase | Khk | P97328 | 91 | 32,75 | 1.65 ↑ |
| 28 | L-lactate dehydrogenase A chain | Ldha | P06151 | 77 | 36,499 | 2,18 ↓ |

Reduced calreticulin level results in oxidative stress mediated mitochondrial damage and kidney injury

| | | | | | | |
|----|--|---------|--------|-----|--------|--------|
| 29 | L-lactate dehydrogenase B chain | Ldhb | P16125 | 190 | 36,572 | 1.75 ↑ |
| 30 | Malate dehydrogenase, cytoplasmic | Mdh1 | P14152 | 50 | 36,511 | 3.58 ↓ |
| 31 | Malate dehydrogenase, mitochondrial | Mdh2 | P08249 | 75 | 35,611 | 2.62 ↓ |
| 32 | Mitochondrial peptide methionine sulfoxide reductase | Msra | Q9D6Y7 | 96 | 25,988 | 2.38 ↓ |
| 33 | Na(+)/H(+) exchange regulatory cofactor NHERF3 | Nherf3 | Q9JIL4 | 126 | 56,499 | 1.74 ↑ |
| 34 | NADH dehydrogenase [ubiquinone] iron-sulfur protein 8, mitochondrial | Ndufs8 | Q8K3J1 | 123 | 24,038 | 1.86 ↓ |
| 35 | Origin recognition complex subunit 3 | Orc3 | Q9JK30 | 81 | 82,342 | 1.96 ↑ |
| 36 | Peroxiredoxin-1 | Prdx1 | P35700 | 120 | 22,176 | 3.25 ↑ |
| 37 | Peroxiredoxin-2 | Prxd2 | Q5M9N9 | 73 | 21,791 | 2.74 ↑ |
| 38 | Peroxiredoxin-6 | Prdx6 | O08709 | 141 | 24,871 | 4.66 ↑ |
| 39 | Phosphoglycerate kinase 1 | Pgk1 | P09411 | 103 | 44,55 | 2.81 ↑ |
| 40 | Protein DJ-1 | PARK7 | Q99LX0 | 160 | 20,021 | 2.91 ↑ |
| 41 | Pyridine nucleotide-disulfide oxidoreductase domain-containing protein 2 | Pyroxd2 | Q3U4I7 | 175 | 62,685 | 4.73 ↓ |
| 42 | Serum albumin | Alb | P07724 | 92 | 68,693 | 3.59 ↑ |
| 43 | Short-chain specific acyl-CoA dehydrogenase, mitochondrial | Acads | Q07417 | 165 | 44,89 | 2.81 ↓ |
| 44 | Sorbitol dehydrogenase | Sord | Q64442 | 193 | 38,249 | 7.13 ↓ |
| 45 | Stress-70 protein, mitochondrial | Grp75 | P38647 | 128 | 73,528 | 2.19 ↑ |
| 46 | Superoxide dismutase [Cu-Zn] | Sod1 | P08228 | 143 | 15,943 | 2.60 ↓ |
| 47 | Toll/interleukin-1 receptor domain-containing adapter protein | Tirap | Q99JY1 | 203 | 26,035 | 2.59 ↑ |
| 48 | Triosephosphate isomerase | Tpi1 | P17751 | 262 | 32,192 | 2.90 ↑ |
| 49 | 60 kDa heat shock protein, mitochondrial | Hspd1 | P63038 | 236 | 60,955 | 1.82 ↑ |
| 50 | 78 kDa glucose-regulated protein | Grp78 | P20029 | 110 | 72,422 | 1.01 |

3.5 Discussion

In this study, we presented the first report for the potential role of reduction of Calr level in triggering renal injury leading to CKD. Morphological analyses of Calr^{+/-} mice indicate a progressive development of kidney injury with marked structural defects such as glomerulosclerosis and tubulointerstitial fibrosis at advanced stage complement with previously reported symptoms of CKD. Glomerulosclerosis is consistent with progressive increase in glomerular volume, mesangial expansion and deposition of ECM, whereas tubulointerstitial fibrosis is characterized by tubular necrosis with deposition of ECM in interstitial spaces. Ultrastructural analysis further demonstrates GBM defects, vacuolated podocyte along with foot process effacement and loss of tubular brush borders. Severely impaired expression of Ezr, a podocyte marker, in Calr^{+/-} kidneys further confirms severe podocyte damage (Hsu et al, 2005). Moreover, expression of S100a4 is extremely enhanced in tubular epithelial cells. S100a4 is also known as FSP1 (fibroblast specific protein 1) expressed specifically in fibrosing cells and involved in the development of fibrosis (Strutz et al, 1995). Finally, the distinct and dramatic renal phenotypes observed with Calr^{+/-} mice suggest that balanced expression of Calr is pivotal in renal health and establish its role in the pathogenesis of renal disease.

Calr is mainly involved in two major functions; as a chaperon and as a Ca²⁺ binding protein within ER (Coe & Michalak, 2009). Therefore, the progression of kidney injury in Calr^{+/-} mice can be anticipated from either improper protein folding or Ca²⁺ cytotoxicity. Malfunctioning of chaperons result in accumulation of misfolded proteins leading to ER stress. ER stress is peer reviewed to play a pathophysiological role in several renal diseases (Chiang et al, ; Cybulsky et al, 2010; Inagi, 2009; Inagi, 2010). It is also known that ER stress results in the activation of UPR, a coordinated stress response that upregulates the capacity of

the ER to process abnormal folded proteins (Hetz, 2012; Ron & Walter, 2007). As an adaptive mechanism, UPR further targets the transcription regulation of proteins, which can restore the proper folding of proteins such as Grp78 (Lee, 2007) or phosphorylation of eukaryotic translation initiation factor-2 α subunit (eif2 α), which decreases the ER load by turning down the general translation (Lee et al, 2010). However, in the present study, expression of Grp78 and eif2 α -phospho are not significantly changed excluding the role of ER stress in renal damage. In addition, prolonged ER stress followed by extended UPR is also known to play hazardous role via triggering cellular apoptosis and Chop/Gadd153 is induced as a proapoptotic signal (Araki et al, 2003). The unaltered expression of Chop in Calr^{+/-} kidneys further rules out the role of ER stress in renal damage.

Calr is also known as a major Ca²⁺ buffering protein of ER. Another hypothesis for the involvement of Calr in renal injury can be because of decreased Ca²⁺ buffering through Calr within ER resulting in increased free reactive intracellular Ca²⁺. Calr^{+/-} mice showed a significant upregulation of a group of EF-hand cytosolic Ca²⁺ binding proteins such as Cam, Pv and S100a4. These proteins, that contain EF-hand motifs, are Ca²⁺ sensors and are mainly involved in Ca²⁺ buffering in the cytosol. Upregulation of these proteins suggests an involvement of disturbance of free intracellular Ca²⁺ levels in Calr^{+/-} kidney injury (Cioffi, 2011). Previous studies have shown similar results, namely that regulation of expression of Calr leads to altered ER Ca²⁺ buffering capacity with almost no impact on protein folding (Bastianutto et al, 1995; Bibi et al, 2011; Opas et al, 1996).

The application of proteomics, a combination of sophisticated techniques including 2D gel electrophoresis, image analysis, mass spectrometry, amino acid sequencing, and bioinformatics, provides major opportunities to elucidate disease mechanisms and to identify new diagnostic markers and therapeutic targets (Chambers et al, 2000; Vidal et al, 2005). In

the present study, we used proteomics to further reveal the molecular mechanisms associated with renal injury in Calr^{+/-} kidneys. Proteomics identification coupled with bioinformatics analysis characterizes the involvement of oxidative stress, mitochondrial dysfunction and energy metabolism in the worsening of kidneys in Calr^{+/-} mice.

Oxidative stress is known as a major culprit in the progression of chronic kidney diseases (Djamali, 2007; Forbes et al, 2008). Generally, oxidative stress is the result of an imbalance between generation of free radicals and radical scavenging antioxidant systems. Therefore, the degree of imbalance defines the degree of oxidative stress (Droge, 2002; Finkel & Holbrook, 2000). Our proteomic analysis of kidneys of Calr^{+/-} mice compared to WT mice revealed regulation of various proteins related to induction of or induced by oxidative stress. Mainly 3 out of 6 isoforms of peroxiredoxins are upregulated in our Calr^{+/-} mice kidneys. Peroxiredoxin along with thioredoxin comprise an important anti-oxidative system which is sensitive to ROS accumulation (Michalak et al, 2002). Induction of ROS sensitive redox system confirms that oxidative stress is operative in the deterioration of kidneys in Calr^{+/-} mice (Immenschuh & Baumgart-Vogt, 2005).

The superoxide dismutase (Sod) family is a major antioxidant system (Kojima et al, 2012). Sod1 is an important antioxidant widely distributed in the tissues and represents 90% of the total Sod activity which protects a range of tissues from various oxidative stresses (Fridovich, 1997). Proteomic analysis further revealed a significant decrease in Sod1 expression in Calr^{+/-} mice. Downregulation of Sod1 might cause vulnerability to oxidative stress mediated renal injury in Calr^{+/-} mice. Several studies have already reported downregulation of Sod1 as a causal link between oxidative stress and progressive renal injury (Inagi et al, 2008; Kapoor et al, 2004; Vaziri et al, 2003; Vaziri & Rodriguez-Iturbe, 2006; Wyatt et al, 2002). Knockout studies also indicate that elimination of the Sod1 gene is associated with a variety of renal

pathological conditions, including acceleration of diabetic renal injury (DeRubertis et al, 2007), ischemia/reperfusion-induced acute renal failure (Yamanobe et al, 2007) salt sensitivity and hypertension in hydronephrosis (Carlstrom et al, 2011).

In addition to downregulation, we showed for the first time an irregular expression of Sod1 in the form of aggregates or inclusion bodies in kidneys of Calr^{+/-} mice compared to homogenous distribution in WT mice kidneys. To our knowledge, such inclusion bodies have been discussed in the neurodegenerative disease amyotrophic lateral sclerosis (ALS) ((Shaw, 2005) but not in any kidney disease. 20% of the familial ALS cases have a mutation of the Sod1 gene and are characterized by progressive degeneration of motor neurons (Wijesekera & Leigh, 2009). Despite the exact mechanism of action, the SOD1 aggregates have been proposed to play a cytotoxic role by reducing the availability of other essential intracellular proteins (Bruening et al, 1999), interfering normal intracellular mechanisms such as proteasome degradation (Allen et al, 2003), oxidative stress (Johnston et al, 2000) or by interacting with cellular organelles like mitochondria leading to dysfunction (Faes & Callewaert, 2011). In a recent study, downregulation of Calr in Sod1 mutant mice further demonstrated a link between these two proteins (Bernard-Marissal et al, 2012).

Mitochondria play vital roles in energy production, metabolism, apoptosis, necrosis, intracellular signaling and Ca²⁺ homeostasis. They are quite sensitive cellular organelles particularly, because of their capacity to change morphology, number and function in response to cellular stressors and diseases including diabetes, neurodegenerative diseases and cancer. Distribution of differentially regulated proteins in Calr^{+/-} mice according to cellular localization and functional categories also showed that 36 % of the regulated proteins belong to mitochondria and mitochondrial functions (Figure 3.7). Electron microscopy further revealed that the mitochondria are vacuolated and dilated with disorganized cristae and

damaged inner membrane, which is in agreement with neuronal mitochondrial damage in ALS (Echaniz-Laguna et al, 2002; Higgins et al, 2003; Meunier et al, 2002; Song et al, 2012; Vande Velde et al, 2011). Upregulation of mitochondrial chaperones Grp75, Hsp60 and Phb further confirmed the mitochondrial damage in Calr^{+/-} mice kidneys.

Chronic low level of Calr coupled with consistent increase in free intracellular Ca²⁺ might play a toxic role leading to mitochondrial damage in Calr^{+/-} mice through dimerization of iNos in its active dimer form. Active iNos is known to produce NO. Under pathological conditions, NO might react with O₂ to produce peroxynitrite (ONOO⁻) species which modifies proteins leading to mitochondrial dysfunction (Radisky et al, 2007; Sandhu et al, 2005). Moreover, accumulation of mitochondrial reactive oxygen species as a result of Sod1 downregulation, might lead to oxidative damage and mitochondrial dysfunction. Oxidative stress is inseparably linked to mitochondrial dysfunction, as mitochondria are both generators of and targets for reactive species (Andreyev et al, 2005; Balaban et al, 2005; Maleki et al, 2012; Small et al, 2012). Previous studies have also shown mitochondrial damage as an important phenomenon related to Sod1 down regulation, Sod1 knockout (Jang et al, 2010), or Sod1 mutation (Faes & Callewaert, 2011; Magrane et al, 2012).

Mitochondria are considered the powerhouse of the cell and play a central role in energy metabolism because of producing more than 80% of the cellular energy. Therefore, mitochondrial dysfunction, as a consequence of calcium load and oxidative stress can lead to impaired energy metabolism in Calr^{+/-} mice kidneys. With the use of the KEGG pathways, a very consistent view related to energy metabolism showed a significant downregulation of enzymes belonging to mitochondrial resident energy pathways such as the oxidative phosphorylation (OxPhos) pathway. On the other hand, cytosolic resident energy production with glycolysis pathway is enhanced. It is well known that the mitochondrial respiratory chain

together with ATP synthase constitutes the OxPhos machinery, which produces 15 times more energy equivalents in the form of ATP than the glycolytic pathway does (Huttemann et al, 2012). Therefore, enhancement of glycolysis might be unable to fulfill cellular energy needs in Calr^{+/-} kidneys leading to starved cellular conditions. Decreased cytochrome c oxidase activity further confirmed the loss of proper mitochondrial function leading to energy crisis in Calr^{+/-} mice kidneys. Ca²⁺ concentration changes are known to directly correlate to changes in mitochondrial energy metabolism and ATP production through interaction with OxPhos and electron transport chain enzymes (Glancy & Balaban, 2012; Griffiths & Rutter, 2009). Moreover, it can also act through the decrease in Vdac1 expression, which is well established to regulate the energy balance of mitochondria and the entire cell by serving as a common pathway for metabolite exchange between mitochondria and cytoplasm (Shoshan-Barmatz et al, 2008). As Vdac1 is absolutely required for PINK1/Parkin-mediated selective autophagy of damaged mitochondria, its downregulation further accelerates the accumulation of necrotic and damaged toxic mitochondria in intracellular environment leading to cell apoptosis (Geisler et al, 2010).

Earlier studies showed that cellular ability to utilize different metabolic pathways in support of energy production is critical for survival under stress, and if compromised, activates the programmed cell death and dies by autophagy; a phenomenon whereby cells can digest themselves from within (Sandhu et al, 2005). Calr^{+/-} mice kidneys show similar results with presence of mitochondrial autophagy and robust increase in number.

In summary, we demonstrated that low level of Calr is responsible for the impairment of entire pathways involved in oxidative stress, mitochondrial structure and function, and energy metabolism at the protein level and is linked to the pathology of renal injury of Calr +/- mice.

Our observations suggest a notion that chronic low level of Calr favors conditions for the onset and progression of chronic kidney disease.

4. SUMMARY

Chronic kidney disease (CKD) is becoming a major public health problem worldwide. The persistent progression of CKD is postulated to result from a self-perpetuating vicious cycle of events activated after initial injury. Being a major excretory and homeostatic organ of the body, kidney is continuously exposed to toxic wastes, excess of water and ions. In an attempt to understand the molecular mechanisms, which lead a normal functioning kidney towards disease state, proteomic screening of renal cells under various physiological conditions such as osmotic stress, oxidative stress and cytokines were performed. The data highlighted the expression regulation of an endoplasmic reticulum resident Ca^{2+} binding protein, calreticulin. Within endoplasmic reticulum (ER), calreticulin plays important function as a chaperon directing proper conformation of proteins, as well as a major ER Ca^{2+} binding protein, which controls cytosolic and ER Ca^{2+} levels. The purpose of this study was to investigate the potential role of calreticulin and mechanisms connecting this protein in regulating the renal cells function and progression of renal injury.

In vitro investigations described in Chapter 2 using two-dimensional fluorescence difference gel electrophoresis combined with mass spectrometry analysis revealed an expression alteration of calreticulin in renal cells under osmotic stress conditions. It was also found that downregulation of calreticulin is combined with continuous change in the level of free intracellular Ca^{2+} . On the other hand, inhibition of the Ca^{2+} release, through IP3R antagonist, prevented calreticulin expression alteration under hyperosmotic stress, whereas the cell viability was significantly impaired. An increase in ER Ca^{2+} storage with decreased cell viability was observed in cells overexpressing wild type calreticulin compared to no significant change in Ca^{2+} level and viability in cells overexpressing mutant calreticulin, lacking the Ca^{2+} binding domain. Furthermore, free Ca^{2+} level and cell survival were significantly improved under osmotic stress conditions by silencing calreticulin with siRNA.

Taken together, our data clearly highlight the crucial role of calreticulin in renal cells functioning and survival through modulating Ca^{2+} homeostasis under osmotic stress conditions.

The work presented in Chapter 3 was performed with adult heterozygote $\text{Calr}^{+/-}$ mice having chronic low level of calreticulin to further investigate the *in vivo* impact of downregulation of calreticulin on kidney structure and function. A progression of renal injury evidenced by development of glomerulosclerosis and tubulointerstitial damage was observed in histological analysis of $\text{Calr}^{+/-}$ mice kidneys from different age groups. The significant overexpression of cytosolic Ca^{2+} binding proteins with an insignificant alteration of ER stress proteins, suggested the role of intracellular Ca^{2+} homeostasis disturbance in renal impairments in $\text{Calr}^{+/-}$ mice. It was also found that endoplasmic reticulum stress protein markers are not significantly induced. Proteomic analysis further highlighted the role of oxidative stress and mitochondrial dysfunction in renal injury in $\text{Calr}^{+/-}$ mice kidneys. Especially, the reactive oxidative species scavenging enzyme, Sod1 expression was not only significantly downregulated but also showed irregular aggregates with immunohistochemical staining. Ultrastructural analysis further indicated significantly impaired mitochondrial morphology characterized by enlarged, swollen mitochondria with disturbed membranous structures in $\text{Calr}^{+/-}$ mice. These morphological changes were accompanied by biochemical abnormalities with specific decreases in the activity of cytochrome c oxidase of the mitochondrial electron transfer chain. Consequently, the oxidative stress together with mitochondrial damage and energy imbalance resulted in kidney injury in $\text{Calr}^{+/-}$ mice. A diagram summarizing the results of this chapter is provided in in Figure 4.1.

In conclusion, the work presented in this thesis, revealed for the first time, the role of calreticulin in renal cells function and in the progression of chronic kidney injury. The study

also points out that low level of calreticulin mediated Ca^{2+} homeostasis disturbances impacts the mitochondrial morphology, function and expression of Sod1. It will be interesting to investigate the exact mechanism by which calreticulin modulates Sod1 downregulation, at the molecular level. This should provide more concentrated foci for future experimentation. However, our findings highlighted a new potential mechanism of the progression of CKD and encourage new directions in CKD research, which in turn should have impact on treatment approach, diagnosis and prevention of CKD.

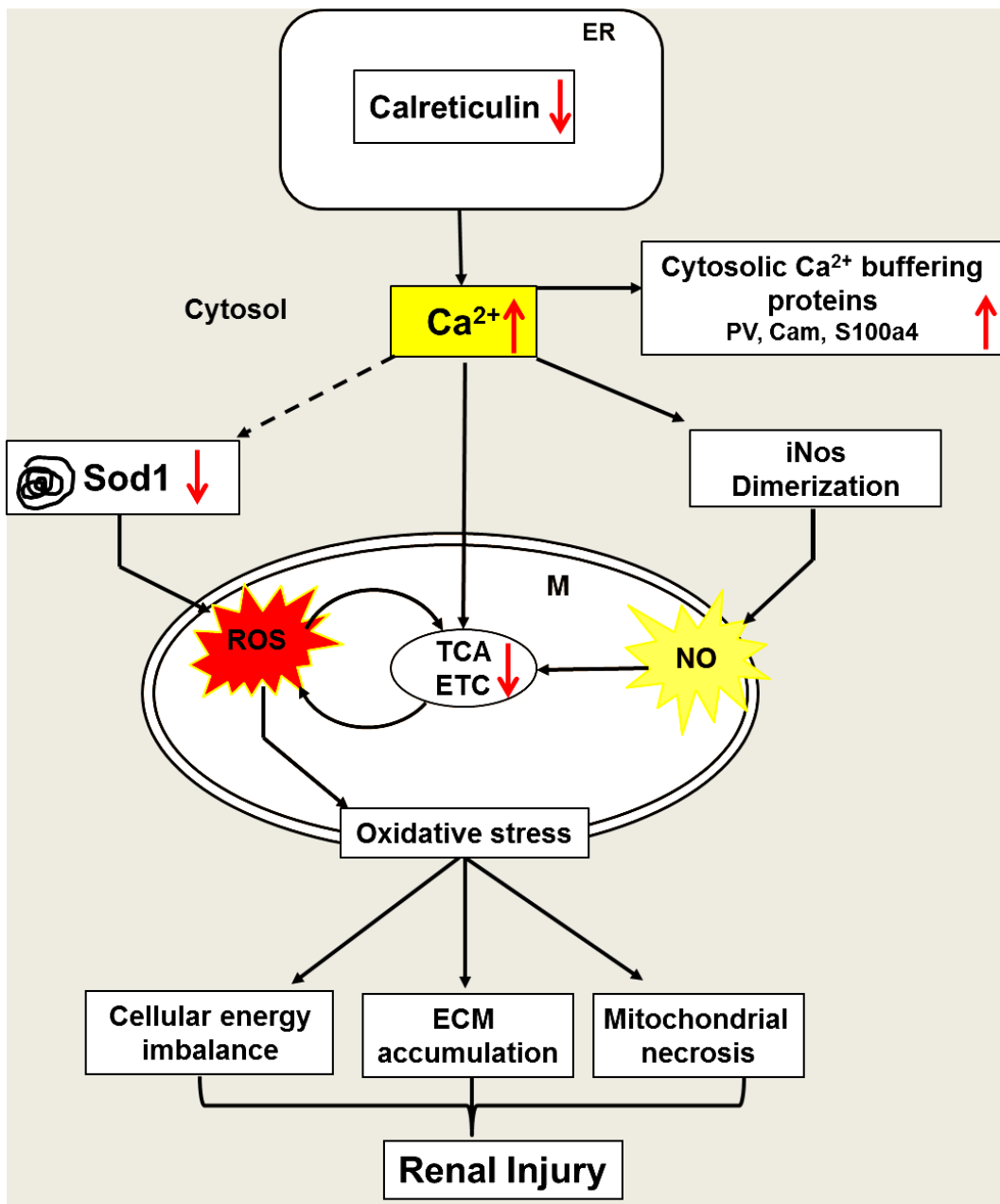


Figure 4.1: Schematic representation of potential pathway of low calreticulin level in the progression of renal injury.

Low expression of calreticulin results in the elevated cytosolic Ca^{2+} level. The present study revealed the overexpression of cytosolic Ca^{2+} buffering proteins; Pv, Cam and S100a4 as a result of increase in Ca^{2+} level. We further observed that low calreticulin level results in the dimerization of iNos, downregulation of Sod1 and expression alteration of proteins related to cellular energy metabolism. Based on the present data and literature, we hypothesized that downregulation of Sod1 results in accumulation of ROS, which may lead to a pathological alteration in mitochondrial function, favouring more ROS generation, and oxidative stress. Oxidative stress in turn results in accumulation of ECM, mitochondrial necrosis and energy imbalance; all these impairments finally converge to renal injury. Red arrows show the up- or downregulation. Broken line indicates the supposed link. Ca^{2+} : calcium ions, Cam: calmodulin, ECM: extracellular matrix, ER: endoplasmic reticulum, ETC: electron transport chain, iNOS: induced nitric oxide synthase, M: mitochondria, , NO: nitric oxide, Pv: parvalbumin, ROS: reactive oxidative species, Sod1: superoxide dismutase 1, TCA: tricarboxylic cycle.

BIBLIOGRAPHY

Afshar N, Black BE, Paschal BM (2005) Retrotranslocation of the chaperone calreticulin from the endoplasmic reticulum lumen to the cytosol. *Mol Cell Biol* 25: 8844-8853

Allen S, Heath PR, Kirby J, Wharton SB, Cookson MR, Menzies FM, Banks RE, Shaw PJ (2003) Analysis of the cytosolic proteome in a cell culture model of familial amyotrophic lateral sclerosis reveals alterations to the proteasome, antioxidant defenses, and nitric oxide synthetic pathways. *J Biol Chem* 278: 6371-6383

Andreyev AY, Kushnareva YE, Starkov AA (2005) Mitochondrial metabolism of reactive oxygen species. *Biochemistry (Mosc)* 70: 200-214

Araki E, Oyadomari S, Mori M (2003) Impact of endoplasmic reticulum stress pathway on pancreatic beta-cells and diabetes mellitus. *Exp Biol Med (Maywood)* 228: 1213-1217

Arendshorst WJ, Thai TL (2009) Regulation of the renal microcirculation by ryanodine receptors and calcium-induced calcium release. *Curr Opin Nephrol Hypertens* 18: 40-49

Baksh S, Burns K, Andrin C, Michalak M (1995) Interaction of calreticulin with protein disulfide isomerase. *J Biol Chem* 270: 31338-31344

Balaban RS, Nemoto S, Finkel T (2005) Mitochondria, oxidants, and aging. *Cell* 120: 483-495

Barri YM (2008) Hypertension and kidney disease: a deadly connection. *Curr Hypertens Rep* 10: 39-45

Barsoum RS (2006) Chronic kidney disease in the developing world. *N Engl J Med* 354: 997-999

Bartek J, Bartkova J, Kyprianou N, Lalani EN, Staskova Z, Shearer M, Chang S, Taylor-Papadimitriou J (1991) Efficient immortalization of luminal epithelial cells from human mammary gland by introduction of simian virus 40 large tumor antigen with a recombinant retrovirus. *Proc Natl Acad Sci U S A* 88: 3520-3524

Bash LD, Selvin E, Steffes M, Coresh J, Astor BC (2008) Poor glycemic control in diabetes and the risk of incident chronic kidney disease even in the absence of albuminuria and retinopathy: Atherosclerosis Risk in Communities (ARIC) Study. *Arch Intern Med* 168: 2440-2447

Bastianutto C, Clementi E, Codazzi F, Podini P, De Giorgi F, Rizzuto R, Meldolesi J, Pozzan T (1995) Overexpression of calreticulin increases the Ca²⁺ capacity of rapidly exchanging Ca²⁺ stores and reveals aspects of their luminal microenvironment and function. *J Cell Biol* 130: 847-855

Baumann O, Walz B (2001) Endoplasmic reticulum of animal cells and its organization into structural and functional domains. *Int Rev Cytol* 205: 149-214

Bedard K, Szabo E, Michalak M, Opas M (2005) Cellular functions of endoplasmic reticulum chaperones calreticulin, calnexin, and ERp57. *Int Rev Cytol* 245: 91-121

Bernard-Marissal N, Moumen A, Sunyach C, Pellegrino C, Dudley K, Henderson CE, Raoul C, Pettmann B (2012) Reduced calreticulin levels link endoplasmic reticulum stress and Fas-triggered cell death in motoneurons vulnerable to ALS. *J Neurosci* 32: 4901-4912

Berridge MJ (1993) Inositol trisphosphate and calcium signalling. *Nature* 361: 315-325

Bibi A, Agarwal NK, Dihazi GH, Eltoweissy M, Van Nguyen P, Mueller GA, Dihazi H (2011) Calreticulin is crucial for calcium homeostasis mediated adaptation and survival of thick ascending limb of Henle's loop cells under osmotic stress. *Int J Biochem Cell Biol* 43: 1187-1197

Bourque CW (2008) Central mechanisms of osmosensation and systemic osmoregulation. *Nat Rev Neurosci* 9: 519-531

Boykin S, Diez-Roux AV, Carnethon M, Shrager S, Ni H, Whitt-Glover M (2011) Racial/ethnic heterogeneity in the socioeconomic patterning of CVD risk factors: in the United States: the multi-ethnic study of atherosclerosis. *J Health Care Poor Underserved* 22: 111-127

Bradford MM (1976) A rapid and sensitive method for the quantitation of microgram quantities of protein utilizing the principle of protein-dye binding. *Anal Biochem* 72: 248-254

Brodsky JL, Skach WR Protein folding and quality control in the endoplasmic reticulum: Recent lessons from yeast and mammalian cell systems. *Curr Opin Cell Biol* 23: 464-475

Bruening W, Roy J, Giasson B, Figlewicz DA, Mushynski WE, Durham HD (1999) Up-regulation of protein chaperones preserves viability of cells expressing toxic Cu/Zn-superoxide dismutase mutants associated with amyotrophic lateral sclerosis. *J Neurochem* 72: 693-699

Buchberger A, Bukau B, Sommer T (2010) Protein quality control in the cytosol and the endoplasmic reticulum: brothers in arms. *Mol Cell* 40: 238-252

Burg MB, Ferraris JD, Dmitrieva NI (2007) Cellular response to hyperosmotic stresses. *Physiol Rev* 87: 1441-1474

Camacho P, Lechleiter JD (1995) Calreticulin inhibits repetitive intracellular Ca²⁺ waves. *Cell* 82: 765-771

Carew RM, Wang B, Kantharidis P The role of EMT in renal fibrosis. *Cell Tissue Res* 347: 103-116

Carlstrom M, Persson AE, Larsson E, Hezel M, Scheffer PG, Teerlink T, Weitzberg E, Lundberg JO (2011)

) Dietary nitrate attenuates oxidative stress, prevents cardiac and renal injuries, and reduces blood pressure in salt-induced hypertension. *Cardiovasc Res* 89: 574-585

Chambers G, Lawrie L, Cash P, Murray GI (2000) Proteomics: a new approach to the study of disease. *J Pathol* 192: 280-288

Chan CS, Gertler TS, Surmeier DJ (2009) Calcium homeostasis, selective vulnerability and Parkinson's disease. *Trends Neurosci* 32: 249-256

Chevet E, Cameron PH, Pelletier MF, Thomas DY, Bergeron JJ (2001) The endoplasmic reticulum: integration of protein folding, quality control, signaling and degradation. *Curr Opin Struct Biol* 11: 120-124

Chiang CK, Hsu SP, Wu CT, Huang JW, Cheng HT, Chang YW, Hung KY, Wu KD, Liu SH (2011) Endoplasmic reticulum stress implicated in the development of renal fibrosis. *Mol Med* 17: 1295-1305

Chouquet A, Paidassi H, Ling WL, Frachet P, Houen G, Arlaud GJ, Gaboriaud C (2011) X-ray structure of the human calreticulin globular domain reveals a peptide-binding area and suggests a multi-molecular mechanism. *PLoS One* 6: e17886

Cioffi DL, Barry, C. J. and Stevens, T. (2011) Role of Calcium as a Second Messenger in Signaling: A Focus on Endothelium. *Textbook of Pulmonary Vascular Disease* 1: 261-272

Coe H, Michalak M (2009) Calcium binding chaperones of the endoplasmic reticulum. *Gen Physiol Biophys* 28 Spec No Focus: F96-F103

Cunard R, Sharma K (2011) The endoplasmic reticulum stress response and diabetic kidney disease. *Am J Physiol Renal Physiol* 300: F1054-1061

Cybulsky AV, Takano T, Papillon J, Kitzler TM, Bijian K (2010) Endoplasmic reticulum stress in glomerular epithelial cell injury. *Am J Physiol Renal Physiol* 301: F496-508

DeRubertis FR, Craven PA, Melhem MF (2007) Acceleration of diabetic renal injury in the superoxide dismutase knockout mouse: effects of tempol. *Metabolism* 56: 1256-1264

Dihazi H, Asif AR, Agarwal NK, Doncheva Y, Muller GA (2005) Proteomic analysis of cellular response to osmotic stress in thick ascending limb of Henle's loop (TALH) cells. *Mol Cell Proteomics* 4: 1445-1458

Dihazi H, Dihazi GH, Mueller C, Lahrichi L, Asif AR, Bibi A, Eltoweissy M, Vasko R, Mueller GA (2011) Proteomics characterization of cell model with renal fibrosis phenotype: osmotic stress as fibrosis triggering factor. *J Proteomics* 74: 304-318

Djamali A (2007) Oxidative stress as a common pathway to chronic tubulointerstitial injury in kidney allografts. *Am J Physiol Renal Physiol* 293: F445-455

Droge W (2002) Free radicals in the physiological control of cell function. *Physiol Rev* 82: 47-95

Echaniz-Laguna A, Zoll J, Ribera F, Tranchant C, Warter JM, Lonsdorfer J, Lampert E (2002) Mitochondrial respiratory chain function in skeletal muscle of ALS patients. *Ann Neurol* 52: 623-627

Efstratiadis G, Divani M, Katsioulis E, Vergoulas G (2009) Renal fibrosis. *Hippokratia* 13: 224-229

El-Nahas AM (2003) Plasticity of kidney cells: role in kidney remodeling and scarring. *Kidney Int* 64: 1553-1563

Elbein AD (1987) Inhibitors of the biosynthesis and processing of N-linked oligosaccharide chains. *Annu Rev Biochem* 56: 497-534

Ellgaard L, Bettendorff P, Braun D, Herrmann T, Fiorito F, Jelesarov I, Guntert P, Helenius A, Wuthrich K (2002) NMR structures of 36 and 73-residue fragments of the calreticulin P-domain. *J Mol Biol* 322: 773-784

Ellgaard L, Helenius A (2003) Quality control in the endoplasmic reticulum. *Nat Rev Mol Cell Biol* 4: 181-191

Eltoweissy M, Muller GA, Bibi A, Nguye PV, Dihazi GH, Muller CA, Dihazi H (2011) Proteomics analysis identifies PARK7 as an important player for renal cell resistance and survival under oxidative stress. *Mol Biosyst* 7: 1277-1288

Faes L, Callewaert G (2011) Mitochondrial dysfunction in familial amyotrophic lateral sclerosis. *J Bioenerg Biomembr* 43: 587-592

Finkel T, Holbrook NJ (2000) Oxidants, oxidative stress and the biology of ageing. *Nature* 408: 239-247

Fliegel L, Burns K, Opas M, Michalak M (1989) The high-affinity calcium binding protein of sarcoplasmic reticulum. Tissue distribution, and homology with calregulin. *Biochim Biophys Acta* 982: 1-8

Fogo AB (2006) Progression versus regression of chronic kidney disease. *Nephrol Dial Transplant* 21: 281-284

Forbes JM, Coughlan MT, Cooper ME (2008) Oxidative stress as a major culprit in kidney disease in diabetes. *Diabetes* 57: 1446-1454

Fridovich I (1997) Superoxide anion radical (O₂⁻), superoxide dismutases, and related matters. *J Biol Chem* 272: 18515-18517

Friedman PA, Figueiredo JF, Maack T, Windhager EE (1981) Sodium-calcium interactions in the renal proximal convoluted tubule of the rabbit. *Am J Physiol* 240: F558-568

Geisler S, Holmstrom KM, Treis A, Skujat D, Weber SS, Fiesel FC, Kahle PJ, Springer W (2010) The PINK1/Parkin-mediated mitophagy is compromised by PD-associated mutations. *Autophagy* 6: 871-878

Gelebart P, Opas M, Michalak M (2005) Calreticulin, a Ca²⁺-binding chaperone of the endoplasmic reticulum. *Int J Biochem Cell Biol* 37: 260-266

Girgert R, Martin M, Kruegel J, Miosge N, Temme J, Eckes B, Muller GA, Gross O Integrin alpha2-deficient mice provide insights into specific functions of collagen receptors in the kidney. *Fibrogenesis Tissue Repair* 3: 19

Glancy B, Balaban RS (2012) Role of mitochondrial Ca²⁺ in the regulation of cellular energetics. *Biochemistry* 51: 2959-2973

Go AS, Chertow GM, Fan D, McCulloch CE, Hsu CY (2004) Chronic kidney disease and the risks of death, cardiovascular events, and hospitalization. *N Engl J Med* 351: 1296-1305

Gold LI, Eggleton P, Sweetwyne MT, Van Duyn LB, Greives MR, Naylor SM, Michalak M, Murphy-Ullrich JE (2010) Calreticulin: non-endoplasmic reticulum functions in physiology and disease. *Faseb J* 24: 665-683

Gorg A, Obermaier C, Boguth G, Csordas A, Diaz JJ, Madjar JJ (1997) Very alkaline immobilized pH gradients for two-dimensional electrophoresis of ribosomal and nuclear proteins. *Electrophoresis* 18: 328-337

Griffiths EJ, Rutter GA (2009) Mitochondrial calcium as a key regulator of mitochondrial ATP production in mammalian cells. *Biochim Biophys Acta* 1787: 1324-1333

Grunewald RW, Fahr M, Fiedler GM, Jehle PM, Muller GA (2001) Volume regulation of thick ascending limb of Henle cells: significance of organic osmolytes. *Exp Nephrol* 9: 81-89

Grupp C, Troche I, Steffgen J, Langhans S, Cohen DI, Brandl L, Muller GA (1998) Highly specific separation of heterogeneous cell populations by lectin-coated beads: application for the isolation of inner medullary collecting duct cells. *Exp Nephrol* 6: 542-550

Hebert DN, Molinari M (2007) In and out of the ER: protein folding, quality control, degradation, and related human diseases. *Physiol Rev* 87: 1377-1408

Hetz C (2012) The unfolded protein response: controlling cell fate decisions under ER stress and beyond. *Nat Rev Mol Cell Biol* 13: 89-102

Higgins CM, Jung C, Xu Z (2003) ALS-associated mutant SOD1G93A causes mitochondrial vacuolation by expansion of the intermembrane space and by involvement of SOD1 aggregation and peroxisomes. *BMC Neurosci* 4: 16

Hohenadel D, van der Woude FJ (2004) Gene expression in diabetic nephropathy. *Curr Diab Rep* 4: 462-469

Hong M, Luo S, Baumeister P, Huang JM, Gogia RK, Li M, Lee AS (2004) Underglycosylation of ATF6 as a novel sensing mechanism for activation of the unfolded protein response. *J Biol Chem* 279: 11354-11363

Hossain MP, Goyder EC, Rigby JE, El Nahas M (2009) CKD and poverty: a growing global challenge. *Am J Kidney Dis* 53: 166-174

Hsu WM, Hsieh FJ, Jeng YM, Kuo ML, Chen CN, Lai DM, Hsieh LJ, Wang BT, Tsao PN, Lee H et al (2005) Calreticulin expression in neuroblastoma--a novel independent prognostic factor. *Ann Oncol* 16: 314-321

Huttemann M, Helling S, Sanderson TH, Sinkler C, Samavati L, Mahapatra G, Varughese A, Lu G, Liu J, Ramzan R et al (2012) Regulation of mitochondrial respiration and apoptosis through cell signaling: cytochrome c oxidase and cytochrome c in ischemia/reperfusion injury and inflammation. *Biochim Biophys Acta* 1817: 598-609

Ihara Y, Kageyama K, Kondo T (2005) Overexpression of calreticulin sensitizes SERCA2a to oxidative stress. *Biochem Biophys Res Commun* 329: 1343-1349

Immenschuh S, Baumgart-Vogt E (2005) Peroxiredoxins, oxidative stress, and cell proliferation. *Antioxid Redox Signal* 7: 768-777

Inagi R (2009) Endoplasmic reticulum stress in the kidney as a novel mediator of kidney injury. *Nephron Exp Nephrol* 112: e1-9

Inagi R (2010) Endoplasmic reticulum stress as a progression factor for kidney injury. *Curr Opin Pharmacol* 10: 156-165

Inagi R, Kumagai T, Nishi H, Kawakami T, Miyata T, Fujita T, Nangaku M (2008) Preconditioning with endoplasmic reticulum stress ameliorates mesangioproliferative glomerulonephritis. *J Am Soc Nephrol* 19: 915-922

Ishii T, Yanagawa T (2007) Stress-induced peroxiredoxins. *Subcell Biochem* 44: 375-384

Jang YC, Lustgarten MS, Liu Y, Muller FL, Bhattacharya A, Liang H, Salmon AB, Brooks SV, Larkin L, Hayworth CR et al (2010) Increased superoxide *in vivo* accelerates age-associated muscle atrophy through mitochondrial dysfunction and neuromuscular junction degeneration. *Faseb J* 24: 1376-1390

Johnston JA, Dalton MJ, Gurney ME, Kopito RR (2000) Formation of high molecular weight complexes of mutant Cu, Zn-superoxide dismutase in a mouse model for familial amyotrophic lateral sclerosis. *Proc Natl Acad Sci U S A* 97: 12571-12576

Kapoor M, Ellgaard L, Gopalakrishnapai J, Schirra C, Gemma E, Oscarson S, Helenius A, Surolia A (2004) Mutational analysis provides molecular insight into the carbohydrate-binding region of calreticulin: pivotal roles of tyrosine-109 and aspartate-135 in carbohydrate recognition. *Biochemistry* 43: 97-106

Kapoor M, Srinivas H, Kandiah E, Gemma E, Ellgaard L, Oscarson S, Helenius A, Surolia A (2003) Interactions of substrate with calreticulin, an endoplasmic reticulum chaperone. *J Biol Chem* 278: 6194-6200

Klahr S, Schreiner G, Ichikawa I (1988) The progression of renal disease. *N Engl J Med* 318: 1657-1666

Kleizen B, Braakman I (2004) Protein folding and quality control in the endoplasmic reticulum. *Curr Opin Cell Biol* 16: 343-349

Kojima T, Wakamatsu TH, Dogru M, Ogawa Y, Igarashi A, Ibrahim OM, Inaba T, Shimizu T, Noda S, Obata H et al (2012) Age-related dysfunction of the lacrimal gland and oxidative stress: evidence from the Cu,Zn-superoxide dismutase-1 (Sod1) knockout mice. *Am J Pathol* 180: 1879-1896

Kolodziejcki PJ, Rashid MB, Eissa NT (2003) Intracellular formation of "undisruptable" dimers of inducible nitric oxide synthase. *Proc Natl Acad Sci U S A* 100: 14263-14268

Kottgen A, Pattaro C, Boger CA, Fuchsberger C, Olden M, Glazer NL, Parsa A, Gao X, Yang Q, Smith AV et al (2010)
New loci associated with kidney function and chronic kidney disease. *Nat Genet* 42: 376-384

Kozlov G, Pocanschi CL, Rosenauer A, Bastos-Aristizabal S, Gorelik A, Williams DB, Gehring K (2010)
Structural basis of carbohydrate recognition by calreticulin. *J Biol Chem* 285: 38612-38620

Kubala M (2006) ATP-binding to P-type ATPases as revealed by biochemical, spectroscopic, and crystallographic experiments. *Proteins* 64: 1-12

Lajdova I, Spustova V, Oksa A, Chorvatova A, Chorvat D, Jr., Dzurik R (2009) Intracellular calcium homeostasis in patients with early stages of chronic kidney disease: effects of vitamin D3 supplementation. *Nephrol Dial Transplant* 24: 3376-3381

Leach MR, Cohen-Doyle MF, Thomas DY, Williams DB (2002) Localization of the lectin, ERp57 binding, and polypeptide binding sites of calnexin and calreticulin. *J Biol Chem* 277: 29686-29697

Lee AS (1992) Mammalian stress response: induction of the glucose-regulated protein family. *Curr Opin Cell Biol* 4: 267-273

Lee AS (2007) GRP78 induction in cancer: therapeutic and prognostic implications. *Cancer Res* 67: 3496-3499

Lee do Y, Lee KS, Lee HJ, Kim do H, Noh YH, Yu K, Jung HY, Lee SH, Lee JY, Youn YC et al (2010)
Activation of PERK signaling attenuates Abeta-mediated ER stress. *PLoS One* 5: e10489

Levey AS, Coresh J (2011) Chronic kidney disease. *Lancet* 379: 165-180

Lindenmeyer MT, Rastaldi MP, Ikehata M, Neusser MA, Kretzler M, Cohen CD, Schlondorff D (2008)
Proteinuria and hyperglycemia induce endoplasmic reticulum stress. *J Am Soc Nephrol* 19: 2225-2236

Little E, Lee AS (1995) Generation of a mammalian cell line deficient in glucose-regulated protein stress induction through targeted ribozyme driven by a stress-inducible promoter. *J Biol Chem* 270: 9526-9534

Liu G, Sun Y, Li Z, Song T, Wang H, Zhang Y, Ge Z (2008) Apoptosis induced by endoplasmic reticulum stress involved in diabetic kidney disease. *Biochem Biophys Res Commun* 370: 651-656

Liu H, Bowes RC, 3rd, van de Water B, Sillence C, Nagelkerke JF, Stevens JL (1997) Endoplasmic reticulum chaperones GRP78 and calreticulin prevent oxidative stress, Ca²⁺ disturbances, and cell death in renal epithelial cells. *J Biol Chem* 272: 21751-21759

Lopez-Novoa JM, Martinez-Salgado C, Rodriguez-Pena AB, Lopez-Hernandez FJ (2010) Common pathophysiological mechanisms of chronic kidney disease: therapeutic perspectives. *Pharmacol Ther* 128: 61-81

Lysaght MJ (2002) Maintenance dialysis population dynamics: current trends and long-term implications. *J Am Soc Nephrol* 13 Suppl 1: S37-40

Magrane J, Sahawneh MA, Przedborski S, Estevez AG, Manfredi G (2012) Mitochondrial dynamics and bioenergetic dysfunction is associated with synaptic alterations in mutant SOD1 motor neurons. *J Neurosci* 32: 229-242

Maleki S, Sepehr R, Staniszewski K, Sheibani N, Sorenson CM, Ranji M (2012) Mitochondrial redox studies of oxidative stress in kidneys from diabetic mice. *Biomed Opt Express* 3: 273-281

Marber MS, Mestrlil R, Chi SH, Sayen MR, Yellon DM, Dillmann WH (1995) Overexpression of the rat inducible 70-kD heat stress protein in a transgenic mouse increases the resistance of the heart to ischemic injury. *J Clin Invest* 95: 1446-1456

Marsh DJ, Azen SP (1975) Mechanism of NaCl reabsorption by hamster thin ascending limbs of Henle's loop. *Am J Physiol* 228: 71-79

Martin V, Groenendyk J, Steiner SS, Guo L, Dabrowska M, Parker JM, Muller-Esterl W, Opas M, Michalak M (2006) Identification by mutational analysis of amino acid residues essential in the chaperone function of calreticulin. *J Biol Chem* 281: 2338-2346

Means AR, Rasmussen CD (1988) Calcium, calmodulin and cell proliferation. *Cell Calcium* 9: 313-319

Meguid El Nahas A, Bello AK (2005) Chronic kidney disease: the global challenge. *Lancet* 365: 331-340

Mery L, Mesaeli N, Michalak M, Opas M, Lew DP, Krause KH (1996) Overexpression of calreticulin increases intracellular Ca²⁺ storage and decreases store-operated Ca²⁺ influx. *J Biol Chem* 271: 9332-9339

Mesaeli N, Nakamura K, Zvaritch E, Dickie P, Dziak E, Krause KH, Opas M, MacLennan DH, Michalak M (1999) Calreticulin is essential for cardiac development. *J Cell Biol* 144: 857-868

Meunier L, Usherwood YK, Chung KT, Hendershot LM (2002) A subset of chaperones and folding enzymes form multiprotein complexes in endoplasmic reticulum to bind nascent proteins. *Mol Biol Cell* 13: 4456-4469

Michalak M, Corbett EF, Mesaeli N, Nakamura K, Opas M (1999) Calreticulin: one protein, one gene, many functions. *Biochem J* 344 Pt 2: 281-292

Michalak M, Milner RE, Burns K, Opas M (1992) Calreticulin. *Biochem J* 285 (Pt 3): 681-692

Michalak M, Robert Parker JM, Opas M (2002) Ca²⁺ signaling and calcium binding chaperones of the endoplasmic reticulum. *Cell Calcium* 32: 269-278

Michea L, Ferguson DR, Peters EM, Andrews PM, Kirby MR, Burg MB (2000) Cell cycle delay and apoptosis are induced by high salt and urea in renal medullary cells. *Am J Physiol Renal Physiol* 278: F209-218

Mimran A, du Cailar G (2008) Dietary sodium: the dark horse amongst cardiovascular and renal risk factors. *Nephrol Dial Transplant* 23: 2138-2141

Mimura I, Nangaku M (2010)

) The suffocating kidney: tubulointerstitial hypoxia in end-stage renal disease. *Nat Rev Nephrol* 6: 667-678

Modlinger PS, Wilcox CS, Aslam S (2004) Nitric oxide, oxidative stress, and progression of chronic renal failure. *Semin Nephrol* 24: 354-365

Morris JA, Dorner AJ, Edwards CA, Hendershot LM, Kaufman RJ (1997) Immunoglobulin binding protein (BiP) function is required to protect cells from endoplasmic reticulum stress but is not required for the secretion of selective proteins. *J Biol Chem* 272: 4327-4334

Nakamura K, Zuppini A, Arnaudeau S, Lynch J, Ahsan I, Krause R, Papp S, De Smedt H, Parys JB, Muller-Esterl W et al (2001) Functional specialization of calreticulin domains. *J Cell Biol* 154: 961-972

Nauseef WM, McCormick SJ, Clark RA (1995) Calreticulin functions as a molecular chaperone in the biosynthesis of myeloperoxidase. *J Biol Chem* 270: 4741-4747

Nguyen Van PP, F; and Soling, HD, (1989) *J Biol Chem* 264: 17494-17501

Nicotera P, Bellomo G, Orrenius S (1992) Calcium-mediated mechanisms in chemically induced cell death. *Annu Rev Pharmacol Toxicol* 32: 449-470

Nicotera P, Orrenius S (1998) The role of calcium in apoptosis. *Cell Calcium* 23: 173-180

Oberg BP, McMenamin E, Lucas FL, McMonagle E, Morrow J, Ikizler TA, Himmelfarb J (2004) Increased prevalence of oxidant stress and inflammation in patients with moderate to severe chronic kidney disease. *Kidney Int* 65: 1009-1016

Okada Y, Sim X, Go MJ, Wu JY, Gu D, Takeuchi F, Takahashi A, Maeda S, Tsunoda T, Chen P et al (2012) Meta-analysis identifies multiple loci associated with kidney function-related traits in east Asian populations. *Nat Genet* 44: 904-909

Opas M, Szewczenko-Pawlikowski M, Jass GK, Mesaeli N, Michalak M (1996) Calreticulin modulates cell adhesiveness via regulation of vinculin expression. *J Cell Biol* 135: 1913-1923

Orantes CM, Herrera R, Almaguer M, Brizuela EG, Hernandez CE, Bayarre H, Amaya JC, Calero DJ, Orellana P, Colindres RM et al Chronic kidney disease and associated risk factors in the Bajo Lempa region of El Salvador: Nefrolempa study, 2009. *MEDICC Rev* 13: 14-22

Ostwald TJ, MacLennan DH (1974) Isolation of a high affinity calcium-binding protein from sarcoplasmic reticulum. *J Biol Chem* 249: 974-979

Peterson JR, Ora A, Van PN, Helenius A (1995) Transient, lectin-like association of calreticulin with folding intermediates of cellular and viral glycoproteins. *Mol Biol Cell* 6: 1173-1184

Pocanschi CL, Kozlov G, Brockmeier U, Brockmeier A, Williams DB, Gehring K (2011) Structural and functional relationships between the lectin and arm domains of calreticulin. *J Biol Chem* 286: 27266-27277

Pollock S, Kozlov G, Pelletier MF, Trempe JF, Jansen G, Sitnikov D, Bergeron JJ, Gehring K, Ekiel I, Thomas DY (2004) Specific interaction of ERp57 and calnexin determined by NMR spectroscopy and an ER two-hybrid system. *Embo J* 23: 1020-1029

Pyram R, Kansara A, Banerji MA, Loney-Hutchinson L (2011) Chronic kidney disease and diabetes. *Maturitas* 71: 94-103

Radisky DC, Kenny PA, Bissell MJ (2007) Fibrosis and cancer: do myofibroblasts come also from epithelial cells via EMT? *J Cell Biochem* 101: 830-839

Rangan GK, Tesch GH (2007) Quantification of renal pathology by image analysis. *Nephrology (Carlton)* 12: 553-558

Rivera VM, Clackson T, Natesan S, Pollock R, Amara JF, Keenan T, Magari SR, Phillips T, Courage NL, Cerasoli F, Jr. et al (1996) A humanized system for pharmacologic control of gene expression. *Nat Med* 2: 1028-1032

Ron D, Walter P (2007) Signal integration in the endoplasmic reticulum unfolded protein response. *Nat Rev Mol Cell Biol* 8: 519-529

Rule AD, Bergstralh EJ, Melton LJ, 3rd, Li X, Weaver AL, Lieske JC (2009) Kidney stones and the risk for chronic kidney disease. *Clin J Am Soc Nephrol* 4: 804-811

Sandhu JK, Sodja C, McRae K, Li Y, Rippstein P, Wei YH, Lach B, Lee F, Bucurescu S, Harper ME et al (2005) Effects of nitric oxide donors on cybrids harbouring the mitochondrial myopathy, encephalopathy, lactic acidosis and stroke-like episodes (MELAS) A3243G mitochondrial DNA mutation. *Biochem J* 391: 191-202

Schiffrin EL, Lipman ML, Mann JF (2007) Chronic kidney disease: effects on the cardiovascular system. *Circulation* 116: 85-97

Schulman G (2012) A nexus of progression of chronic kidney disease: tryptophan, profibrotic cytokines, and charcoal. *J Ren Nutr* 22: 107-113

Shaw PJ (2005) Molecular and cellular pathways of neurodegeneration in motor neurone disease. *J Neurol Neurosurg Psychiatry* 76: 1046-1057

Shoshan-Barmatz V, Keinan N, Zaid H (2008) Uncovering the role of VDAC in the regulation of cell life and death. *J Bioenerg Biomembr* 40: 183-191

Small DM, Coombes JS, Bennett N, Johnson DW, Gobe GC (2012) Oxidative stress, anti-oxidant therapies and chronic kidney disease. *Nephrology (Carlton)* 17: 311-321

Song W, Song Y, Kincaid B, Bossy B, Bossy-Wetzel E (2012) Mutant SOD1(G93A) triggers mitochondrial fragmentation in spinal cord motor neurons: Neuroprotection by SIRT3 and PGC-1alpha. *Neurobiol Dis*

Sonnichsen B, Fullekrug J, Nguyen Van P, Diekmann W, Robinson DG, Mieskes G (1994) Retention and retrieval: both mechanisms cooperate to maintain calreticulin in the endoplasmic reticulum. *J Cell Sci* 107 (Pt 10): 2705-2717

Strutz F, Okada H, Lo CW, Danoff T, Carone RL, Tomaszewski JE, Neilson EG (1995) Identification and characterization of a fibroblast marker: FSP1. *J Cell Biol* 130: 393-405

Sugawara S, Takeda K, Lee A, Dennert G (1993) Suppression of stress protein GRP78 induction in tumor B/C10ME eliminates resistance to cell mediated cytotoxicity. *Cancer Res* 53: 6001-6005

Susic D, Frohlich ED (2012) Salt consumption and cardiovascular, renal, and hypertensive diseases: clinical and mechanistic aspects. *Curr Opin Lipidol* 23: 11-16

Syntichaki P, Tavernarakis N (2003) The biochemistry of neuronal necrosis: rogue biology? *Nat Rev Neurosci* 4: 672-684

Taylor A, Windhager EE (1979) Possible role of cytosolic calcium and Na-Ca exchange in regulation of transepithelial sodium transport. *Am J Physiol* 236: F505-512

Tedla FM, Brar A, Browne R, Brown C (2011) Hypertension in chronic kidney disease: navigating the evidence. *Int J Hypertens* 2011: 132405

Thastrup O, Cullen PJ, Drobak BK, Hanley MR, Dawson AP (1990) Thapsigargin, a tumor promoter, discharges intracellular Ca^{2+} stores by specific inhibition of the endoplasmic reticulum Ca^{2+} -ATPase. *Proc Natl Acad Sci U S A* 87: 2466-2470

Timmins JM, Ozcan L, Seimon TA, Li G, Malagelada C, Backs J, Backs T, Bassel-Duby R, Olson EN, Anderson ME et al (2009) Calcium/calmodulin-dependent protein kinase II links ER stress with Fas and mitochondrial apoptosis pathways. *J Clin Invest* 119: 2925-2941

Tjoelker LW, Seyfried CE, Eddy RL, Jr., Byers MG, Shows TB, Calderon J, Schreiber RB, Gray PW (1994) Human, mouse, and rat calnexin cDNA cloning: identification of potential calcium binding motifs and gene localization to human chromosome 5. *Biochemistry* 33: 3229-3236

Tonelli M, Wiebe N, Culeton B, House A, Rabbat C, Fok M, McAlister F, Garg AX (2006) Chronic kidney disease and mortality risk: a systematic review. *J Am Soc Nephrol* 17: 2034-2047

Towbin H, Staehelin T, Gordon J (1979) Electrophoretic transfer of proteins from polyacrylamide gels to nitrocellulose sheets: procedure and some applications. *Proc Natl Acad Sci U S A* 76: 4350-4354

Treves S, De Mattei M, Landfredi M, Villa A, Green NM, MacLennan DH, Meldolesi J, Pozzan T (1990) Calreticulin is a candidate for a calsequestrin-like function in Ca^{2+} -storage compartments (calciosomes) of liver and brain. *Biochem J* 271: 473-480

Trombetta ES, Helenius A (1998) Lectins as chaperones in glycoprotein folding. *Curr Opin Struct Biol* 8: 587-592

Tuomilehto J, Jousilahti P, Rastenyte D, Moltchanov V, Tanskanen A, Pietinen P, Nissinen A (2001) Urinary sodium excretion and cardiovascular mortality in Finland: a prospective study. *Lancet* 357: 848-851

Vamvakas S, Anders MW (1990) Perturbation of calcium homeostasis as a link between acute cell injury and carcinogenesis in the kidney. *Toxicol Lett* 53: 115-120

Vande Velde C, McDonald KK, Boukhedimi Y, McAlonis-Downes M, Lobsiger CS, Bel Hadj S, Zandona A, Julien JP, Shah SB, Cleveland DW (2011)

) Misfolded SOD1 associated with motor neuron mitochondria alters mitochondrial shape and distribution prior to clinical onset. *PLoS One* 6: e22031

Vanderheyden V, Devogelaere B, Missiaen L, De Smedt H, Bultynck G, Parys JB (2009) Regulation of inositol 1,4,5-trisphosphate-induced Ca²⁺ release by reversible phosphorylation and dephosphorylation. *Biochim Biophys Acta* 1793: 959-970

Vassilakos A, Michalak M, Lehrman MA, Williams DB (1998) Oligosaccharide binding characteristics of the molecular chaperones calnexin and calreticulin. *Biochemistry* 37: 3480-3490

Vaziri ND, Dicus M, Ho ND, Boroujerdi-Rad L, Sindhu RK (2003) Oxidative stress and dysregulation of superoxide dismutase and NADPH oxidase in renal insufficiency. *Kidney Int* 63: 179-185

Vaziri ND, Rodriguez-Iturbe B (2006) Mechanisms of disease: oxidative stress and inflammation in the pathogenesis of hypertension. *Nat Clin Pract Nephrol* 2: 582-593

Vehaskari VM (2011) Genetics and CKD. *Adv Chronic Kidney Dis* 18: 317-323

Verkhatsky A (2007) Calcium and cell death. *Subcell Biochem* 45: 465-480

Vidal BC, Bonventre JV, S IHH (2005) Towards the application of proteomics in renal disease diagnosis. *Clin Sci (Lond)* 109: 421-430

Walensky LD, Snyder SH (1995) Inositol 1,4,5-trisphosphate receptors selectively localized to the acrosomes of mammalian sperm. *J Cell Biol* 130: 857-869

Weir MR Recognizing the link between chronic kidney disease and cardiovascular disease. *Am J Manag Care* 17 Suppl 15: S396-402

Wijesekera LC, Leigh PN (2009) Amyotrophic lateral sclerosis. *Orphanet J Rare Dis* 4: 3

Wu J, Kaufman RJ (2006) From acute ER stress to physiological roles of the Unfolded Protein Response. *Cell Death Differ* 13: 374-384

Wyatt SE, Tsou PL, Robertson D (2002) Expression of the high capacity calcium-binding domain of calreticulin increases bioavailable calcium stores in plants. *Transgenic Res* 11: 1-10

Xu W, Longo FJ, Wintermantel MR, Jiang X, Clark RA, DeLisle S (2000) Calreticulin modulates capacitative Ca²⁺ influx by controlling the extent of inositol 1,4,5-trisphosphate-induced Ca²⁺ store depletion. *J Biol Chem* 275: 36676-36682

Yamanobe T, Okada F, Iuchi Y, Onuma K, Tomita Y, Fujii J (2007) Deterioration of ischemia/reperfusion-induced acute renal failure in SOD1-deficient mice. *Free Radic Res* 41: 200-207

Yoshida H (2007) ER stress and diseases. *Febs J* 274: 630-658

Zeisberg M, Strutz F, Muller GA (2000) Role of fibroblast activation in inducing interstitial fibrosis. *J Nephrol* 13 Suppl 3: S111-120

Zhang QL, Koenig W, Raum E, Stegmaier C, Brenner H, Rothenbacher D (2009) Epidemiology of chronic kidney disease: results from a population of older adults in Germany. *Prev Med* 48: 122-127

Zhang QL, Rothenbacher D (2008) Prevalence of chronic kidney disease in population-based studies: systematic review. *BMC Public Health* 8: 117

Zhang Y, Liu R, Ni M, Gill P, Lee AS (2010)
) Cell surface relocalization of the endoplasmic reticulum chaperone and unfolded protein response regulator GRP78/BiP. *J Biol Chem* 285: 15065-15075

Zhao L, Ackerman SL (2006) Endoplasmic reticulum stress in health and disease. *Curr Opin Cell Biol* 18: 444-452

Zile MR, Gaasch WH (2011)
) Abnormal calcium homeostasis: one mechanism in diastolic heart failure. *J Am Coll Cardiol* 58: 155-157

APPENDIX

Construction of CALR-expression and CALR-siRNA vectors

The pCMV2 flag-tag-CALR construct was generated by insertion of flag DNA fragment into pVCM2 with the KDEL retention signal at the 3'-end. In brief, the flag-KDEL-construct (generated by PCR) was inserted into the MluI-XbaI-sites of pCMV2

ACGCGTAGATCTAAGCTTGATTACAAGGACGATGACGATAAGATCGATTRRSKLD
YKDDDDKIDAGTGAGAAGGACGAGCTATGAATCGATAGATCTTGAAAGCTTAGT
 GAGSEKDE L * ID S E * KLSEAAA GAT GAG CTT TGA TCT AGA KDEL * SR

* Bold underline: flag peptide sequence; faint underline: Restriction sites MluI and XbaI

CALR fragment was generated by PCR using the sense primer (5'-AAG CTT GAA TTC CCT CGG CCC GCC ATGCTCCTT TCGGTG CCG CTC-3'), and antisense primer (without EKDEL coded nucleotides and flanked by MluI site): (5'-CATAGCACGCGTTGATGTATC CTCTTCACCAG-3') and inserted into pCMV2-flag-KDEL via EcoRI and MluI.

The production of CALR without the calcium binding site (Δ CALR) was carried out by standard PCR procedure using the same sense primer for CALR as above and the antisense primer (5'-GC GAATTC AAGCTTCTACAGCTCATCCTTCTGCTTGTCCTTCATCTGCT TCTC-3'). The insertion of Δ CALR into the pCMV2 was performed via EcoRI (Sonnichsen et al, 1994).

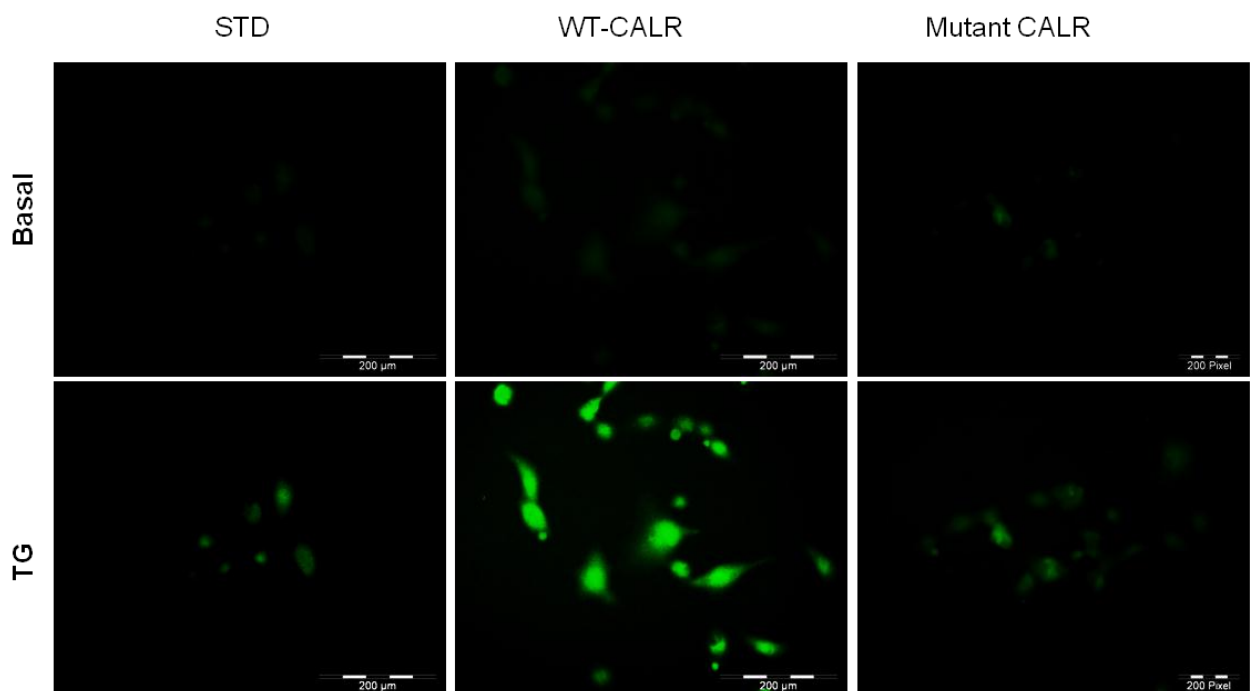
siRNA oligonucleotides specific for the knockdown of CALR expression (sense strand: 5'-ACCTCGGCGATCAGGAGAAAGATAAAATCAAGAGTTTATCTTTCTCCTGATCGCCT T3'),(antisense strand: 3'-CAAAAAGGCGATCAGGAGAAAGATAAACTCTTGATTTAT-CTTTCTCCTGATCGCCG-5'), were designed in our laboratory and synthesized by Eurofins MWG Operon. siRNA vector was constructed by ligating oligonucleotides in psiRNAh7SK

neo vector (Invivogen). Stable clones were selected by adding 1 mg/ml Neomycin. All constructs were verified by sequencing. TALH-cells cultured to approximately 80% confluence were transfected with siRNA containing vector for the knockdown of CALR using transfection reagent Lipofectamine 2000™ (Invitrogen) according to standard protocol of manufacturer.

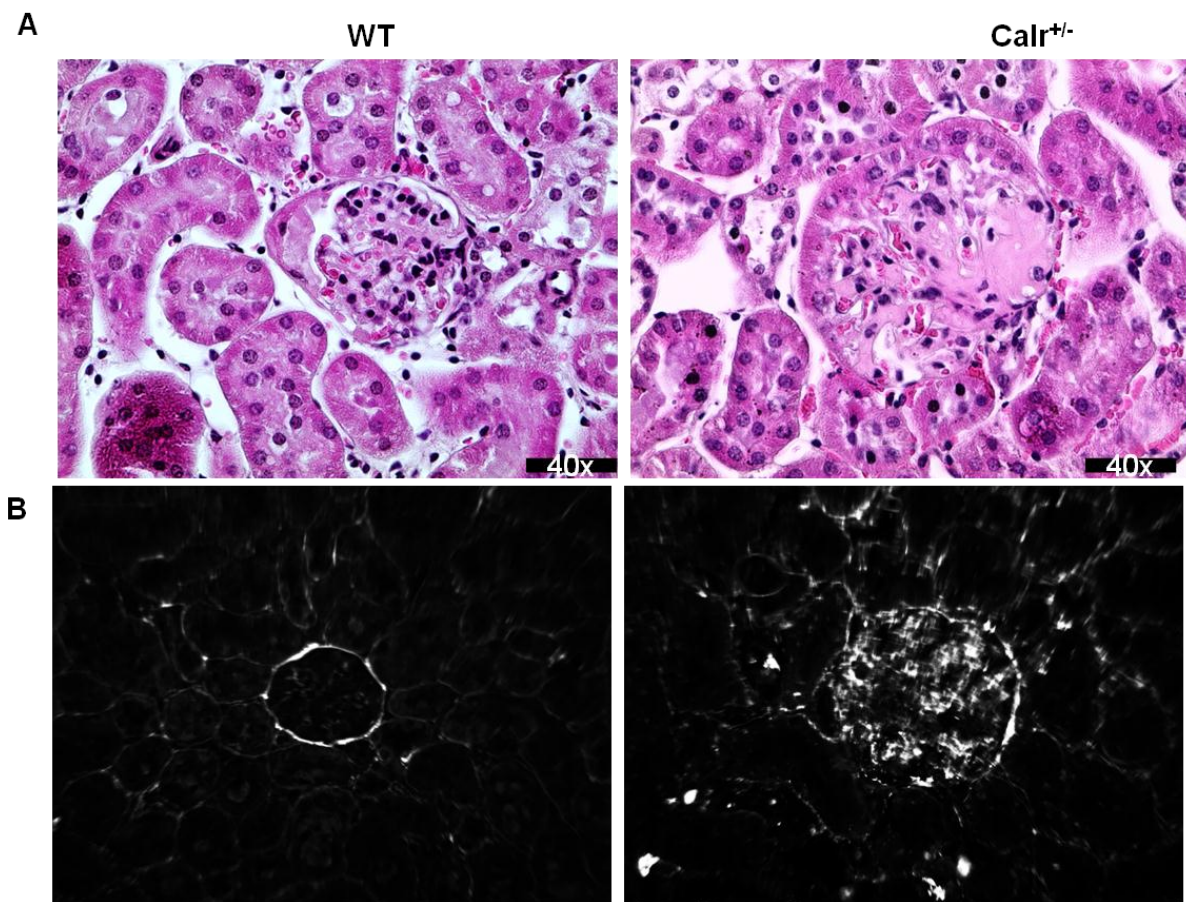
Supplemental Figure 2.1: Measurement of free intracellular Ca^{2+} in TALH-cells overexpressing WT-CALR and mutant CALR compared to TALH-STD cells.

Cells grown on cover slides were loaded with fura-2/AM in a final concentration of 8 μM .

Imaging was carried out at 37 °C on the stage of an inverted microscope for the measurement of free intracellular Ca^{2+} in terms of fluorescence intensity emitted by fura-2.AM.

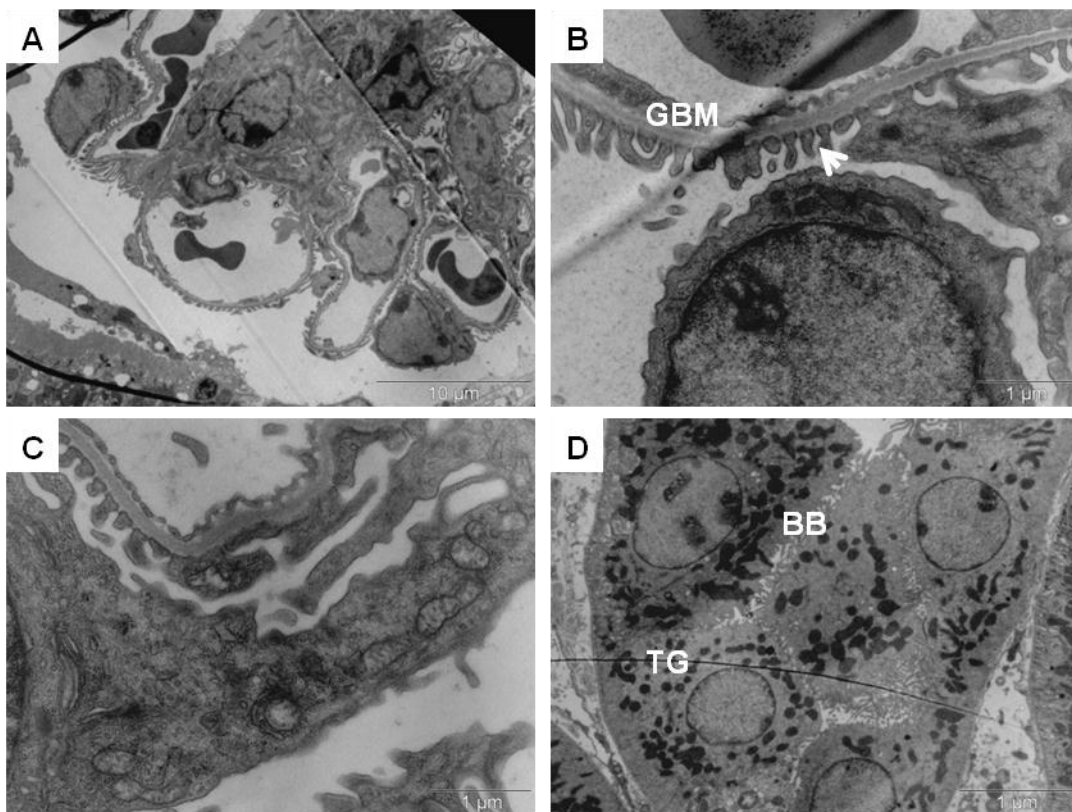


Supplemental Figure 3.1: Histological analysis of $Calr^{+/-}$ mice kidneys. (A) Paraffin embedded kidney sections ($3\mu\text{m}$) were stained with H&E to compare the kidney structures of $Calr^{+/-}$ at age of 40 wk with WT mice at the same age. (B) Immunofluorescence staining of Fn1 of 40 wk old WT and $Calr^{+/-}$ kidneys.

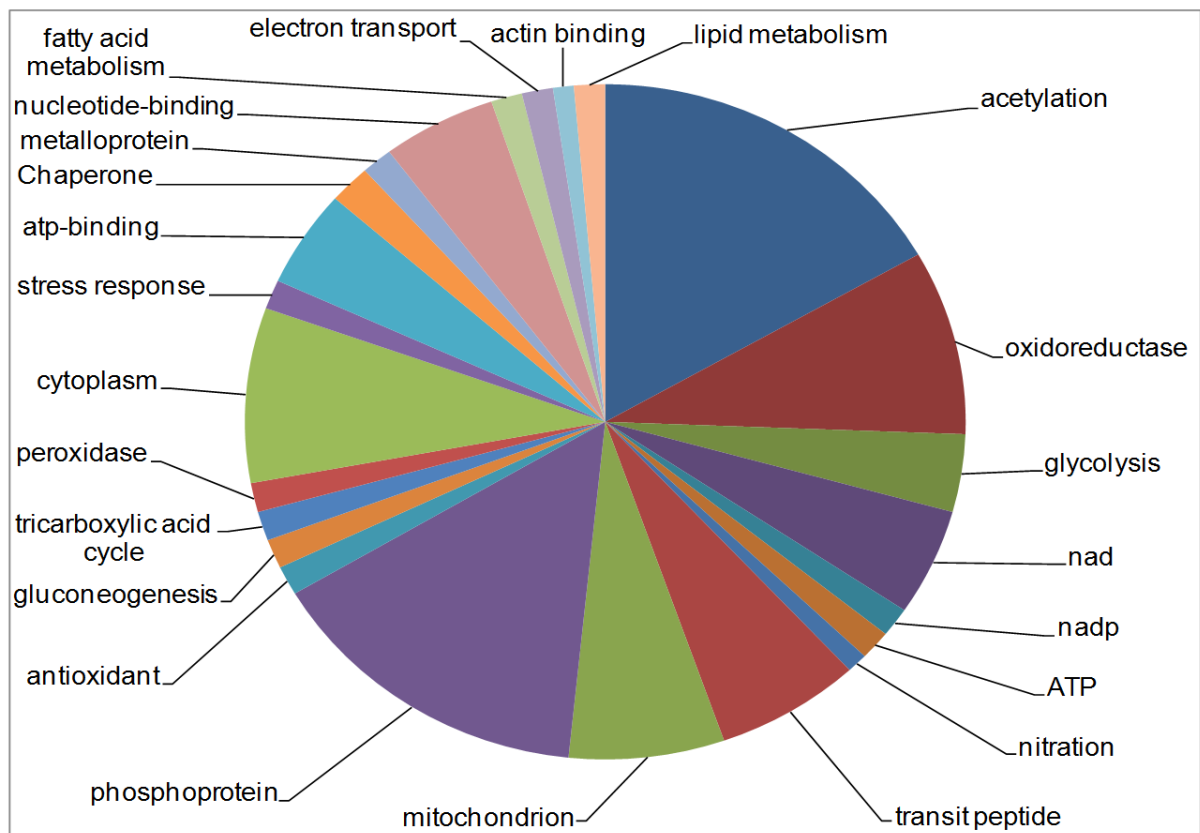


Supplemental Figure 3.2: Electron microscopy analysis of young Calr^{+/-} mice kidneys.

Kidney section from 12-weeks-old WT and Calr^{+/-} mice were assessed by electron microscopy. Representative electron microscopic images show normal structures in young Calr^{+/-} (A) lower magnification shows no deposition of ECM (10 μ m) (B) Normal glomerular basement membrane indicated with GBM and podocyte foot process indicated with arrow (2 μ m). (C) Podocyte with normal mitochondria (1 μ m). (E) Representative micrographs of proximal tubular cells from showing normal TJ and BB in 12 wk Calr^{+/-} mice (10 μ m). GBM: glomerular basement membrane, BB: brush borders, TJ: tight junction



Supplemental Figure 3.3: Functional classification of differentially regulated proteins on the basis of functional protein categories. Distribution of all differentially regulated proteins, according to the Gene Ontology (GO) annotation system, was performed using the DAVID database bioinformatic resources (<http://david.abcc.ncifcrf.gov/>).



ACKNOWLEDGEMENTS

In the name of Allah, the most Merciful, the most Gracious. I am thankful to Allah Almighty, that after four year's journey, I finally arrived at the end of the road. But this was not a lonely trip, and I would like to thank a number of great people who helped me to achieve this goal.

First, I would like to express my gratitude to my supervisor, Prof. Dr. Hassan Dihazi for giving me opportunity to work as a member of "AG Dihazi". He has been a great source of inspiration and motivation throughout my PhD period, and without whom, this thesis would not have been a reality. I have enjoyed being taught and guided by him, and I hope that this project serves as the foundation for many more years of collaboration.

This thesis owes a great deal to the support and guidance of Prof. Dr. Sigrd Hoyer-Fender and Prof. Dr. med. Jürgen Brockmüller. I would like to take opportunity to thank them for accepting to be my supervisors and the interest they have shown throughout in my work.

Special thanks go to Elke Brünst-Knoblich, who not only guided and helped me in lab work but also was very helpful in private issues throughout my stay in Germany. I would also like to thank to my research colleagues and friends Marwa, Gry, Ivana, Constanze and Diana for their support, guidance and friendship. I am proud to have such fellows who deserve my high appreciation. I would also like to thank to Prof. Dr. Gerhard A. Müller, who kindly provided me opportunity to stay in Department of Nephrology, University Medical Center Goettingen.

I am thankful to Jenny Krugel for providing support in Electron Microscopy, Dr. Abdul Rahman Asif for Proteomic Analysis and Dr. Phuc Von Nugvan for providing guidance in Molecular Biology work. I would also like to thank to Prof. Dr. Michalak, Alberta, Canada who kindly provided "Calreticulin knockout mice" for my PhD project.

None of the work offered here would have been possible without the financial support afforded from Higher Education Commission of Pakistan and German Academic Exchange Service (DAAD). I am very thankful to both of these organizations for their support.

Friends, I am so fortunate to have you all. I am thankful to Rehana, Mubeen, Zia bhai, Tayyab, Aneela and many others for their support, company and entertainment to make my PhD period, a memorable time of my life. Thanks to my very dear and near friend, Zakia for her never-ending emotional and moral support. I would also like to mention my little sweet and cute friend Khadija Zia for her lovely chit chats.

I would like to thank to a very special category. They are friends but I find them more like a family in Goettingen. Maliha, Shahid bhai, Seemin aapi, Abid bhai, Sana, Imran bhai, and very sweet and cute Mashal, Eshal and Hamza, for their love, support, homelike environment and a lot more during my stay in Germany. Especially our memorable tours; I can never forget those fantastic moments.

Very special thanks go to all my family members in Pakistan; my mother, sisters, brothers, sisters-in-law, brothers-in-law, nieces and nephews. In all aspects of my life they have provided me endless support encouragement and love. In particular, I am deeply grateful to my brother Waqar Alam for being a pillar of support and love, during all stressful moments of my PhD project.

Asima

CURRICULUM VITAE

Personal Data

Name Asima Bibi
Place and date of Birth Gujrat, 02-04-1983
Country of Origin Pakistan
Email asmaalam11@hotmail.com



Academic Career

2008-2012 PhD (Biology), George August University, Goettingen, Germany
2006-2008 M.Phil (Zoology), University of Agriculture, Faisalabad, Pakistan
2004-2006 M.Sc. (Zoology), University of Agriculture, Faisalabad, Pakistan
2002-2004 B.Sc (Zoology, Botany and Chemistry), University of Punjab, Lahore, Pakistan

Research presentations/Published abstracts:

- **Bibi A.**, Müller GA., and Dihazi H. Nuclear translocation of ER calcium binding proteins under hyper osmotic stress in TALH cells. Kongress der Gesellschaft für Nephrologie, page 432 Nieren-und Hochdruck-ankheiten, 38/9 September 2009, Göttingen, Germany
- **Bibi, A.**, Dihazi, G.H., Van Nguyen, P., Mueller, G.A., El-Toweissy, M., Dihazi, H., Role of calreticulin (CRT) by regulating calcium homeostasis in the osmotic stress adaption of thick ascending limb of Henle's loop (TALH) cells, XLVII ERA-EDTA Congress-II DGfN Congress, June, 25–28, 2010, Nephrol. Dial. Transpl. Vol. 3 Supplement 3 iii315, Munich, Germany.
- El-Toweissy, M., Mueller, G.A., **Bibi, A.**, Dihazi, H., Oxidative stress pathways in the pathogenesis of renal fibrosis: the role of the vasoactive compound angiotensin II (ANGII) and the platelet derived growth factor (PDGF), XLVII ERA-EDTA Congress-II DGfN Congress, June, 25–28, 2010, Nephrol. Dial. Transpl. Vol.3 Supplement 3 iii314, Munich, Germany.
- Oral presentation: **Bibi A.**, Calreticulin (CALR) expression and calcium homeostasis regulation plays important role in the osmotic stress adaptation of thick ascending limb of Henle's loop (TALH) cells, Göttinger Transporttage 2010, October 16-17.2010, Göttingen, Germany.

- Poster presentation in Göttingen Proteomic Forum, 18 November 2010, Göttingen, Germany.
- Eltoweissy M., Müller G.A., **Bibi A.**, and Dihazi H. Proteomics analysis identify PARK7 as an important player for renal cell resistance and survival under oxidative stress. Deutsche Physiologische Gesellschaft Regensburg, March 26-29 2011, Regensburg, Acta Physiol. March 2011 Volume 201 Suppl. 682 page 248.
- Eltoweissy, M., Dihazi, G.H., **Bibi, A.**, Mueller, G.A., and Dihazi, H., Proteomics characterization of cell model with renal fibrosis phenotype: Osmotic stress as fibrosis triggering factor. Deutsche Physiologische Gesellschaft Regensburg, March 26-29 2011, Regensburg, Acta Physiol. March 2011 Volume 201 Suppl. 682 page 144.
- Eltoweissy, M., Mueller, G.A., **Bibi, A.**, Van Nguyen, P., Dihazi, G.H., Mueller, C.A., and Dihazi, H., Functional proteomics analyses identify PARK7 as an important player for renal cell resistance and survival under oxidative stress, 10th HUPO World Congress 2011, September 4-7, 2011, Page 502, Geneva, Switzerland.
- **Bibi, A.**, Buchmeier, B., Eltoweissy, M., Dihazi, G.H., Mueller, G.A., and Dihazi, H., Expression and reorganization of vimentin play a vital role in osmotic stress resistance of renal cells, 3. Jahrestagung der Deutschen Gesellschaft für Nephrologie 2011, DGfN Heft 03/2011, September 10-13, 2011, P273, Berlin, Germany.

List of Publications:

- **Bibi, A.**, Agarwal, N.K., Dihazi, G.H., El Toweissy, Nguyen, P.V., Mueller, G.A. and Dihazi, H., Calreticulin is crucial for calcium homeostasis mediated adaptation and survival of thick ascending limb of Henle's loop cells under osmotic stress. Int. J. Biochem. Cell. Biol., (2011),
- Dihazi, H., Dihazi, G.H., Mueller, A.C., Lahrichi, L., Asif, A.R., **Bibi, A.**, El Toweissy, M., Vasko, R. and Mueller, G.A., Proteomics characterization of cell model with renal fibrosis phenotype: Osmotic stress as fibrosis triggering factor, J. Proteomic., (2011), 74:304-318.
- El Toweissy, M., Mueller, G.A., **Bibi, A.**, Nguyen, P.V., Dihazi, G.H., Mueller, A.C. and Dihazi, H., Proteomics analysis identifies PARK7 as an important player for renal cell resistance and survival under oxidative stress, Mol. BioSyst., (2011), 7(4):1277-88.
- Buchmaier, B., **Bibi, A.**, Dihazi, G.H., Mueller, G.A., El Toweissy, M., Renal cells express different forms of vimentin, the independent expression regulation alteration of these forms is important in cell resistance to osmotic stress and apoptosis. Plos One, (In revision).
- Dihazi, G.H., **Bibi, A.**, Jahn, O., Nolte, J., Mueller, G.A.,v Engel, W., Dihazi, H., Impact of the antiproliferative agent ciclopirox olamine treatment on stem cells

- proteome, World J. Stem Cells, (In revision).
- Reduced calreticulin level results in oxidative stress mediated mitochondrial damage and kidney injury (in process).

Key qualifications:

- Certificate for Laser capture microdissection coupled with mass spectrometry, Eurokup Training School, May 25-27, 2009, Rotterdam, Netherlands.
- Certificate for MALDI imaging mass spectrometry, Eurokup Training School, October 12-14, 2010, Helsinki, Finland.
- Introduction to laboratory animal science, February 21-25, 2011, Central animal facility, University Medical center, Goettingen, Germany.

Distinction and awards:

- Scholarship award for doctoral studies in Germany by Higher education commission of Pakistan (HEC) (2008-2012).
- First position holder in class through the period of 2004-2008 in University of Agriculture, Faisalabad, Pakistan.

Referenc:

Prof. Dr. Hassan Dihazi

Department of Nephrology and Rheumatology,
University Medical Center Goettingen, Germany.

Telefon: +49 551-39-91221

Fax: +49 551-39-8906

Email: dihazi@uni.med-goettingen.de